CAPÍTULO 5: PARTE EXPERIMENTAL

CAPÍTULO 5: PARTE EXPERIMENTAL

5.1. MATERIAIS E MÉTODOS

5.1.1. Difração de Raios X

A coleta dos dados de difração de raios X dos compostos **1**, **3**, **4**, **5**, **6**, **7**, **8**, **9**, **17**, **18** e **19** foi realizada sob condições de temperatura ambiente (20°C) em um difratômetro de quatro círculos CAD-4 (Enraf-Nonius), dotado de um monocromador de grafite, de radiação Mo-Kα (λ = 0,71073 Å).[69] (Freie Universität Berlin – Alemanha).

Os parâmetros da cela elementar para esses compostos, foram obtidos com base no refinamento de 25 reflexões obtidas em diferentes quadrantes da Esfera de Ewald e refinadas pelo método dos mínimos quadrados ao final da coleta de dados das intensidades.[70]

As intensidades coletadas foram submetidas à redução (correções de polarização e de Lorentz) com o programa HELENA[71] e posteriormente avaliadas na sua totalidade para a identificação das condições de reflexão/extinção e determinação do grupo espacial, para a solução e refinamento das estruturas.

Para os compostos **10** e **12** foi utilizado um difratômetro automático com detector de área, SMART CCD (**C**harge **C**oupled **D**evice Detector – Bruker) e fonte de radiação Mo-Kα (λ = 0,71073 Å).[72] Já para os compostos **14** e **16** foi usado um difratômetro automático com detector de área IPDS – Bruker, utilizando Mo-Kα (λ = 0,71073 Å) como fonte de radiação.[73] (Ambos difratômetros da Freie Universität Berlin – Alemanha).

Finalmente, para os compostos **2**, **HL²**, **H₂L⁷**, **11**, **13** e **15** o difratômetro utilizado foi do tipo Bruker CCD X8 APEX II, dotado de um sistema de detecção por área, monocromador de grafite e fonte de radiação Mo-Kα (λ = 0,71073 Å).[74] (UFSM)

As estruturas foram solucionadas empregando-se métodos diretos através do programa SHELXS97.[75,76] O refinamento baseou-se nos quadrados dos fatores estruturais (F^2) e na técnica da matriz completa/mínimos quadrados.

Os átomos não hidrogenóides foram localizados através de sucessivas diferenças de Fourier e refinados com parâmetros anisotrópicos. Os átomos de

hidrogênio foram refinados isotropicamente na forma de grupos vinculados geometricamente aos respectivos átomos não hidrogenóides. Os dados de refinamento foram obtidos com o emprego do programa SHELXL97.[77] Outros programas complementares foram utilizados para facilitar o desempenho da rotina dos referidos cálculos.[78] As projeções gráficas foram executadas utilizando-se os programas ORTEP-3[78] e DIAMOND[79].

As Tabelas 5.1, 5.2, 5.3, 5.4, 5.5 e 5.6 reúnem as informações da coleta de dados e refinamento das estruturas cristalinas dos compostos cristalinos obtidos.

Tabela 5.1. Dados da coleta de intensidades e do refinamento das estruturas cristalinas dos compostos **HL^2**, [UO$_2$(L^1)$_2$] **(1)** e [UO$_2$(L^2)(dmf)$_2$](NO$_3$) **(2)**.

Composto	HL^2	1	2
Fórmula molecular	C$_{14}$H$_{14}$N$_4$O	C$_{28}$H$_{24}$N$_6$O$_4$U	C$_{20}$H$_{27}$N$_7$O$_8$U
Massa molecular (g mol^{-1})	254,29	746,56	731,52
Sistema cristalino	Ortorrômbico	Ortorrômbico	Monoclínico
Grupo espacial	*Pbca* (N° 61)	*Pbcn* (N° 60)	*C2/c* (N° 15)
Parâmetros de cela			
a (Å)	11,4752(19)	14,641(2)	26,2373(13)
b (Å)	14,766(3)	7,834(1)	7,9459(4)
c (Å)	15,177(3)	23,163(3)	25,4549(12)
α (°)	90	90	90
β (°)	90	90	107,507(3)
γ (°)	90	90	90
V (Å^3)	2571,6(8)	2656,7(6)	5061,0(4)
Z	8	4	8
Coeficiente linear de absorção μ (mm^{-1})	0,087	6,156	6,472
Região de varredura angular θ (°)	3,55 – 29,47	3,08 – 28,97	1,63 – 30,10
Índices de varredura *h, k, l*	-8 ≤ *h* ≤ 15 -20 ≤ *k* ≤ 13 -21 ≤ *l* ≤ 19	-19 ≤ *h* ≤ 0 -10 ≤ *k* ≤ 1 -31 ≤ *l* ≤ 31	-36 ≤ *h* ≤ 34 -10 ≤ *k* ≤ 11 -35 ≤ *l* ≤ 35
Número de reflexões: Coletadas Independentes Observadas	 12645 3562 1599	 7990 3517 1791	 31092 7429 5582
Critério de observação	[*I* >2σ(*I*)]	[*I* >2σ(*I*)]	[*I* >2σ(*I*)]
Número de parâmetros	169	178	325
Correção de absorção	Multi-scan (SADABS) T$_{min}$=0,790382 T$_{max}$=1,00	Psi-scan T$_{min}$ =0,0495 T$_{max}$ =0,1047	Multi-scan (SADABS) T$_{min}$=0,595546 T$_{max}$=1,00
F(000)	1072	1432	2816
Goodness-of-fit (*F^2*)	0,994	0,966	0,854
Índices de discordância finais	R$_1$ = 0,0484 *w*R$_2$ = 0,1073	R$_1$ = 0,0495 *w*R$_2$ = 0,1047	R$_1$ = 0,0295 *w*R$_2$ = 0,0776
Densidade eletrônica residual (e. Å^{-3})	0,135 [0,81 Å de O1] -0,144 [1,10 Å de C6]	2,64 [0,76 Å de O10] -3,45 [0,91 Å de U]	1,07 [0,37 Å de N4] -1,16 [0,91 Å de U1]
Depósito N°	CCDC 606778	CCDC 229651	CCDC 609303

Tabela 5.2. Dados da coleta de intensidades e do refinamento das estruturas cristalinas dos complexos [UO$_2$(L^3)(dmso)] **(3)**, [UO$_2$(L^4)(dmso)] **(4)**, [UO$_2$(L^5)][UO$_2$(L^5)(dmso)]·dmso·H$_2$O **(5)** e [UO$_2$(L^6)] **(6)**.

Composto	3	4	5	6
Fórmula molecular	C$_{25}$H$_{27}$N$_7$O$_5$SU	C$_{25}$H$_{25}$N$_5$O$_7$SU	C$_{50}$H$_{54}$N$_{14}$O$_{11}$S$_2$U$_2$	C$_{23}$H$_{20}$N$_6$O$_4$U
Massa molecular (g mol^{-1})	775,63	777,60	1567,25	682,48
Sistema cristalino	Ortorrômbico	Ortorrômbico	Triclínico	Monoclínico
Grupo espacial	*Pnma* (N° 62)	*Pnma* (N° 62)	*P$\bar{1}$* (N° 2)	*P2$_1$/n* (N° 14)
Parâmetros de cela				
a (Å)	18,304(1)	17,979(2)	8,284(1)	8,141(2)
b (Å)	17,535(5)	17,716(1)	15,283(2)	10,985(2)
c (Å)	8,288(2)	8,300(1)	23,700(3)	29,120(2)
α (°)	90	90	75,52(1)	90
β (°)	90	90	88,92(1)	93,71(9)
γ (°)	90	90	78,30(1)	90
V (Å^3)	2660,3(9)	2642(5)	2843,1(7)	2598,7(8)
Z	4	4	2	4
Coeficiente linear de absorção μ (mm^{-1})	6,230	6,276	5,832	6,284
Região de varredura angular θ (°)	3,22 – 26,96	3,22 – 25,00	3,01 – 27,01	3,16 – 18,50
Índices de varredura *h, k, l*	-23 ≤ *h* ≤ 0 0 ≤ *k* ≤ 22 -1 ≤ *l* ≤ 10	-1 ≤ *h* ≤ 9 0 ≤ *k* ≤ 20 0 ≤ *l* ≤ 21	-1 ≤ *h* ≤ 10 -19 ≤ *k* ≤ 19 -30 ≤ *l* ≤ 30	-1 ≤ *h* ≤ 7 0 ≤ *k* ≤ 9 -25 ≤ *l* ≤ 25
Número de reflexões: Coletadas Independentes Observadas	3411 2993 2052	3148 2970 1789	14998 12389 7724	3849 3048 1447
Critério de observação	[*I* >2σ(*I*)]	[*I* >2σ(*I*)]	[*I* >2σ(*I*)]	[*I* >2σ(*I*)]
Número de parâmetros	172	197	716	307
Correção de absorção	DELABS T$_{min}$=0,331 T$_{max}$=0,759	Psi-scans T$_{min}$=0,7583 T$_{max}$=0,9750	Psi-scans T$_{min}$=0,7094 T$_{max}$=0,9783	DELABS T$_{min}$=0,230 T$_{max}$=0,391
F(000)	1496	1496	1512	1296
Goodness-of-fit (*F^2*)	1,046	0,973	0,997	1,034
Índices de discordância finais	R$_1$ = 0,0485 *w*R$_2$ = 0,1129	R$_1$ = 0,0626 *w*R$_2$ = 0,0906	R$_1$ = 0,0459 *w*R$_2$ = 0,0922	R$_1$ = 0,0677 *w*R$_2$ = 0,1535
Densidade eletrônica residual (e. Å^{-3})	2,74 [0,29 Å de H6] -0,89 [0,52 Å de C14]	0,73 [0,26 Å de C12] -0,93 [0,69 Å de O12]	1,71 [1,07 Å de O60] -1,44 [0,97 Å de U2]	1,77 [1,10 Å de O10] -2,316 [1,06 Å de U]
Depósito Nº	-	CCDC 229650	CCDC 230959	CCDC 230960

Tabela 5.3. Dados da coleta de intensidades e do refinamento das estruturas cristalinas dos compostos **H_2L^7**, $(Et_3NH)_2[\{UO_2(L^7)\}_2(\mu\text{-}OMe)_2]\cdot 2H_2O$ **(7)**, $[UO_2(L^7)(H_2O)(py)]\cdot 2py$ **(8)** e $[UO_2(L^7)(dmso)_2]_2$ **(9)**.

Composto	H_2L^7	7	8	9
Fórmula molecular	$C_{15}H_{15}N_3O_2$	$C_{22}H_{34}N_4O_6U$	$C_{30}H_{30}N_6O_5U$	$C_{38}H_{50}N_6O_{12}S_4U_2$
Massa molecular (g mol^{-1})	269,30	688,56	792,63	1387,14
Sistema cristalino	Ortorrômbico	Monoclínico	Monoclínico	Monoclínico
Grupo espacial	$Pna2_1$ (N° 33)	$P2_1/n$ (N° 14)	$P2_1/n$ (N° 14)	$P2_1/n$ (N° 14)
Parâmetros de cela				
a (Å)	8,9022(1)	13,348(3)	15,45(2)	7,6152(9)
b (Å)	5,6764(6)	13,348(3)	12,10(2)	28,805(4)
c (Å)	26,360(3)	13,832(3)	16,58(4)	21,826(3)
α (°)	90	90	90	90
β (°)	90	91,58(2)	102,385(1)	93,254(1)
γ (°)	90	90	90	90
V (Å^3)	1332,1(3)	2463,6(1)	3027(1)	4780,0(1)
Z	4	4	4	4
Coeficiente linear de absorção μ (mm^{-1})	0,092	6,632	5,411	7,005
Região de varredura angular θ (°)	1,54 – 22,53	3,05 – 25,00	3,03 – 26,97	3,03 – 25,00
Índices de varredura h, k, l	$-9 \leq h \leq 5$ $-6 \leq k \leq 4$ $-25 \leq l \leq 28$	$-15 \leq h \leq 15$ $0 \leq k \leq 15$ $0 \leq l \leq 16$	$-1 \leq h \leq 19$ $-1 \leq k \leq 15$ $-21 \leq l \leq 20$	$-9 \leq h \leq 9$ $0 \leq k \leq 34$ $-1 \leq l \leq 25$
Número de reflexões: Coletadas Independentes Observadas	2497 1502 1119	4327 4327 2459	7994 6572 3565	9082 8381 4747
Critério de observação	$[I > 2\sigma(I)]$	$[I > 2\sigma(I)]$	$[I > 2\sigma(I)]$	$[I > 2\sigma(I)]$
Número de parâmetros	181	298	344	562
Correção de absorção	Multi-scan (SADABS) $T_{min}=0,9660$ $T_{max}=1,00$	DIFABS $T_{min}=0,2136$ $T_{max}=0,5152$	DIFABS $T_{min}=0,287$ $T_{max}=0,732$	Psi-scans $T_{min}=0,8833$ $T_{max}=0,9744$
F(000)	568	1336	1536	2656
Goodness-of-fit (F^2)	1,152	0,929	0,971	1,017
Índices de discordância finais	$R_1 = 0,0431$ $wR_2 = 0,1141$	$R_1 = 0,0588$ $wR_2 = 0,0988$	$R_1 = 0,0504$ $wR_2 = 0,0723$	$R_1 = 0,0596$ $wR_2 = 0,1094$
Densidade eletrônica residual (e. Å^{-3})	0,31 [1,511Å de H4] -0,31 [0,98 de C1]	1,12 [1,47 Å de U1] 1,02 [1,02 Å de U1]	0,90 [1,72 Å de O20] -1,27 [0,10 Å de U1]	3,23 [0,974 Å de U2] -1,30 [0,16 Å de S4]
Depósito Nº	CCDC 606779	-	-	-

Tabela 5.4. Dados da coleta de intensidades e do refinamento das estruturas cristalinas dos compostos $(Et_3NH)_2[\{UO_2(L^8)\}_2]$ **(10)** e $[\{UO_2(L^9)\}_2(\mu\text{-}OH_2)_2]\cdot 4dmf$ **(11)**.

Composto	10	11
Fórmula molecular	$C_{42}H_{54}N_6O_{10}U_2$	$C_{15}H_{25}N_5O_7U$
Massa molecular (g mol^{-1})	1278,97	625,43
Sistema cristalino	Ortorrômbico	Ortorrômbico
Grupo espacial	*Pbca* (N° 61)	*Pbca* (N° 61)
Parâmetros de cela		
a (Å)	19,413(4)	11,7025(2)
b (Å)	8,7519(2)	17,0883(3)
c (Å)	26,986(5)	21,5706(3)
α (°)	90	90
β (°)	90	90
γ (°)	90	90
V (Å^3)	4585(2)	4313,60(12)
Z	4	8
Coeficiente linear de absorção μ (mm^{-1})	7,115	7,569
Região de varredura angular θ (°)	1,84 – 30,57	1,89 – 30,11
Índices de varredura *h, k, l*	$-27 \leq h \leq 26$ $-12 \leq k \leq 12$ $-38 \leq l \leq 38$	$-16 \leq h \leq 14$ $-24 \leq k \leq 23$ $-30 \leq l \leq 30$
Número de reflexões: Coletadas Independentes Observadas	53696 7039 3708	92373 6341 5389
Critério de observação	$[I > 2\sigma(I)]$	$[I > 2\sigma(I)]$
Número de parâmetros	271	253
Correção de absorção	Multi-scan (SADABS) $T_{min}=0,3303$ $T_{max}=0,8352$	Multi-scan (SADABS) $T_{min}=0,559582$ $T_{max}=1,00$
F(000)	2448	2384
Goodness-of-fit (F^2)	0,817	1,223
Índices de discordância finais	$R_1 = 0,0376$ $wR_2 = 0,0820$	$R_1 = 0,0194$ $wR_2 = 0,0584$
Densidade eletrônica residual (e. Å^{-3})	1,27 [0,76 Å de O10] -1,80 [0,04 Å de U1]	0,66 [0,81 Å de H15B] -1,22 [0,03 Å de H3A]
Depósito N$^\circ$	CCDC 235134	-

Tabela 5.5. Dados da coleta de intensidades e do refinamento das estruturas cristalinas dos compostos $(Et_3NH)_3[\{UO_2(L^{10})\}_3]$ **(12)**, $(Et_3NH)_3[\{UO_2(L^{11})\}_3]$ **(13)**, $[UO_2(HL^{11})(dmso)_2]$ **(14)**.

Composto	12	13	14
Fórmula molecular	$C_{23}H_{29}N_3O_6U$	$C_{23}H_{30}N_4O_6U$	$C_{21}H_{27}N_3O_8S_2U$
Massa molecular (g mol^{-1})	681,52	696,54	751,61
Sistema cristalino	Trigonal	Trigonal	Triclínico
Grupo espacial	$P\text{-}3c_1$ (N° 165)	$P\text{-}3c_1$ (N° 165)	$P\bar{1}$ (N° 2)
Parâmetros de cela			
a (Å)	21,413(3)	21,4151(1)	7,5219(9)
b (Å)	21,413(3)	21,4151(1)	12,071(2)
c (Å)	23,615(5)	24,003(3)	14,279(2)
α (°)	90	90	86,631(1)
β (°)	90	90	82,235(1)
γ (°)	120	120	83,308(1)
V (Å^3)	9377(2)	9532,9(2)	1274,6(3)
Z	12	12	2
Coeficiente linear de absorção μ (mm^{-1})	5,226	5,143	6,581
Região de varredura angular θ (°)	1,10 – 26,37	1,10 – 25,57	2,88 – 21,50
Índices de varredura h, k, l	$-26 \le h \le 26$ $-26 \le k \le 26$ $-29 \le l \le 29$	$-23 \le h \le 19$ $-25 \le k \le 25$ $-28 \le l \le 29$	$-7 \le h \le 7$ $-12 \le k \le 12$ $-14 \le l \le 14$
Número de reflexões: Coletadas Independentes Observadas	82889 6403 4632	186334 5954 4847	5624 2876 2600
Critério de observação	$[I > 2\sigma(I)]$	$[I > 2\sigma(I)]$	$[I > 2\sigma(I)]$
Número de parâmetros	294	272	316
Correção de absorção	Multi-scan (SADABS) T_{min}=0,249906 T_{max}=0,374395	Multi-scan (SADABS) T_{min}=0,815339 T_{max}=1,00	Numérico T_{min}=0,2118 T_{max}=0,7349
F(000)	3936	4032	724
Goodness-of-fit (F^2)	0,977	1,068	1,085
Índices de discordância finais	R_1 = 0,0373 wR_2 = 0,1002	R_1 = 0,0541 wR_2 = 0,1535	R_1 = 0,0404 wR_2 = 0,0986
Densidade eletrônica residual (e. Å^{-3})	1,73 [0,93 Å de U1] -1,19 [2,74 Å de H6]	2,31 [0,07 Å de U1] -0,84 [1,24 Å de U1 Å]	0,07 [1,61 Å de H10C] -0,03 [0,80 Å de H51C]
Depósito Nº	-	-	-

Tabela 5.6. Dados da coleta de intensidades e do refinamento das estruturas cristalinas dos complexos [(UO$_2$)$_2$(L^{12})(dmf)$_4$] **(15)** e [{UO$_2$(L^{13A})(dmso)}$_4$] **(16)**.

Composto	**15**	**16**
Fórmula molecular	C$_{36}$H$_{46}$N$_8$O$_{12}$U$_2$	C$_{48}$H$_{56}$O$_{28}$S$_4$U$_4$
Massa molecular (g mol^{-1})	1258,87	2161,29
Sistema cristalino	Triclínico	Triclínico
Grupo espacial	$P\bar{1}$ (N° 2)	$P\bar{1}$ (N° 2)
Parâmetros de cela		
a (Å)	13,109(6)	13,978(5)
b (Å)	13,212(5)	15,306(5)
c (Å)	14,973(7)	22,965(5)
α (°)	79,874(2)	104,257(5)
β (°)	71,160(2)	102,777(5)
γ (°)	63,231(3)	104,097(5)
V (Å^3)	2189,88(2)	4407(2)
Z	2	2
Coeficiente linear de absorção μ (mm^{-1})	7,541	7,480
Região de varredura angular θ (°)	1,44 – 28,45	2,60 – 25,00
Índices de varredura h, k, l	-17 ≤ h ≤ 15 -17 ≤ k ≤ 17 -20 ≤ l ≤ 19	-16 ≤ h ≤ 16 -18 ≤ k ≤ 17 -27 ≤ l ≤ 27
Número de reflexões: Coletadas Independentes Observadas	42063 10995 7118	30561 15384 7120
Critério de observação	[I >2σ(I)]	[I >2σ(I)]
Número de parâmetros	523	757
Correção de absorção	Multi-scan (SADABS) T$_{min}$=0,67259 T$_{max}$=1,00	Numérico T$_{min}$=0,3127 T$_{max}$=0,6325
F(000)	1196	2000
Goodness-of-fit (F^2)	1,034	0,799
Índices de discordância finais	R$_1$ = 0,0343 wR$_2$ = 0,0810	R$_1$ = 0,0582 wR$_2$ = 0,1246
Densidade eletrônica residual (e. Å^{-3})	0,73 [1,26 Å de U2] -0,93 [0,87 Å de U2]	1,76 [1,21 Å de U3] -2,60 [1,00 Å de U3]
Depósito Nº	-	-

Tabela 5.7. Dados da coleta de intensidades e do refinamento das estruturas cristalinas dos compostos $(Et_3NH)[UO_2(L^{14})(OMe)]$ **(17)**, $[UO_2(L^{14})(dmso)]$ **(18)** e $(Et_3NH)_2[\{UO_2(L^{15})\}_3(\mu_3\text{-}O)]\cdot H_2O$ **(19)**.

Composto	17	18	19
Fórmula molecular	$C_{27}H_{41}N_3O_9U$	$C_{22}H_{28}N_2O_9SU$	$C_{51}H_{73}N_5O_{20}U_3$
Massa molecular (g mol^{-1})	789,66	734,55	1790,23
Sistema cristalino	Monoclínico	Triclínico	Monoclínico
Grupo espacial	$P2_1/c$ (N° 14)	$P\bar{1}$ (N° 2)	$P2_1/n$ (N° 14)
Parâmetros de cela			
a (Å)	11,524(7)	8,908(1)	19,754(4)
b (Å)	15,959(2)	11,337(2)	14,312(3)
c (Å)	17,061(2)	13,783(2)	22,241(4)
α (°)	90	110,39(1)	90
β (°)	94,84(1)	91,14(1)	107,12(1)
γ (°)	90	93,59(2)	90
V (Å^3)	3126(2)	1300,9(3)	6009(2)
Z	4	2	4
Coeficiente linear de absorção μ (mm^{-1})	1,678	6,370	8,139
Região de varredura angular θ (°)	3,10 – 26,93	3,07 – 26,99	1,21 – 30,62
Índices de varredura h, k, l	$-1 \leq h \leq 14$ $0 \leq k \leq 20$ $-21 \leq l \leq 21$	$-1 \leq h \leq 11$ $-14 \leq k \leq 14$ $-17 \leq l \leq 17$	$-25 \leq h \leq 28$ $-20 \leq k \leq 20$ $-29 \leq l \leq 31$
Número de reflexões: Coletadas Independentes Observadas	7777 6763 4787	6764 5653 3884	53009 12304 10701
Critério de observação	$[I > 2\sigma(I)]$	$[I > 2\sigma(I)]$	$[I > 2\sigma(I)]$
Número de parâmetros	362	316	712
Correção de absorção	Psi-scans $T_{min}=0,440$ $T_{max}=0,890$	DIFABS $T_{min}=0,322$ $T_{max}=0,753$	DELABS $T_{min}=0,235$ $T_{max}=0,672$
F(000)	1552	708	3392
Goodness-of-fit (F^2)	0,738	1,007	0,936
Índices de discordância finais	$R_1 = 0,0521$ $wR_2 = 0,0881$	$R_1 = 0,0484$ $wR_2 = 0,1122$	$R_1 = 0,0345$ $wR_2 = 0,0628$
Densidade eletrônica residual (e. Å^{-3})	4,55 [0,77 Å de U1] -2,64 [1,17 Å de H32C]	1,39 [1,05 Å de U1] -1,92 [1,00 Å de U1]	2,22 [0,81 Å de U1] -1,74 [0.85 Å de U3]
Depósito N°	CCDC 208434	CCDC 208435	CCDC 235135

5.1.2. Espectroscopia Vibracional de Infravermelho

A espectroscopia de infravermelho foi utilizada como um procedimento para a caracterização dos compostos com os seguintes objetivos:

✓ Realizar a caracterização dos pré-ligantes, de acordo com os modos vibracionais dos grupos funcionais existentes.

✓ Verificar a presença dos ligantes e do íon UO_2^{2+} nos complexos obtidos.

✓ Conhecer que átomos doadores de elétrons dos ligantes coordenam-se com o átomo de urânio na formação dos complexos, mediante a observação das modificações que se produzem na posição de algumas bandas de absorção, como conseqüência das interações doador-receptor e também pela observação do surgimento de novas bandas nos complexos.

Os espectros de absorção de infravermelho foram registrados na forma sólida em KBr (entre 2-3 mg do composto para cada 100 mg de KBr). A calibração dos aparelhos foi realizada mediante um filme de poliestireno de 0,05 mm, utilizando a absorção presente em 1601 cm^{-1}. Utilizou-se o seguinte aparelho:

- Espectrofotômetro Shimadzu FT-IR (Freie Universität Berlin) com uma janela espectral desde 4000 até 400 cm^{-1}.

A atribuição das bandas mais características dos pré-ligantes e seus complexos com urânio(VI) estão listadas nas tabelas de I.V. 5.8, 5.9, 5.10, 5.11 e 5.12.

Tabela 5.8. Freqüências de infravermelho mais significativas (cm^{-1}) para HL^1, [UO$_2$(L^1)$_2$] **(1)**, **HL^2** e [UO$_2$(L^2)(dmf)$_2$](NO$_3$) **(2)**.

	ν(NH)*	ν(CO)	ν(CN)+ν(CC)	ν(NN)	ν(UO$_2^{2+}$)
HL^1	3176F 3008F	1656MF 1612f	1575f 1541MF 1461m	979m	--
[UO$_2$(L^1)$_2$]	3421f 3060m	1591MF 1564f	1517MF 1469MF 1433MF	1033m 993f	910MF
HL^2	3436F 3332F 3278f	1651MF 1616MF	1585m 1562m 1512MF 1249MF	1030f	--
[UO$_2$(L^2)(dmf)$_2$](NO$_3$)	3400m 3355m 3263f	1685F 1616F	1562f 1508F 1469F 1427m 1373MF	1099m 1045m	910MF

* Pode estar associadas com OH e/ou H$_2$O
MF: muito forte,   F: forte,   m: média,   f: fraca

Tabela 5.9. Freqüências de infravermelho mais significativas (cm^{-1}) para H$_2$L^3, [UO$_2$(L^3)(dmso)] **(3)**, H$_2$L^4, [UO$_2$(L^4)(dmso)] **(4)**, H$_2$L^5, [UO$_2$(L^5)] [UO$_2$(L^5)(dmso)]·dmso·H$_2$O **(5)**, H$_2$L^6, [UO$_2$(L^6)] **(6)**.

	ν(NH)*	ν(CO)	ν(CN)+ν(CC)	ν(NN)	ν(UO$_2$$^{2+}$)
H$_2$L^3	3456m 3352F 3232f	1697m 1654MF 1616f	1581f 1527F 1454F 1357F	1080f	--
[UO$_2$(L^3)(dmso)]	3429F 3309f 3271f	1612m	1577f 1519F 1419f 1377MF	1026F	894F
H$_2$L^4	3209MF 3058MF 2929MF	1695F 1649MF	1602f 1550MF 1496f 1454MF	1089m 989f	--
[UO$_2$(L^4)(dmso)]	3053f 2993f	1650f	1591m 1539m 1488m 1450m 1377F	1031MF	914MF
H$_2$L^5	3379MF 3201MF 3091MF	1687MF	1598m 1533MF 1442MF	1097f 1031f	--
[UO$_2$(L^5)(dmso)]·dmso·H$_2$O	3409f 3246f 3074f 3006f	1602m	1571m 1540f 1492F 1409f 1334MF	1029F 952f	908MF
H$_2$L^6	3377F 3199F 3082m	1687MF 1656F	1589m 1533MF 1444MF 1365m	1083f 993f	--
[UO$_2$(L^6)]	3409m 3089f	1687f	1591f 1508MF 1434f 1407MF 1365MF	1151F 1107f 1029F	908MF

* Pode estar associadas com OH e/ou H$_2$O
MF: muito forte,   F: forte,   m: média,   f: fraca

Tabela 5.10. Freqüências de infravermelho mais significativas (cm^{-1}) para **H$_2$L^7**, (Et$_3$NH)$_2$[{UO$_2$(L^7)}$_2$(μ-OMe)$_2$]·2H$_2$O **(7)**, [UO$_2$(L^7)(H$_2$O)(py)]·2py **(8)**, [UO$_2$(L^7)(dmso)$_2$]$_2$ **(9)**, H$_3$L^8, (Et$_3$NH)$_2$[{UO$_2$(L^8)}$_2$] **(10)**, H$_2$L^9 e [{UO$_2$(L^9)}$_2$(μ-OH$_2$)$_2$]·4dmf **(11)**.

	ν(NH)*	ν(CO)	ν(CN)+ν(CC)	ν(NN)	ν(UO$_2^{2+}$)
H$_2$L^7	3475F 3363F 3209F 3028f	1627MF 1608f	1573m 1523m 1492f 1450m	1026F 975f	--
(Et$_3$NH)$_2$[{UO$_2$(L^7)}$_2$(μ-OMe)$_2$] ·2H$_2$O	3394F 3224f	1612m	1593f 1508F 1470m 1438m	1010F	887MF
UO$_2$(L^7)(H$_2$O)(py)]·2py	3406F 3274f	1616f	1593F 1542m 1504F 1438MF	1068m	898MF
[UO$_2$(L^7)(dmso)$_2$]$_2$	3463m 3386m 3263m	1612m	1573m 1539m 1512F 1473m 1434F	999MF	898MF
H$_3$L^8	3261f 3045MF	1622MF	1570f 1542m 1490m 1448m	1035m 977m	--
(Et$_3$NH)$_2$[{UO$_2$(L^8)}$_2$]	3444m 3053m	1587MF	1533m 1469f 1438F	1026F	893MF
H$_2$L^9	3506m 3429f 3159F 3055f	1705MF	1593MF 1473F 1438F	1037f	--
[{UO$_2$(L^9)}$_2$(μ-OH$_2$)$_2$]·4dmf	3294m 3116f	1654MF	1593m 1539F 1477m 1438m	1099F	894MF

* Pode estar associadas com OH e/ou H$_2$O
MF: muito forte,   F: forte,   m: média,   f: fraca

Tabela 5.11. Freqüências de infravermelho mais significativas (cm⁻¹) para H_3L^{10}, $(Et_3NH)_3[\{UO_2(L^{10})\}_3]$ **(12)**, H_3L^{11}, $(Et_3NH)_3[\{UO_2(L^{11})\}_3]$ **(13)**, $[UO_2(HL^{11})(dmso)_2]$ **(14)**, H_4L^{12}, $[(UO_2)_2(L^{14})(dmf)_4]$ **(15)**, H_2L^{15} e $[\{UO_2(L^{13A})(dmso)\}_4]$ **(16)**.

	ν(NH)*	ν(CO)	ν(CN)+ν(CC)	ν(NN)	ν(UO₂²⁺)
H_3L^{10}	3564f 3392m 3205m 3003f	1641MF	1581f 1523m 1485m 1433f 1363m	1053m 1024f	--
$(Et_3NH)_3[\{UO_2(L^{10})\}_3]$	3435m	1591MF	1556f 1523f 1483f 1363m	1053m	893MF
H_3L^{11}	3467F 3359MF	1658F 1612F	1585m 1558f 1520m 1485f 1434f	1049m 952m	--
$(Et_3NH)_3[\{UO_2(L^{11})\}_3]$	3406F	1650f 1620f	1581MF 1558f 1508m	1053m 956f	887F
$[UO_2(HL^{11})(dmso)_2]$	3429F 3263f	1640f 1612m	1542m 1512m 1477f 1419f	1002F 952F	894MF
H_4L^{12}	3444m 3296f 3205m 3006m	1647MF	1585f 1531f 1487m 1431f	1049m 952m	--
$[(UO_2)_2(L^{12})(dmf)_4]$	3421m	1654MF 1639f	1589F 1542F 1488m 1438f	1064m	898MF
H_2L^{13}	3409f 3278m 3178m	1635MF	1590f 1488F	1049m 952m	--
$[\{UO_2(L^{13A})(dmso)\}_4]$	3425m	1635f	1558MF	--	902F

* Pode estar associadas com OH e/ou H_2O
MF: muito forte,   F: forte,   m: média,   f: fraca

149

Tabela 5.12. Freqüências de infravermelho mais significativas (cm^{-1}) para H$_2$L^{14}, (Et$_3$NH)[UO$_2$(L^{14})(OMe)] **(17)**, [UO$_2$(L^{14})(dmso)] **(18)**, H$_2$L^{15} e (Et$_3$NH)$_2$[{UO$_2$(L^{15})}$_3$(μ$_3$-O)]·H$_2$O **(19)**.

	ν(NH)*	ν(CO)	ν(CN)+ν(CC)	ν(NN)	ν(UO$_2$$^{2+}$)
H$_2$L^{14}	3089f 2977F	1708MF 1635MF	1573f 1504f 1407F	--	--
(Et$_3$NH)[UO$_2$(L^{14})(OMe)]	2977m 2941f 2900f	1689MF	1571MF 1436MF 1392MF	--	896MF
[UO$_2$(L^{14})(dmso)]	3436m 2979f	1698MF	1569MF 1438F 1388F	--	906MF
H$_2$L^{15}	3186F 2977f	1703F 1670m 1625F	1552f 1467m 1409m	--	--
(Et$_3$NH)$_2$[{UO$_2$(L^{15})}$_3$(μ$_3$-O)]·H$_2$O	3554m 3134f 3058f 2981f	1679F	1587MF 1481f 1444F 1388F	--	896MF

* Pode estar associadas com OH e/ou H$_2$O
MF: muito forte,   F: forte,   m: média,   f: fraca

5.1.3. Espectroscopia de Ressonância Magnética Nuclear

Os espectros de RMN ^{1}H foram obtidos no aparelho Bruker DPX-400 (400 MHz), na Freie Universität Berlin. Os deslocamentos químicos (δ) são registrados em ppm, em relação ao tetrametilsilano (TMS, utilizado como padrão interno para os espectros).

Para os espectros de ^{1}H, as atribuições são relatadas da seguinte maneira: primeiro o valor numérico do sinal e após, entre parênteses, a multiplicidade, o número de hidrogênios deduzidos da integral relativa, e finalmente o hidrogênio ou ao conjunto de átomos de hidrogênio que foi atribuído o sinal. As abreviaturas utilizadas para indicar as multiplicidades são: s – singleto, d – dubleto, t – tripleto, q – quarteto e m – multipleto.[80]

Os espectros de RMN de próton foram realizados com o seguinte objetivo:

- ✓ Caracterizar os pré-ligantes e seus correspondentes complexos.

- ✓ Observar os deslocamentos dos sinais para analisar a possibilidade de coordenação.

- ✓ Conhecer a forma em que se encontram os pré-ligantes e seus complexos, como por exemplo, se estão protonados ou desprotonados.

Entretanto, não foi realizada uma discussão detalhada dos espectros de ressonância magnética nuclear de próton devido à baixa solubilidade dos compostos e a necessidade de utilizar um solvente coordenante (DMSO-d_6) para dissolver as amostras.

Os complexos ao serem tratados com solventes diferenciados, demonstraram modificações estruturais em comparação as suas respectivas estruturas no estado sólido. Podem ser citados como exemplos, o composto **8** que é gerado a partir do composto **7** na presença de piridina, e o composto **14**, que foi obtido da dissolução de **13**, em dimetilsulfóxido, tornando assim, muito difícil a correta identificação dos sinais de ^{1}H.

Outro fator que deve ser levado em consideração é a ausência de detalhes mais conclusivos nos espectros de RMN de ^{1}H, no qual são observadas apenas pequenas variações entre os espectros dos pré-ligantes e dos complexos.

Comparando-se o espectro de RMN de próton para o composto HL[1], δ (ppm): CH_3 2,46 (s, 3H); CH - aromático 7,42-8,91 (m, 9H); NH 10,87 (s, 1H) com o espectro de RMN de próton para o complexo **1**, δ (ppm): CH_3 2,75 (s, 3H); CH - aromático 6,76-8,36 (m, 9H); não se obtém uma contribuição significativa que justifique a discussão de cada espectro individualmente, aonde o maior diferencial entre eles é apenas a desprotonação do ligante na formação do complexo.

Os deslocamentos químicos nos espectros de RMN ^{1}H dos pré-ligantes e seus correspondentes complexos, nos quais foi possível uma melhor identificação, estão citados juntamente com as descrições das sínteses.

5.1.4. Reagentes, Solventes e Informações Gerais

O derivado de urânio $UO_2(NO_3)_2 \cdot 6H_2O$ foi adquirido comercialmente através da Merck e os reagentes de partida para a obtenção dos pré-ligantes foram adquiridos da Sigma-Aldrich e Acros Organics.

Os solventes utilizados foram adquiridos da Merck e Vetec. Não houve a necessidade da utilização de solventes secos, haja vista que nas reações de obtenção dos pré-ligantes utiliza-se água como solvente no meio reacional, e nas reações de obtenção dos complexos, o próprio derivado de urânio encontra-se hidratado e a presença de moléculas de água, em alguns casos, facilita a cristalização dos produtos atuando como solvente de cristalização ou coordenando-se ao átomo de urânio.

O urânio é um metal tóxico, sendo os isótopos ^{235}U e ^{238}U radioativos. É necessário que o manuseio deste metal seja efetuado em um laboratório, que apresente condições mínimas de segurança para o trabalho com materiais radioativos, como por exemplo, a presença de detectores de radioatividade.

Os resíduos radioativos devem ser armazenados em recipientes fechados, até serem recolhidos por uma entidade competente que se responsabilize pelo descarte dos mesmos. No caso do Brasil, os resíduos radioativos são recolhidos pelo IPEN (Instituto de Pesquisas Energéticas e Nucleares), que é gerenciado pela CNEN (Comissão Nacional de Energia Nuclear).

Quando houve a necessidade de purificar os produtos obtidos realizaram-se recristalizações.

5.2 SÍNTESE DOS PRÉ-LIGANTES

Os pré-ligantes foram sintetizados por reações de condensação, no qual um aldeído ou cetona reage com hidrazidas ou semicarbazidas para formar hidrazonas e semicarbazonas, denominadas também de bases de Schiff, com a eliminação de uma molécula de água, como demonstrado na reação baixo.[81]
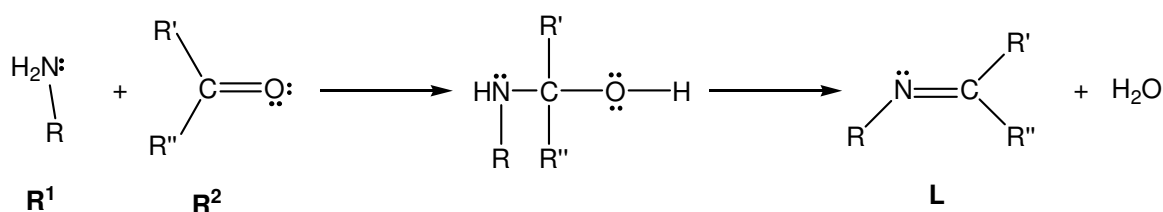
Para:

L = HL^1 ⟹ R^1 = benzoil-hidrazida e R^2 = 2-acetilpiridina

L = HL^2 ⟹ R^1 = 2-aminobenzoil-hidrazida e R^2 = 2-acetilpiridina

L = H$_2$L^3 ⟹ R^1 = 2-aminobenzoil-hidrazida e R^2 = 2,6-diacetilpiridina

L = H$_2$L^4 ⟹ R^1 = salicil-hidrazida e R^2 = 2,6-diacetilpiridina

L = H$_2$L^5 ⟹ R^1 = 4-fenilsemicarbazida e R^2 = 2,6-diacetilpiridina

L = H$_2$L^6 ⟹ R^1 = 4-fenilsemicarbazida, benzoil-hidrazida e R^2 = 2,6-diacetilpiridina

L = H$_2$L^7 ⟹ R^1 = 2-aminobenzoil-hidrazida e R^2 = 2-hidroxiacetofenona

L = H$_3$L^8 ⟹ R^1 = salicil-hidrazida e R^2 = 2-hidroxiacetofenona

L = H$_2$L^9 ⟹ R^1 = semicarbazida e R^2 = 2-hidroxiacetofenona

L = H$_3$L^{10} ⟹ R^1 = benzoil-hidrazida e R^2 = 4,6-diacetilresorcinol

L = H$_3$L^{11} ⟹ R^1 = 2-aminobenzoil-hidrazida e R^2 = 4,6-diacetilresorcinol

L = H$_4$L^{12} ⟹ R^1 = benzoil-hidrazida e R^2 = 4,6-diacetilresorcinol

L = H$_3$L^{13} ⟹ R^1 = tiossemicarbazida e R^2 = 4,6-diacetilresorcinol

### 5.2.1. Síntese do composto 2-acetilpiridina-benzoil-hidrazona (HL^1)

2-Acetilpiridina (0,34 mL, 3 mmol) foi adicionada a um balão contendo uma solução de benzoil-hidrazida (408 mg, 3 mmol), dissolvidos em 10 mL de H$_2$O e 10 mL de EtOH. Deixou-se a mistura reacional sob refluxo por 3h. Obteve-se um precipitado amarelado, que foi filtrado. Rendimento: 645 mg, 90%.
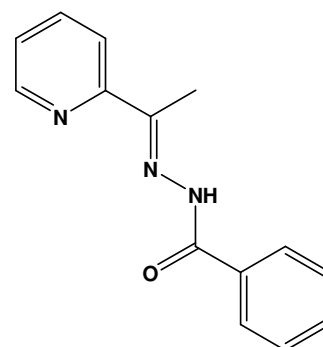
Análise elementar, valores encontrados: C 70,33; H 5,42; N 17,47% e valores calculados para C$_{14}$H$_{13}$N$_3$O$_1$: C 70,28; H 5,48; N 17,56%. ^{1}H NMR (400 MHz, dmso-d$_6$): δ (ppm): CH$_3$ 2,46 (s, 3H); CH - aromático 7,42-8,91 (m, 9H); NH 10,87 (s, 1H). I.V. (ν_{max}/cm^{-1}): 3176 e 3008 (N-H), 1656,7 (C=O), 1541 (C=N).

5.2.2. Síntese do composto 2-acetilpiridina-aminobenzoil-hidrazona (HL^2)

Adicionou-se 2-acetilpiridina (0,34 mL, 3 mmol) a um balão contendo 2-aminobenzoil-hidrazida (453 mg, 3 mmol), com 15 mL de isopromanol e 5 mL de H$_2$O. Deixou-se a solução sob refluxo por 4h, obtendo-se uma solução amarela. Com a evaporação lenta do solvente, obtiveram-se cristais amarelos que foram analisados por difração de raios X. Rendimento: 708 mg, 93%.
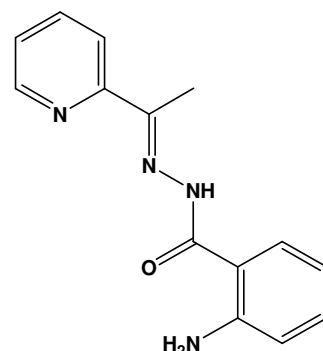
Análise elementar, valores encontrados: C 66,05; H 5,68; N 22,37% e valores calculados para C$_{14}$H$_{14}$N$_4$O: C 66,13; H 5,55; N 22,03%. ^{1}H NMR (400 MHz, dmso-d$_6$): δ (ppm): CH$_3$ 2,45 (s, 3H); CH - aromático 6,27-8,64 (m, 8H); NH 10,67 (s, 1H). I.V. (ν_{max}/cm^{-1}): 3436 e 3332 (N-H), 1651 e 1616 (C=O), 1512 (C=N).

### 5.2.3. Síntese do composto 2,6-diacetilpiridina-bis(aminobenzoil-hidrazona) (H₂L³)

Dissolveu-se em um balão 2,6-diacetilpiridina (245 mg, 1,5 mmol), em 10 mL de EtOH e 10 mL de H₂O. Adicionou-se à essa solução 2-aminobenzoil-hidrazida (453 mg, 3 mmol) e deixou-se a mistura sob refluxo por 3h. Obteve-se um precipitado amarelo, que foi filtrado. Rendimento: 650 mg, 85%.
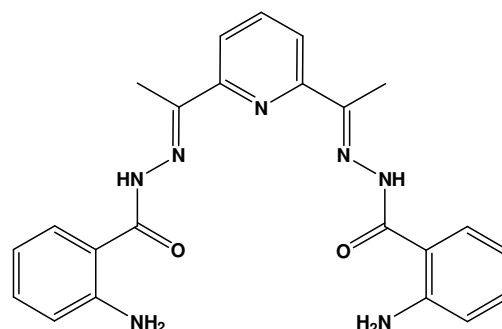
Análise elementar, valores encontrados: C 64,02; H 5,34; N 22,82% e valores calculados para $C_{23}H_{23}N_7O_2$: C 64,32; H 5,40; N 22,83%. ^{1}H NMR (400 MHz, dmso-d_6): δ (ppm): CH_3 2,70 (s, 6H); CH - aromático 6,24-8,31 (m, 11H); NH 10,63 (s, 2H); NH_2 10,71 (s, 4H). I.V. (ν_{max}/cm^{-1}): 3352 (N-H), 1697 e 1654 (C=O), 1581 e 1527 (C=N).

5.2.4. Síntese do composto 2,6-diacetilpiridina-bis(salicil-hidrazona) (H₂L⁴)

Dissolveu-se em um balão 2,6-diacetilpiridina (245 mg, 1,5 mmol), em 10 mL de EtOH e 10 mL de H₂O. Adicionou-se a essa solução salicil-hidrazida (456 mg, 3 mmol) e deixou-se a mistura sob refluxo por 3h. Obteve-se um precipitado amarelo pálido, que foi filtrado. Rendimento: 537 mg, 83%.
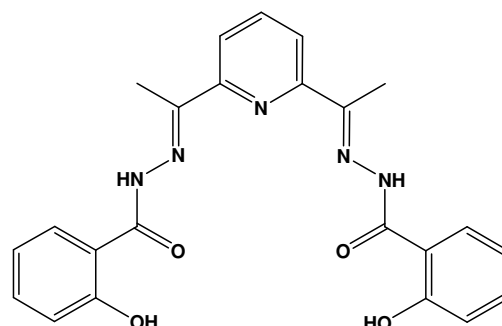
Análise elementar, valores encontrados: C 64,07; H 4,94; N 16,47% e valores calculados para $C_{23}H_{21}N_5O_4$: C 64,03; H 4,91; N 16,23%. ^{1}H NMR (400 MHz, dmso-d_6): δ (ppm): CH_3 2,68 (s, 6H); CH - aromático 6,99-8,15 (m, 11H); NH 11,49 (s, 2H). I.V. (ν_{max}/cm^{-1}): 3209 e 3058 (OH, NH), 1695 e 1649 (C=O), 1550 (C=N).

5.2.5. Síntese do composto 2,6-diacetilpiridina-bis(fenilsemicarbazona) (H$_2$L^5)

Em um balão dissolveu-se 2,6-diacetilpiridina (245 mg, 1,5 mmol), em 15 mL de isopropanol. Adicionou-se a essa solução 4-fenilsemicarbazida (471 mg, 3 mmol) e deixou-se a mistura sob refluxo por 3h. Obteve-se um precipitado amarelo pálido, que foi filtrado. Rendimento: 380 mg, 59%.

Análise elementar, valores encontrados: C 64,07; H 5,31; N 22,41% e valores calculados para C$_{23}$H$_{23}$N$_7$O$_2$: C 64,32; H 5,40; N 22,83%. ^{1}H NMR (400 MHz, dmso-d$_6$): δ (ppm): CH$_3$ 2,41 (s, 6H); CH - aromático 7,01–8,39 (m, 13H); NH 9,03 (s, 2H) e 9,95 (s, 2H). I.V. (ν$_{max}$/cm^{-1}): 3379 e 3201 (NH), 1687 (C=O), 1533 (C=N).
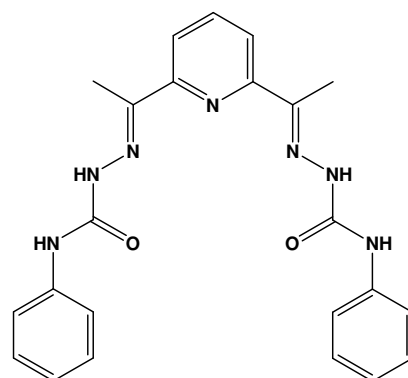
5.2.6. Síntese do composto 2,6-diacetilpiridina(fenilsemicarbazona)-benzoil-hidrazona (H$_2$L^6)

2,6-Diacetilpiridina (1,63 g, 10,0 mmol) foi dissolvida em 50 mL de uma mistura quente 1:1 de EtOH e H$_2$O. A solução de 4-fenilsemicarbazida (1,51 g, 10,0 mmol) em 75 mL de água, foi adicionada lentamente à mistura reacional. Deixou-se sob refluxo por 1h, obtendo-se um precipitado esbranquiçado **(HL^6)** que foi filtrado e lavado com MeOH. Rendimento: 2,75 g, 93%.

Análise elementar, valores encontrados: C 64,6; H 5,5; N 19,1% e valores encontrados para C$_{16}$H$_{16}$N$_4$O$_2$: C 64,9; H 5,4; N 18,9%. ^{1}H NMR (400 MHz, dmso-d$_6$): δ (ppm): CH$_3$ 2,20 (s, 3H), 2,67 (s, 3H); CH - aromático 7,03–8,65 (m, 8H); NH 9,01, 10,03 (s, 2H). I.V. (ν$_{max}$/cm^{-1}): 3375, 3194 (NH), 1697,1680 (C=O).
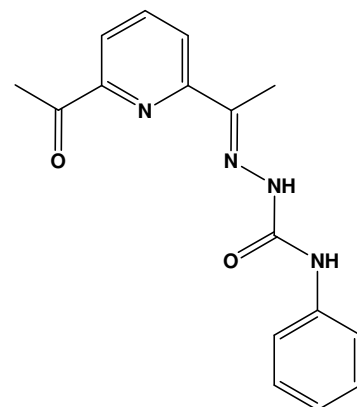
Deixou-se o ligante HL[6] (340 mg, 1,2 mmol) sob refluxo por 36h em um balão com benzoil-hidrazida (160 mg, 1,2 mmol) em 30 mL de isopropanol. A mistura reacional, ainda quente, foi filtrada e o precipitado amarelo pálido obtido foi lavado com 5 mL de MeOH. Rendimento: 330 mg, 66%.
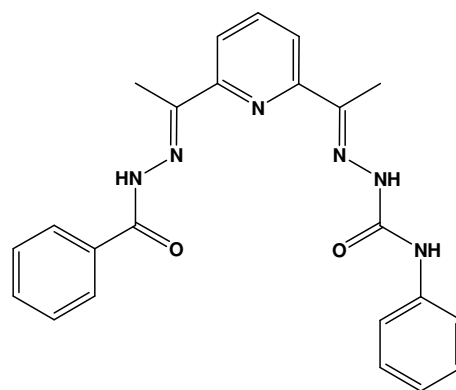
Análise elementar, valores encontrados: C 66,5; H 5,6; N 19,9% e valores encontrados para $C_{23}H_{22}N_6O_2$: C 66,7; H 5,4; N 20,3%. ^{1}H NMR (400 MHz, dmso-d6): δ (ppm): CH_3 2,41 (s, 3H,); 2,64 (s, 3H); CH - aromático 6,97–8,40 (m, 13H); NH 8,96 (s, 1H), 9,92 (s, 1H), 10,85 (s, 1H). I.V. (v_{max}/cm^{-1}): 3377 e 3199 (NH), 1687 e 1656 (C=O).

### 5.2.7. Síntese do composto 2-hidroxiacetofenona-aminobenzoil-hidrazona (H₂L⁷)

Em um balão dissolveu-se 2-aminobenzoil-hidrazida (302 mg, 2 mmol), em 15 mL de isopropanol e 5 mL de H_2O. Deixou-se sob refluxo e após 15 min e adicionou-se 2-hidroxiacetofenona (0,24 mL, 2 mmol), permanecendo a mistura reacional por mais 3h de refluxo. Obteve-se um precipitado microcristalino amarelo pálido e da solução mãe, com a evaporação lenta do solvente, obteve-se cristais incolores que foram analisados por difração de raios X. Rendimento: 392 mg, 73%.
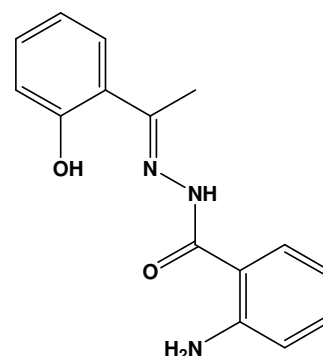
Análise elementar, valores encontrados: C 66,90; H 5,91; N 15,72% e valores calculados para $C_{15}H_{15}N_3O_2$: C 66,90; H 5,61; N 15,60%. ^{1}H NMR (400 MHz, dmso-d6): δ (ppm): CH_3 2,53 (s, 3H); OH 4,41 (s, 1H); CH - aromático 6,35–7,66 (m, 8H); NH 9,49 (s, 1H); NH_2 13,47 (s, 2H). I.V. (v_{max}/cm^{-1}): 3363 e 3209 (OH, NH), 1627 (C=O), 1573 (C=N).

### 5.2.8. Síntese do composto 2-hidroxiacetofenona-salicil-hidrazona (H₃L⁸)

Em um balão dissolveu-se salicil-hidrazida (304 mg, 2 mmol), em 10 mL de isopropanol e 5 mL de H_2O. Deixou-se sob refluxo e após 15 min. Adicionou-se 2-hidroxiacetofenona (0,24 mL, 2 mmol), ficando a reação por mais 3h sob refluxo. Obteve-se um sólido branco, que foi filtrado. Rendimento: 378 mg, 70%.
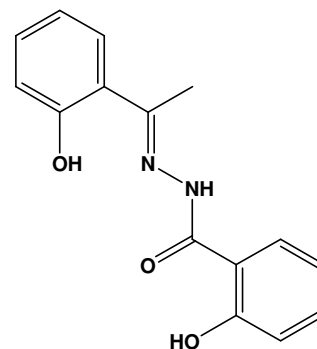
Análise elementar, valores encontrados: C 66,41; H 5,13; N 10,25% e valores calculados para $C_{15}H_{14}N_2O_3$: C 66,66; H 5,22; N 10,36%. ^1H NMR (400 MHz, dmso-d₆): δ (ppm): CH₃ 2,35 (s, 3H); CH - aromático 6,84–7,94 (m, 8H); NH 11,50 (s, 1H). I.V. (ν_{max}/cm^{-1}): 3261 e 3045 (OH, NH), 1622 (C=O), 1570 (C=N).

5.2.9. Síntese do composto 2-hidroxiacetofenona-semicarbazona (H₂L⁹)

Semicarbazida (557 mg, 5 mmol) foi dissolvida, em um balão com 15 mL de isopropanol e 5 mL de H_2O. Adicionou-se a esta solução 2-hidroxiacetofenona (0,603 mL, 5 mmol). A mistura reacional ficou sob refluxo por 3h, formando um sólido amarelo, que foi filtrado. Rendimento: 733 mg, 76%.
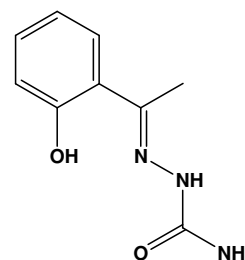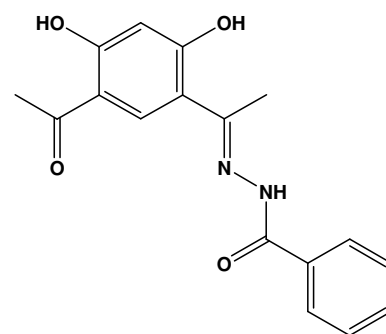
Análise elementar, valores encontrados: C 55,05; H 4,87; N 21.69% e valores calculados para $C_9H_{11}N_3O_2$: C 55,95; H 5,74; N 21.75%. ^1H NMR (400 MHz, dmso-d₆): δ (ppm): CH₃ 2,48 (s, 3H); OH 6,21 (s, 1H), CH - aromático 6,83–7,49 (m, 4H); NH 9,72 (s, 1H). I.V. (ν_{max}/cm^{-1}): 3506 e 3159 (OH, NH), 1705 (C=O), 1593 (C=N).

### 5.2.10. Síntese do composto 4,6-diacetilresorcinol(benzoil-hidrazona) (H₃L¹⁰)

Dissolveu-se em um balão benzoil-hidrazida (272 mg, 2 mmol), em 15 mL de EtOH e 5 mL de H₂O. Adicionou-se a esta solução 4,6-diacetilresorcinol (388 mg, 2 mmol) e deixou-se sob refluxo por 3h. Obteve-se um precipitado amarelo pálido, que foi filtrado. Rendimento: 487 mg, 78%.

Análise elementar, valores encontrados: C 65,53; H 4,89; N 9,047% e valores calculados para $C_{17}H_{16}N_2O_4$: C 65,38; H 5,16; N 8,97%. ^{1}H NMR (400 MHz, dmso-d_6): δ (ppm): CH₃ 2,34 (s, 3H), 2,39 (s, 3H); OH 6,21 (s, 2H); CH - aromático 7,37–8,57 (m, 7H); NH 12,47 (s, 1H). I.V. (v_{max}/cm^{-1}): 3392 e 3205 (OH, NH), 1641 (C=O), 1523 (C=N).

### 5.2.11. Síntese do composto 4,6-diacetilresorcinol(aminobenzoil-hidrazona) (H₃L¹¹)

Adicionou-se a um balão 2-aminobezoil-hidrazida (302 mg, 2 mmol) e dissolveu-se com 15 mL de EtOH e 5 mL de H₂O. A está solução adicionou-se 4,6-diacetilresorcinol (388 mg, 2 mmol) e deixou-se a mistura sob refluxo por 2:30h. Obteve-se um sólido amarelo. Rendimento: 530 mg, 81%.
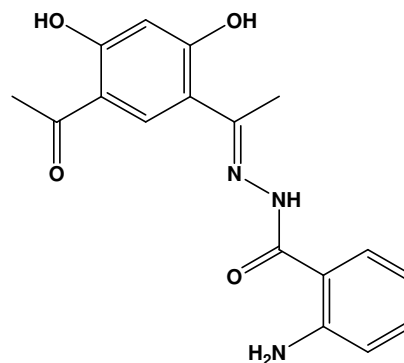
Análise elementar, valores encontrados: C 61,63; H 5,58; N 12,10% e valores calculados para $C_{17}H_{17}N_3O_4$: C 62,38; H 5,23; N 12,84%. ^{1}H NMR (400 MHz, dmso-d_6): δ (ppm): CH₃ 2,52 (s, 3H) 2,64 (s, 3H); OH 6,33 (s, 2H); CH - aromático 6,56–8,08 (m, 6H); NH 8,39 (s, 1H); NH₂ 12,61 (s, 2H). I.V. (v_{max}/cm^{-1}): 3467 e 3359 (OH, NH), 1658 e 1612 (C=O), 1585 (C=N).

5.2.12. Síntese do composto 4,6-diacetilresorcinol-bis(benzoil-hidrazona) (H₄L¹²)

Dissolveu-se ,4,6-diacetilresorcinol (194 mg, 1 mmol), em 10 mL de isopropanol. Separadamente, dissolveu-se benzoil-hidrazida (364 mg, 4 mmol) também em 10 mL de isopropanol. Juntaram-se as duas soluções em um balão e deixou-se sob refluxo por 5h, ocorrendo à formação de um sólido amarelo pálido que foi filtrado. Rendimento: 374 mg, 87%.
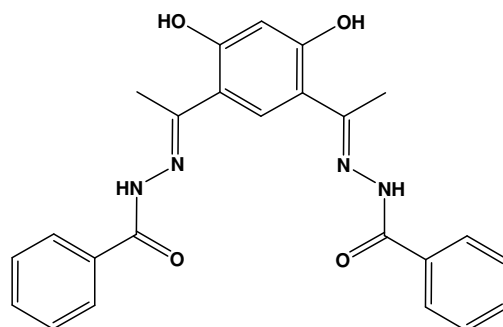
Análise elementar, valores encontrados: C 65,13; H 5,18; N 12,97% e valores calculados para $C_{24}H_{22}N_4O_4$: C 66,97; H 5,15; N 13,02%. ^{1}H NMR (400 MHz, dmso-d_6): δ (ppm): CH_3 2,53 (s, 6H); OH 6,35 (s, 2H); CH - aromático 7,43–8,10 (m, 12H); NH 11,38 (s, 1H), 12,61 (s, 1H). I.V. (ν_{max}/cm^{-1}): 3444 e 3205 (OH, NH), 1647 (C=O), 1585 (C=N).

5.2.13. Síntese do composto 4,6-diacetilresorcinol(tiossemicarbazona) (H₃L¹³)

Em um balão pesou-se tiossemicarbazida (182 mg, 2 mmol) e acrescentou-se 15 mL de EtOH e 5 mL de H_2O. Deixou-se sob refluxo até solubilização completa, adicionando-se posteriormente a esta solução 4,6-diacetilresorcinol (388 mg, 2 mmol). A mistura reacional permaneceu sob refluxo por 3h, ocorrendo à formação de um precipitado amarelo. Rendimento: 448 mg, 84%.
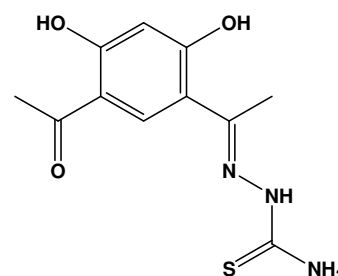
Análise elementar, valores encontrados: C 49,81; H 5,19; N 15,87; S 12,34% e valores calculados para $C_{11}H_{13}N_3O_3S$: C 49,43; H 4,90; N 15,72; S 11,99%. ^{1}H NMR (400 MHz, dmso-d_6): δ (ppm): CH_3 2,32 (s, 3H), 2,52 (s, 3H); OH 6,32 e 6,37 (s, 2H); CH - aromático 7,97–8,39 (s, 2H); NH 12,55 (s, 1H); NH_2 12,73 (s, 2H). I.V. (ν_{max}/cm^{-1}): 3425 (OH), 1635 (C=O), 1558 (C=N).

5.3 SÍNTESE DOS COMPLEXOS

5.3.1. Síntese do complexo [UO$_2$(L^1)$_2$], (1)

Foi dissolvido em um balão o pré-ligante HL^1 (53 mg, 0,22 mmol), e aproximadamente 5 mL de metanol e, posteriormente, adicionou-se uma solução de UO$_2$(NO$_3$)$_2$·6H$_2$O (50 mg, 0,1 mmol) em 5 mL de metanol. A mistura ficou sob refluxo por 1h. Durante este período a solução passa de uma cor amarela para vermelha. A adição de algumas gotas de Et$_3$N pode ser usada para a desprotonação mais rápida de HL^1, mas não influencia no produto final. Após mais uma hora de refluxo obteve-se a formação de uma pequena quantidade de sólido vermelho. Os cristais de coloração laranja foram obtidos diretamente da solução mãe. Rendimento: 59,5 mg, 80%.

Análise elementar, valores encontrados: C 45,2; H 3,3; N 11,6% e valores calculados para C$_{28}$H$_{24}$N$_6$O$_4$U: C 45,0; H 3,2; N 11,3%. ^{1}H NMR (400 MHz, dmso-d$_6$): δ (ppm): CH$_3$ 2,75 (s, 3H); CH - aromático 6,76-8,36 (m, 9H). I.V. (ν$_{max}$/cm^{-1}): 1591 (C=O), 1517, 1469 (C=N), 910 (O=U=O).

5.3.2. Síntese do composto [UO$_2$(L^2)(dmf)$_2$](NO$_3$), (2)

Dissolveu-se em um balão o pré-ligante HL^2 (50 mg, 0,2 mmol), em 5 mL de MeOH. A esta solução adicionou-se UO$_2$(NO$_3$)$_2$·6H$_2$O (100 mg, 0,2 mmol) dissolvido em 5 mL de metanol. À mistura reacional adicionou-se 2 gotas de Et$_3$N e deixou-se sob refluxo por 2h. A solução passa de uma coloração amarela para laranja, ocorrendo a formação de um sólido laranja que foi filtrado e recristalizado em 3 mL de dmf a quente. Com a evaporação do solvente observou-se a formação de cristais de coloração laranja. Rendimento: 94,7 mg, 65%.

Análise elementar, valores encontrados: C 32,62; H 3,48; N 13,83% e valores calculados para C$_{20}$H$_{27}$N$_7$O$_8$U: C 32,84; H 3,72; N 13,40%. ^{1}H NMR (400 MHz, dmso-d$_6$): δ (ppm): CH$_3$ 2,71 (s, 6H), 2,87 (s, 6H), 2,91 (s, 3H); CH 6,6 (s, 4H) CH - aromático 6,80-7,94 (m, 8H), NH$_2$ 8,40 (s, 2H). I.V. (ν$_{max}$/cm^{-1}): 1685 (C=O), 1508 (C=N), 910 (O=U=O).

5.3.3. Síntese do complexo [UO₂(L³)(dmso)], (3)

Dissolveu-se em um balão o pré-ligante H_2L^3 (86 mg, 0,2 mmol), em 10 mL de MeOH. A esta solução adicionou-se $UO_2(NO_3)_2 \cdot 6H_2O$ (100 mg, 0,2 mmol) dissolvido em 5 mL de metanol. À mistura reacional adicionou-se 2 gotas de Et_3N e deixou-se sob refluxo por 90 min, obtendo-se um precipitado laranja, que foi filtrado e recristalizado em 3 mL de dmso a quente. Rendimento: 120 mg, 78%.

Análise elementar, valores encontrados: C 38,78; H 3,47; N 12,58; S 4,65% e valores calculados para $C_{25}H_{27}N_7O_5SU$: C 38,71; H 3,51; N 12,64; S 4,13%. ¹H NMR (400 MHz, dmso-d_6): δ (ppm): CH_3 2,67 (s, 6H), CH - aromático 6,22-8,28 (m, 11H), NH_2 10,63 (s, 4H). I.V. (ν_{max}/cm^{-1}): 1612 (C=O), 1519 (C=N), 894 (O=U=O).

5.3.4. Síntese do complexo [UO₂(L⁴)(dmso)], (4)

$[UO_2(L_4)]$ foi obtido através da mistura de $UO_2(NO_3)_2 \cdot 6H_2O$ (50,2 mg, 0,1 mmol) e H_2L^4 (51,7 mg, 0,12 mmol), em 10 mL de metanol, em condições de refluxo. Inicialmente, obteve-se uma solução amarela. Após 15 min de refluxo, observou-se a formação de um precipitado amarelo. Deixou-se sob refluxo por mais 2h e posteriormente filtrou-se o precipitado formado. A reação ocorre mais rápido com a adição de 2 gotas de Et_3N. Neste caso, a precipitação do sólido é completada após 30 mim de refluxo. Rendimento: 629 mg, 90%.

Análise elementar, valores encontrados: C 39,2; H 2,7; N 10,3% e valores calculados para $C_{23}H_{19}N_5O_6U$: C 39,5; H 2,7; N 10,0%. I.V. (ν_{max}/cm^{-1}): 1650 (C=N), 914 (O=U=O).

O complexo $[UO_2(L_4)(dmso)]$ foi preparado através da recristalização do composto $[UO_2(L_4)]$ em 2-3 mL de dmso a quente. Cristais vermelhos são obtidos da evaporação lenta da difusão de água e dmso. Rendimento: 60%.

Análise elementar, valores encontrados: C 38,5; H 3,2; N 8,8; S 4,4% e valores calculados para $C_{25}H_{25}N_5O_7SU$: C 38,6; H 3,2; N 9,0; S 4,1%. ¹H NMR (400 MHz, dmso-d_6): δ (ppm): CH_3 1,15 (s, 3H), 3,0 (s, 3H), CH - aromático 7,06-8,61 (m, 11H), NH 11,52 (s, 1H), 12,93 (s, 1H). I.V. (ν_{max}/cm^{-1}): 3053 (OH), 1591 (C=N), 914,2 (O=U=O).

5.3.5. Síntese do composto [UO$_2$(L^5)][UO$_2$(L^5)(dmso)]·dmso·H$_2$O, (5)

O composto [UO$_2$(L^5)] foi preparado em um balão, com UO$_2$(NO$_3$)$_2$·6H$_2$O (502 mg, 1 mmol) e H$_2$L^5 (515 mg, 1,2 mmol) em 10 mL de metanol, sob refluxo por 2h, obtendo-se um sólido amarelo. Rendimento: 418 mg, 60%.

Análise elementar, valores encontrados: C 40,0; H 3,1; N 14,0% e valores encontrados para C$_{23}$H$_{21}$N$_7$O$_4$U: C 39,6; H 3,0; N 14,1. I.V. (ν_{max}/cm^{-1}): 1570 (C=N), 905 (O=U=O).

Quando o composto [UO$_2$(L^5)] (348 mg, 0,5 mmol) é dissolvido em aproximadamente 3 mL dmso a quente e são adicionadas sobre esta solução algumas gotas de água, ocorre a formação de cristais vermelhos que apresentam a seguinte composição, [UO$_2$(L^5)][UO$_2$(L^5)(dmso)](dmso)(H$_2$O). Rendimento: 176 mg, 45%.

Análise elementar, valores encontrados: C 41,2; H 3,3; N 9,7; S 4,5% e valores calculados para C$_{25}$H$_{25}$N$_5$O$_5$SU: C 41,2; H 3,4; N 9,6; S 4,4%. ^{1}H NMR (400 MHz, dmso-d$_6$): δ (ppm): CH$_3$ 2,80 (s, 3H), CH - aromático 6,95-8,37 (m, 7H), NH 9,70 (s, 1H). I.V. (ν_{max}/cm^{-1}): 1602 (C=O), 1571 (C=N), 908 (O=U=O).

5.3.6. Síntese do complexo [UO$_2$(L^6)], (6)

H$_2$L^6 (45,3 mg, 0,11 mmol) foi parcialmente dissolvido em 5 mL de metanol e adicionado a uma solução de UO$_2$(NO$_3$)$_2$·6H$_2$O (50,2 mg, 0,1 mmol) em 3 mL de metanol. A mistura tornou-se uma solução amarela com a agitação e refluxo e uma pequena quantidade de precipitado amarelo começou a se formar após 15 min de refluxo. Deixou-se sob refluxo por um tempo total de 2h. A mistura foi filtrada e obtiveram-se cristais amarelos para difração de raios X, direto da solução mãe. A reação pode tornar-se mais rápida com a adição de duas gotas de Et$_3$N, onde a precipitação do sólido é completa depois de 30 min. Rendimento: 27,3 mg, 40%.

Análise elementar, valores encontrados: C 40,1; H 3,4; N 11,7% e valores calculados para C$_{23}$H$_{20}$N$_6$O$_4$U: C 40,5; H 2,9; N 12,3%. ^{1}H NMR (400 MHz, dmso-d$_6$): δ (ppm): CH$_3$ 2,83 (s, 3H) e 3,06 (s, 3H), CH - aromático 7,00-8,53 (m, 13H), NH 9,78 (s, 1H). I.V. (ν_{max}/cm^{-1}): 1687 (C=O), 1591, 1508 (C=N), 908 (O=U=O).

5.3.7. Síntese do composto (Et₃NH)₂[{UO₂(L⁷)}₂(μ-OMe)₂]·2H₂O, (7)

O pré-ligante H_2L^7 (81 mg, 0,3 mmol) foi dissolvido em um balão, com 8 mL de MeOH. A esta solução adicionou-se $UO_2(NO_3)_2 \cdot 6H_2O$ (150 mg, 0,3 mmol), dissolvido em 5 mL de MeOH. Três gotas de Et_3N foram adicionadas à mistura reacional, que permaneceu sob refluxo por 2h. Obteve-se um sólido laranja avermelhado, que foi filtrado e da solução mãe após alguns dias, observou-se cristais de coloração laranja. Rendimento: 140 mg, 68%.

Análise elementar, valores encontrados: C 37,97; H 5,12; N 8,28% e valores calculados para $C_{44}H_{68}N_8O_{12}U_2$: C 38,38; H 4,98; N 8,14%. ^1H NMR (400 MHz, dmso-d_6): δ (ppm): CH_3 2,75 (s, 3H), 3,16 (s, 3H), H_2O 4,40 (s, 4H), CH - aromático 6,64-7,71 (m, 8H), NH 8,35 (s, 2H). I.V. (ν_{max}/cm⁻¹): 1612 (C=O), 1593, 1508 (C=N), 887 (O=U=O).

5.3.8. Síntese do composto [UO₂(L⁷)(H₂O)(py)]·2py, (8)

O composto **7** (138 mg, 0,1 mmol) foi dissolvido em 5 mL de piridina a quente. Com a diminuição da temperatura e evaporação do solvente observou-se a formação de cristais vermelhos bem formados. Rendimento: 48 mg, 60%.

Análise elementar, valores encontrados: C 45,23; H 4,53; N 10,44% e valores calculados para $C_{30}H_{30}N_6O_5U$: C 45,46; H 3,81; N 10,60%. ^1H NMR (400 MHz, dmso-d_6): δ (ppm): CH_3 2,75 (s, 3H); CH - aromático 6,66-8,56 (m, 23H). I.V. (ν_{max}/cm⁻¹): 1660 (C=O), 1593, 1508 (C=N), 898 (O=U=O).

5.3.9. Síntese do complexo [UO₂(L⁷)(dmso)₂]₂, (9)

Quando o composto **7** (138 mg, 0,1 mol) foi dissolvido em 3 mL de dmso a quente. Observa-se, com a diminuição da temperatura e evaporação do solvente, a formação de cristais vermelhos. Rendimento: 42 mg, 63%.

Análise elementar, valores encontrados: C 32,07; H 3,79; N 5,95; S 9,15% e valores calculados para $C_{19}H_{25}N_3O_6S_2U$: C 32,90; H 3,63; N 6,06; S 9,24%. ^1H NMR (400 MHz, dmso-d_6): δ (ppm): CH_3 2,75 (s, 3H), CH - aromático 6,66-7,71 (m, 8H). I.V. (ν_{max}/cm⁻¹): 16121 (C=O), 1573, 1512 (C=N), 898 (O=U=O).

5.3.10. Síntese do composto (Et$_3$NH)$_2$ [{UO$_2$(L^8)}$_2$], (10)

UO$_2$(NO$_3$)$_2$·6H$_2$O (50,2 mg, 0,1 mmol) foi dissolvido em 5 mL de metanol e adicionado a uma solução contendo o pré-ligante H$_3$L^8 (54 mg, 0,2 mmol) em 5 mL de metanol. Três gotas de Et$_3$N foram adicionadas à mistura e deixou-se sob refluxo por 2h. Obteve-se um precipitado laranja avermelhado, que foi filtrado e recristalizado em dmso a quente. Com a evaporação do solvente, obtiveram-se cristais vermelhos bem formados. Rendimento: 44,7 mg, 70%.

Análise elementar, valores encontrados: C 39,43; H 4,21; N 6,48%; valores calculados para C$_{42}$H$_{54}$N$_6$O$_{10}$U$_2$: C 39,42; H 4,26; N 6,57%. ^{1}H NMR (400 MHz, dmso-d$_6$): δ (ppm): CH$_3$ 2,71 (s, 3H), CH - aromático 6,49-8,32 (m, 8H). I.V. (v_{max}/cm^{-1}): 1587 (C=O), 1533 (C=N), 893 (O=U=O).

5.3.11. Síntese do composto [{UO$_2$(L^9)}$_2$(μ-OH$_2$)$_2$]·4dmf, (11)

Adicionou-se a um balão o pré-ligante H$_2$L^9 (58 mg, 0,3 mmol) e acrescentou-se 8 mL de MeOH. Separadamente, dissolveu-se em 5 mL de MeOH UO$_2$(NO$_3$)$_2$·6H$_2$O (150 mg, 0,3 mmol). Juntaram-se as duas soluções e adicionou-se 3 gotas de Et$_3$N. Deixou-se sob refluxo por 2h. Obteve-se um precipitado vermelho, que foi filtrado e recristalizado em dmf a quente. Cristais laranja foram obtidos da solução em dmf. Rendimento: 145 mg, 78%.

Análise elementar, valores encontrados: C 28,14; H 4,34; N 11,83% e valores calculados para C$_{30}$H$_{50}$N$_{10}$O$_{14}$U$_2$: C 28,81; H 4,03; N 11,20%. ^{1}H NMR (400 MHz, dmso-d$_6$): δ (ppm): CH$_3$ 2,58 (s, 3H), 2,71 (s, 6H), 2,87 (s, 3H), OH$_2$ 5,82 (s, 2H), CH - aromático 6,56-7,52 (m, 4H), NH$_2$ 7,94 (s, 2H). I.V. (v_{max}/cm^{-1}): 1654 (C=O), 1593, 1539 (C=N), 894 (O=U=O).

5.3.12. Síntese do composto (Et$_3$NH)$_3$[{UO$_2$(L^{10})}$_3$], (12)

O pré-ligante H$_3$L^{10} (31,2 mg, 0,1 mmol) foi parcialmente dissolvido em 5 mL de metanol e adicionado a uma solução de UO$_2$(NO$_3$)$_2$·6H$_2$O (50,2 mg, 0,1 mmol) em 5 mL de metanol. Algumas gotas de Et$_3$N foram adicionadas à mistura, que ficou sob refluxo por 2h. Obteve-se um precipitado vermelho microcristalino, que foi filtrado e recristalizado em uma mistura de 2-3 mL de MeOH/CH$_3$NO$_2$, obtendo-se assim cristais vermelhos bem formados, ideais para difração de raios X. Rendimento: 61,4 mg, 83%.

Análise elementar, valores encontrados: C 39,79; H 4,57; N 6,65% e valores calculados para $C_{69}H_{87}N_9O_{18}U_3$: C 40,53; H 4,29; N 6,17%. I.V. (ν_{max}/cm^{-1}): 1591 (C=O), 1556, 1523 (C=N), 893 (O=U=O).

5.3.13. Síntese do composto (Et₃NH)₃[{UO₂(L¹¹)}₃], (13)

O pré-ligante H_3L^{11} (65,4 mg, 0,2 mmol) foi dissolvido em 5 mL de metanol e adicionado a uma solução de $UO_2(NO_3)_2 \cdot 6H_2O$ (100,4 mg, 0,2 mmol) em 5 mL de metanol. Foram adicionadas também algumas gotas de Et₃N e a mistura reacional foi deixada sob refluxo por 2h, obtendo-se um sólido vermelho microcristalino. Cristais vermelhos foram obtidos após a recristalização do precipitado, em uma mistura, 2-3mL de MeOH/CH₃NO₂. Rendimento: 86,4 mg, 62%.

Análise elementar, valores encontrados: C 39,28; H 4,40; N 8,76% e valores calculados para $C_{69}H_{90}N_{12}O_{18}U_3$: C 39,66; H 4,34; N 8,04%. I.V. (ν_{max}/cm^{-1}): 1650 (C=O), 1581, 1558 (C=N), 887 (O=U=O).

5.3.14. Síntese do complexo [UO₂(HL¹¹)(dmso)₂], (14)

O composto [{UO₂(L¹¹)}₂](Et₃NH)₃ (42 mg, 0,02 mmol) foi dissolvido em aproximadamente 2 mL de dmso a quente e obteve-se cristais vermelhos, com a evaporação lenta do solvente. Rendimento: 27 mg, 60%.

Análise elementar, valores calculados: C 33,38; H 3,53; N 5,44; S 8,96% e valores calculados para: $C_{21}H_{27}N_3O_8S_2U$: C 33,56; H 3,62; N 5,59; S 8,53%. ^{1}H NMR (400 MHz, dmso-d₆): δ (ppm): CH₃ 2,63 (s, 3H), 2,84 (s, 3H); OH 6,49 (s, 2H); CH - aromático 6,65-8,35 (m, 6H); NH 12,82 (s, 2H). I.V. (ν_{max}/cm^{-1}): 1612 (C=O), 1542, 1512 (C=N), 894 (O=U=O).

5.3.15. Síntese do complexo [(UO₂)₂(L¹²)(dmf)₄], (15)

O pré-ligante H_4L^{12} (43 mg, 0,1 mmol) e o composto $UO_2(NO_3)_2 \cdot 6H_2O$ (100 mg, 0,2 mmol) foram colocados em um balão e dissolvidos em aproximadamente 8 mL de dmf. Adicionou-se uma gota de Et₃N a mistura reacional e deixou-se sob refluxo por 2h obtendo-se assim uma solução vermelha bem escura. Cristais pretos/vermelhos escuros foram obtidos diretamente da solução mãe após vários dias, com a evaporação lenta do solvente. Rendimento: 107 mg, 85%.

Análise elementar, valores encontrados: C 34,13; H 3,39; N 8,82% e calculados para $C_{36}H_{46}N_8O_{12}U_2$: C 34,35; H 3,68; N 8,90%. ^{1}H NMR (400 MHz, dmso-d_6): δ (ppm): CH_3 2,73 (s, 6H), 2,89 (s, 12H); CH 6,60 (s, 4H); CH - aromático 7,51-8,41 (m, 12H). I.V. (ν_{max}/cm $^{-1}$): 1654, 1639 (C=O), 1589, 1542 (C=N), 898 (O=U=O).

5.3.16. Síntese do complexo [{UO$_2$(L^{13A})(dmso)}$_4$], (16)

O pré-ligante H_2L^{13} (27 mg, 0,1 mmol) foi dissolvido em 3 mL de metanol e adicionado a uma solução de $UO_2(NO_3)_2 \cdot 6H_2O$ (50,2 mg, 0,1 mmol) em 5 mL de metanol. Algumas gotas de Et_3N foram adicionadas à mistura que ficou sob refluxo por 2h. Obteve-se um precipitado laranja que foi filtrado e recristalizado em dmso a quente, obtendo-se dessa forma cristais laranja, ideais para difração de raios X. Rendimento: 46 mg, 85%.

Análise elementar, valores encontrados: C 26,32; H 3,33; S 6,22% e valores calculados para $C_{48}H_{56}O_{28}S_4U_4$: C 26,67; H 2,61; S 5,93%. I.V. (ν_{max}/cm $^{-1}$): 1635 (C=O), 1558 (C=C), 902 (O=U=O).

5.3.17. Síntese do composto (Et$_3$NH)[UO$_2$(L^{14})(OMe)], (17)

$UO_2(NO_3)_2 \cdot 6H_2O$ (50,2 mg, 0,1 mmol) foi dissolvido em 5 mL de metanol e adicionado a um solução contendo o pré-ligante H_2L^{14} (38,8 mg, 0,1 mmol) com 15 mL de metanol e algumas gotas de Et_3N. Deixou-se sob refluxo e rapidamente a solução passa de uma coloração amarelada para vermelha e, após uma hora de refluxo um sólido vermelho se deposita no fundo do balão. Cristais vermelhos apropriados para a difração de raios X foram obtidos diretamente da solução mãe. Rendimento: 68,6 mg, 87%.

Análise elementar, valores encontrados: C 41,38; H 5,21; N 5,22% e valores calculados para $C_{27}H_{41}N_3O_9U$: C 41,07; H 5,23; N 5,32%. ^{1}H NMR (400 MHz, dmso-d_6): δ (ppm): CH_3 1,23 (t, 9H), 1,27 (t, 6H), 2,41 (s, 3H), 2,85 (s, 6H); CH 3,14 (s, 2H), CH_2 4,11-4,23 (q, 10H), CH - aromático 7,41-7,51 (d, 4H), NH 9,49 (s, 1H). I.V. (ν_{max}/cm $^{-1}$): 1689 (C=O), 1571, 1436 (C=N), 896 (O=U=O).

5.3.18. Síntese do complexo [UO$_2$(L^{14})(dmso)], (18)

Dissolveu-se o complexo **(17)** em 2-3 mL de dmso e obteve-se cristais vermelhos bem formados e ideais para difração de raios X, após alguns dias com a evaporação lenta do solvente. Rendimento: 80%.

Análise elementar, valores encontrados: C 35,99; H 3,80; N 3,75; S 4,84% e valores calculados para C$_{22}$H$_{28}$N$_2$O$_9$SU: C 35,97; H 3,84; N 3,81; S 4,36%. ^{1}H NMR (400 MHz, dmso-d$_6$): δ (ppm): CH$_3$ 1,21 (s, 3H), 2,81 (s, 3H); CH$_2$ 4,16 (s, 2H), CH - aromático 7,35-7,46 (d, 2H). I.V. (ν_{max}/cm^{-1}): 1698 (C=O), 1569, 1438 (C=N), 906 (O=U=O).

5.3.19. Síntese do composto (Et$_3$NH)$_2$[{UO$_2$(L^{15})}$_3$(μ$_3$-O)]·H$_2$O, (19)

UO$_2$(NO$_3$)$_2$·6H$_2$O (50,2 mg, 0,1 mmol) foi dissolvido em 5 mL de metanol e adicionado a um solução contendo o pré-ligante H$_2$L^{15} (47 mg, 0,2 mmol) com 5 mL de metanol. Três gotas de Et$_3$N foram adicionadas à mistura, que foi mantida sob refluxo por 2h. O volume resultante da solução vermelha obtida foi reduzido para aproximadamente 3 mL. Cristais vermelhos foram obtidos com a evaporação do solvente a temperatura ambiente. Rendimento: 36 mg, 60%.

Análise elementar, valores encontrados: C 34,2; H 4,0; N 3,8%; valores calculados para C$_{51}$H$_{73}$N$_5$O$_{20}$U$_3$: C 34,2; H 4,1; N 3,9%. ^{1}H NMR (400 MHz, dmso-d$_6$): δ (ppm): CH$_3$ 0,61 (t, 9H), 0,97 (t, 3H), 2,16 (s, 3H); CH$_2$ 3,87-3,88 (q, 8H), CH - aromático 6,28-6,97 (m, 4H), NH 9,14 (s, 1H). I.V. (ν_{max}/cm^{-1}): 1679 (C=O), 1587 (C=N), 896 (O=U=O).

CAPÍTULO 6:
CONCLUSÕES

Tendo em vista os objetivos propostos e considerando os resultados obtidos, levando-se em conta o conjunto de experimentos, os estudos realizados e a cristaloquímica de complexos de urânio(VI) com hidrazonas, semicarbazonas e ligantes relacionados, podem ser feitas as seguintes considerações finais:

I.   os compostos orgânicos, com diferentes estruturas e geometrias, utilizados neste trabalho, direcionaram a formação dos complexos de urânio(VI), demonstrando capacidade para formar monômeros, dímeros, trímeros e até tetrâmeros, o que indica a grande versatilidade desses ligantes na formação de sistemas polinucleares;

II. em todos os complexos obtidos, o átomo de urânio apresenta um poliedro de coordenação na forma de um bipirâmide pentagonal e/ou bipirâmide hexagonal;

III. todas as hidrazonas e semicarbazonas estudadas aqui neste trabalho foram desprotonadas, o que as torna nucleófilos fortes para reagir com centros deficientes de elétrons e formar assim complexos com o urânio(VI);

IV. as ligações de hidrogênio tiveram um papel importante na cristalização dos complexos de urânio, existindo ligações intra e intermoleculares entre as moléculas dos ligantes, moléculas de solventes e também através do grupo oxo da uranila. Observa-se que essas ligações não influenciaram na coordenação do átomo metálico;

V.   nas estruturas cristalinas de **HL^2** e **H$_2$L^7**, observa-se a presença de ligações de hidrogênio intra e intermoleculares. A existência dessas ligações permite considerar estes compostos como um agregado supramolecular constituído por cadeias contínuas;

VI. nos dímeros **7**, **10** e **11** e no trímero **19**, observa-se que as distâncias entre os átomos de urânio são maiores do que a soma dos raios de van der Waals, o que sugere que essas distâncias impossibilitam interações urânio-urânio;

VII. do ponto de vista estrutural, os complexos **12**, **13** e **16** possuem características próprias. Entre elas, destaca-se a existência de cavidades de forma e tamanhos definidos, que os tornam interessantes por seu potencial de aplicação em, por exemplo, transporte e armazenamento de espécies nanométricas;

VIII. realizou-se a caracterização estrutural de duas novas hidrazonas e dezenove novos complexos de urânio. Os índices de discordância verificados nas medidas de raios X apresentam baixos valores, indicando boa correlação entre as estruturas propostas e aquelas avaliadas experimentalmente.

Acredita-se que esta Tese de Doutorado tenha contribuído para um melhor entendimento da química de coordenação do urânio, bem como, do comportamento coordenativo de hidrazonas, semicarbazonas e ligantes relacionados, no qual a difração de raios X de monocristal foi uma ferramenta indispensável para a elucidação estrutural e estudo das interações presentes nas estruturas cristalinas dos compostos sintetizados.

CAPÍTULO 7: REFERÊNCIAS BIBLIOGRÁFICAS

CAPÍTULO 7: REFERÊNCIAS BIBLIOGRÁFICAS

1.Sessler, J.L.; Melfi, P.J.; Pantos, G.D. *Coord. Chem. Reviews* **2006**, *250*, 816.

2.Hayton, T.W.; Boncella, J.M.; Scott, B.L.; Palmer, P.D.; Batista, E.R.; Hay, P.J. *Science* **2005**, *310*, 1941.

3.Horn, J.D.V.; Huang, H. *Coord. Chem. Reviews* **2006**, *250*, 765.

4.Pacansky, J.; McLean, A. D. *J. Phys. Chem.* **1990**, *94*, 90.

5.Barreiro, E. J.; Fraga, C. A. M.; Miranda, L. P.; Rodrigues, C. R. *Química Nova* **2002**, *25*, 129.

6.Ainscough, E. W.; Brodie, A. M.; Dobbs, A. J.; Ranford, J. D.; Waters, J. M. *Inorg. Chim. Acta* **1998**, *267*, 27.

7.Patole, J.; Sandbhor, U.; Padhye, S.; Deobagkar, D.N.; Anson, C.E.; Powell, A. *Biorg. Med. Chem. Letters* **2003**, *13*, 51.

8.Tai, X.; Yin, X.; Liu, D.; Tan, M.; Yu, K. *Chem. Res. Chin. Univ.* **2003**, *19*, 434.

9.Thomas, J.E.; Palenik, R.C.; Palenik, G.J.; *Inorg. Chim. Acta* **1979**, *37*, L459.

10.Abram, U.; Gatto, C.C.; Bonfada, E.; Lang, E.S. *Inorg. Chem. Commun.* **2002**, *5*, 461.

11.Gatto, C.C. *Dissertação de Mestrado*, Universidade Federal de Santa Maria, Santa Maria – RS, **2002**.

12.Grewe, J.; Hagenbach, A.; Stromburg, B.; Alberto, R.; Lopez, E.V.; Abram, U. *Z. Anorg. Allg. Chem.* **2003**, *629*, 303.

13.Beraldo, H.; Gambino, D. *Mini Reviews in Medicinal Chemistry* **2004**, *4*, 159.

14.Beraldo, H. *Química Nova* **2004**, *27*, 461.

15.Casas, J.S.; García-Tasende, M.S.; Sordo, J. *Coord. Chem. Rev.* **2000**, *209*, 197.

16.La-Scalea, M.A.; Menezes, C.M.; Julião, M.S.S.; Chung, M.C.; Serrano, S.H.; Ferreira, E.I. *J. Braz. Chem. Soc.* **2005**, *16*, 774.

17.Patole, J.; Dutta, S.; Padhye, S.; Sinn, E. *Inorg. Chim. Acta* **2001**, *318*, 207.

18.Kasuga, N.C.; Sekino, K.; Ishikawa, M.; Honda, A.; Yokiyama, M.; Nakano, S.; Shimada, N.; Koumo, C.; Nomiya, K. *J. Inorg. Biochem.* **2003**, *96*, 298.

19.Carcelli, M.; Ianelli, S.; Pelagatti, P.; Pelizzi, G. *Inorg. Chim. Acta* **1999**, *292*, 121.

20.Jagst, A.; Sanchez, A.; Lopez, E.M.V.; Abram, U. *Inorg. Chem.* **2005**, *44*, 5738.

21.Jäger, E.G.; Häussler, E.; Rudolph, M.; Schneider, A. *Z. Anorg. Allg. Chem.* **1985**, *525*, 67.

22. Jäger, E.G.; Gräfe, F. *Z. Anorg. Allg. Chem.* **1988**, *561*, 25.

23. Müller, K.; Seidel, D.; Jäger, E.G. *Z. Anorg. Allg. Chem.* **1988**, *561*, 38.

24. Jäger, E.G.; Knaudt, J.; Rudolph, M.; Rost, M. *Chem. Ber.* **1996**, *129*, 1041.

25. Hess, D.; Elias, H.; Paulus, H. *Z. Anorg. Allg. Chem.* **1989**, *577*, 135.

26. Ellias, H.; Hess, D.; Paulus, H.; Jäger, E.G.; Gräfe, F. *Z. Anorg. Allg. Chem.* **1990**, *589*, 101.

27. Keutel, H.; Seidel, D.; Klussmann, M.; Görls, H. *Inorg. Chem.* **2000**, *39*, 1608.

28. Abram, U.; Abram, S.; Münze, R.; Jäger, E.G.; Stach, J.; Kirmse, R.; Admiraal, G.; Beurskens, P.T. *Inorg. Chim. Acta* **1991**, *182*, 233.

29. Abram, U.; Münze, R.; Jäger, E.G.; Stach, J.; Kirmse, R. *Inorg. Chim. Acta* **1989**, *162*, 171.

30. Bagnall, K.W. *Comprehensive Coordination Chemistry*, The Actinides, Wilkinson, G.; Gillard, R.D.; McCleverty, J.A., Pergamon Press Oxford, **1987**.

31. Miessler, G.L.; Tarr, D.A. *Inorganic Chemistry*, Editora Prentice-Hall do Brasil Ltda, Rio de Janeiro, RJ – Brasil, **1991**.

32. Russel, J.B. *Química Geral*, 2ª Edição, Editora Pearson Makron Books, São Paulo, SP – Brasil, **1994**.

33. Lee, J.D. *Química Inorgânica não tão Concisa*, 5ª Edição, Editora Edgard Blücher Ltda, São Paulo, SP – Brasil, **2003**.

34. Shiver, D.F.; Atkins, P.W. *Química Inorgânica*, 3ª Edição, Editora Bookman, Porto Alegre, RS – Brasil, **2003**.

35. Greenwood, N.N.; Earnshaw, A. *Chemistry of the Elements*, 2ª Edition, Pergamon Press, Oxford, **1997**.

36. Bandoli, G.; Clemente, D.A.; Marangoni, G.; Paolucci, G. *J. Chem. Soc. Chem. Comm.* **1978**, 235.

37. Paolucci, G.; Marangoni, G.; Bandoli, G.; Clemente, D.A. *J. Chem. Soc. Dalton Trans.* **1980**, 459.

38. Paolucci, G.; Marangoni, G.; Bandoli, G.; Clemente, D.A. *J. Chem. Soc. Dalton Trans.* **1980**, 1304.

39. Bino, A.; Frim, R.; Genderen, M.V. *Inorg. Chim. Acta* **1987**, *127*, 95.

40. Kyriakidis, C.E.; Christidis, P.C.; Rentzeperis, P.J.; Tossidis, I.A. *Z. Kristallogr.* **1992**, *200*, 15.

41. Gulbaev, Y.I.; Azizov, T.A.; Khudoyarov, A.B.; Sharipov, K.T. *Uzb. Khim. Sh.(Russ.)(Uzbek Chem. J.)* **1997**, 28-5.

42. Abram, U.; Lang, E.S.; Bonfada, E. *Z. Anorg. Allg. Chem.* **2002**, *628*, 1873.

43. Santos, I.G.; Abram, U. *Inorg. Chem. Commun.* **2004**, *7*, 400.

44. Cotton, F.A.; Marler, D.O.; Schwotzer, W. *Inorg. Chim. Acta* **1984**, *85*, L31.

45. Gatto, C.C.; Lang, E.S.; Kupfer, A.; Hagenbach, A.; Wille, D.; Abram, U. *Z. Anorg. Allg. Chem.* **2004**, *630*, 735.

46. Gatto, C.C.; Lang, E.S.; Burrow, R.A.; Abram, U. *J. Bras. Chem. Soc.* **2006** (artigo já aceito para publicação).

47. Hahn, T. *International Tables for Crystallography*, Vol. A Space-Group Symmetry, **1987**, 2nd Ed., The International Union of Crystallograpy, D. Reidel Publishing Company, Dordrecht, Holland.

48. Nakamoto, D. *Infrared and Raman Spectra of Inorganic and Coordination Compounds*, V.1 and V.2, 5th ed., New York, Joh Wiley & Sons, New York, NY – USA, **1997**.

49. Gatto, C.C.; Lang, E.S.; Jagst, A.; Abram, U. *Inorg. Chim. Acta* **2004**, *357*, 4405.

50. Bermejo, M.R.; Pedrido, R.; Noya, A.M.G.; Romero, M.J.; Vazquez, M.; Sorace, L. *New J. Chem. (Nouv. J. Chim.)* **2003**, *27*, 1753.

51. Harrowfield, J.M.; Kepert, D.L.; Patrick, J.M.; White, A.H.; Lincoln, S.F. *J. Chem. Soc. Dalton Trans.* **1983**, 393.

52. Dinda, R.; Sengupta, P.; Ghosh, S.; Figge, H.M.; Sheldrick, W.S. *J. Chem. Soc. Dalton Trans.* **2002**, 4434.

53. Ghosh, T.; Roy, A.; Bhattacharya, S.; Banerjee, S. *Transition Met. Chem.* **2005**, *30*, 419.

54. Kim, J.H.; Yoon, H.J.; Chae, W.K. *Bull. Korean Chem. Soc.* **2004**, *25*, 1448.

55. Kokila, M.K.; Puttaraja K.A.N.; Shamala, N. *Acta Cryst.* **1992**, *C48*, 1133

56. Drain, C.M.; Lehn, J.M. *J. Chem. Soc., Chem. Commun.* **1994**, 2313.

57. Krishnamohan; C.V.; Griffin; S.T.; Rogers; R.D. *Chem. Commun.* **1998**, 215.

58. Burkhart, D.J.; Vij, A.; Natale, N.R. *J. Chem. Cryst.* **1999**, *29*, 749.

59. Thuéry, P.; Villiers, C.; Jaud, J.; Ephritikhine, M.; Masci, B. *J. Am. Chem. Soc.* **2004**, *126*, 6838.

60. Hueso-Ureña, F.; Illán-Cabeza, N.A.; Moreno-Carreteto, M.N.; Peñas-Chamorro, A.L. *Transition Met. Chem.* **2001**, *26*, 160.

61. Sousa, G.F.; Deflon, V.M.; Ganbardella, M.T.P.; Francisco, R.H.P.; Ardisson, J.D.; Niquet, E. *Inorg. Chem.* **2006**, *45*, 4518.

62. Takano, A.; Ohba, M. *Mol. Cryst. Liq. Cryst. Sci. Technol., Sect. A* **1999**, *335*, 229.

63. Gatto, C.C.; Lang, E.S.; Abram, U. *Inorg. Chem. Comm.* **2003**, *6*, 1001.

64. Gatto, C.C.; Lang, E.S.; Kupfer, A.; Hagenbach, A.; Abram, U. *Z. Anorg. Allg. Chem.* **2004**, *630*, 1286.

65. Lintvedt, R.L.; Heeg, M.J.; Ahmad, N.; Glick, M.D. *Inorg. Chem.* **1982**, *21*, 2350.

66. Charpin, P.; Lance, M.; Nierlich, M.; Vigner, D.; Livet, J.; Musikas, C. *Acta Crystallogr.* **1986**, *C42*, 1691.

67. Bossche, G.; Spirlet, M.R.; Rebizant, J.; Goffart, J. *Acta Crystallogr.* **1987**, *C43*, 837.

68. Turpeinen, U.; Hamalainen, R.; Mutikainen, I.; Orama, O. *Acta Crystallogr.* **1996**, C52, 1169.

69. ENRAF-NONIUS CAD-4 EXPRESS. Version 5.1/1.2. Enraf-Nonius, Delft, The Netherlands, **1994**.

70. Enraf-Nonius, *CAD4-Express Software; Enraf-Nonius Inc.* **1992**, Delf, The Netherlands.

71. Spek, A. *PLATON and HELENA – Programs for Data Reduction e Handling of X-ray Structure Data* **1995**, University of Utrecht, the Netherlands.

72. Bruker, *SMART and SAINT* **1997**, Bruker AXS Inc., Madison, Wisconsis, EUA

73. STOE IPDS 2T - STOE X-AREA **2004**.

74. CCD Bruker – SMART, X8 APEX II (SADABS. SMART and SAINT, Brucker AXS Inc. Madison Wisconsin, **2005**).

75. Farrugia, L.J. *J.Appl. Cryst.* **1999**, 32, 837; *WinGX* – Version 1.70.01.

76. Sheldrick, G.M.; *SHELXS-97 - Program for Crystal Structure Solution*, University of Göttingen, Germany, **1997**.

77. Sheldrick, G.M.; *SHELXL-97 - Program for Crystal Structure Refinement*, University of Göttingen, Germany, **1997**.

78. Farrugia, L.J.; ORTEP-3 - Program for ellipsoid representation of crystal structures *J. Appl. Cryst.* **1997**, *30*, 565, Version 1.08.

79. Brandenburg, H., *DIAMOND; A program for the representation of crystal structures*, Bohn, Germany, **2006**.

80.Silverstein, R. M.; Webster, F.X. *Spectrometric Identification of Organic Compounds*, 6th edition, John Wiley & Sons, New York, NY – USA, **1998**.

81.Solomons, R.W.G.; Fryhle, C.B. *Química Orgânica v.2*, Tradução de Matos, R.M.; Revisão Técnica de Raslan, D.S.; Rio de Janeiro, LTC, **2006**.

ANEXO I:
ARTIGOS
PUBLICADOS

Este trabalho de Doutorado propiciou até o presente momento a publicação de cinco artigos científicos:

1. Gatto, C.C.; Lang, E.S.; Abram, U. *Inorganic Chemistry Comunnications* **2003**, 6, 1001-1003.

2. Gatto, C.C.; Lang, E.S.; Kupfer, A.; Hagenbach, A.; Wille, D.; Abram, U. *Zeitschrift für Anorganische und Allgemeine Chemie* **2004**, 630, 735-41.

3. Gatto, C.C.; Lang, E.S.; Kupfer, A.; Hagenbach, A.; Abram, U. *Zeitschrift für Anorganische und Allgemeine Chemie* **2004**, 630, 1286-1295.

4. Gatto, C.C.; Lang, E.S.; Jagst, A.; Abram, U. *Inorganica Chimica Acta* **2004**, 357, 4405-4412.

5. Gatto, C.C.; Lang, E.S.; Burrow, R.A.; Abram, U. *Journal of the Brazilian Chemical Society* **2006**.

INORGANIC CHEMISTRY COMMUNICATIONS

Dioxouranium complexes with 'Jaeger-type' ligands

Claudia C. Gatto [a], Ernesto Schulz Lang [a,1], Ulrich Abram [b,*]

[a] *Departamento de Quimica, Universidade Federal de Santa Maria, Santa Maria-RS 97111.970, Brazil*
[b] *Freie Universität Berlin, Institut für Chemie, Fabeckstr. 34-36, D-14195 Berlin, Germany*

Abstract

Azomethine ligands with electron-withdrawing groups such as bis{N,N'-(2-ethoxycarbonyl-3-oxo-but-1-en(1)yl)-1,2-diamino-benzene (H_2L^1) or N-(2-ethoxycarbonyl-3-oxo-but-1-en(1)yl)-2-aminophenol (H_2L^2) react with uranyl nitrate under deprotonation and formation of chelate complexes. The composition of the products can be controlled by the reaction conditions and the denticity of the ligands. Structure determinations have been performed on $[NEt_3H][UO_2(L^1)(OMe)]$, $[UO_2(L^1)(DMSO)]$ and $[NEt_3H]_2$ $[\{UO_2(L^2)\}_3(\mu_3\text{-}O)]$.
© 2003 Elsevier Science B.V. All rights reserved.

Keywords: Uranium; Jäger-type ligands; Actinides; Crystal structure

Azomethine ligands with ester or ether groups have been introduced and extensively studied by Jäger [1]. They form stable complexes with a large number of metal ions [2] and have been considered for their catalytic behaviour and used to mimic metal sides in enzymes [3]. Complexes of actinide elements with this ligands, however, have not yet been described to the best of our knowledge.

Here we report synthesis and characterisation of dioxouranium(VI) complexes with bis{N,N'-(2-ethoxycarbonyl-3-oxo-but-1-en(1)yl)-1,2-diaminobenzene (H_2L^1) and N-(2-ethoxycarbonyl-3-oxo-but-1-en(1)yl)-2-aminophenol (H_2L^2). Both compounds react with $UO_2(NO_3)_2 \cdot 6H_2O$ in methanol after addition of NEt_3 under formation of red solids which slowly precipitate from the reaction mixtures [4]. The products contain the chelating ligands in their deprotonated forms. This can be concluded from the bathochromic shifts of their $\nu_{C=O}$ and $\nu_{C=N}$ bands by about 40 cm^{-1} in the infrared spectra of the products.

H_2L^1 H_2L^2
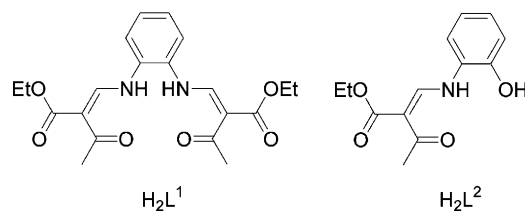
The IR spectrum of the product with H_2L^1 in addition shows a band at 2800 cm^{-1} which suggests hydrogen bonded protons and could be assigned to a $[NEt_3H]^+$ cation. In agreement with the analytical data a composition of $[NEt_3H][UO_2(L^1)(OMe)]$ can be concluded, which has been confirmed by an X-ray structure analysis of the product [5]. The uranium atom shows a distorted pentagonal–bipyramidal co-ordination geometry with a central *trans*-$[UO_2]^{2+}$ core and almost coplanar equatorial donor atoms (mean deviation from planarity: 0.105(5)Å, r.m.s. 0.0747). The chelate rings are not coplanar with the co-ordinating atoms and the central phenyl ring is bent towards O20 forming an angle of 25° with the least-square plane formed by the equatorial donor atoms. The six-membered chelate rings with the peripheral ester substituents are directed into the opposite direction towards O10. An ellipsoid representation of the complex is shown in Fig. 1. The bonding situation in the azomethine changes when it is

* Corresponding author. Tel.: +49-30-838-54002; fax: +49-30-838-52676.
E-mail address: abram@chemie.fu-berlin.de (U. Abram).
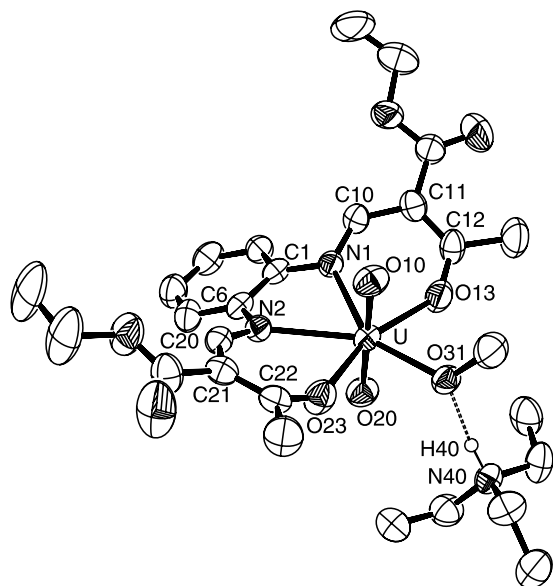[1] Also corresponding author.

Fig. 1. Ellipsoid representation [6] of the molecular structure of [NEt₃H][UO₂(L¹)(OMe)]. Selected bond lengths: U-O10 1.774(7); U-O20 1.772(7); U-O13 2.349(7); U-O23 2.336(7); U-O31 2.234(6); U-N1 2.539(7); U-N2 2.568(7), O13-C12 1.27(1); C12-C11 1.38(1); C11-C10 1.42(1); C10-N1 1.29(1); N1-C1 1.43(1); C6-N2 1.42(1); N2-C20 1.29(1); C20-C21 1.43(1); C21-C22 1.41(1); C22-O23 1.25(1) Å.

Fig. 2. Ellipsoid representation [6] of the molecular structure of [U-O₂(L¹)(DMSO)]. Selected bond lengths: U-O10 1.761(6); U-O20 1.759(6); U-O13 2.321(6); U-O23 2.297(6); U-O30 2.374(5); U-N1 2.496(6); U-N2 2.493(7), O13-C12 1.28(1); C12-C11 1.41(1); C11-C10 1.42(1); C10-N1 1.31(1); N1-C1 1.40(1); C6-N2 1.42(1); N2-C20 1.29(1); C20-C21 1.44(1); C21-C22 1.40(1); C22-O23 1.29(1) Å.

co-ordinated to uranium. Whereas the double bond is mainly located between the carbon atoms in the unco-ordinated compound as is shown in the formula of H_2L^1 [8], a considerable double bond character is found for the C10–N1 and C20–N2 bonds in $[UO_2(L^1)(OMe)]^-$. Similar results have been obtained for copper, nickel and technetium complexes with 'jaeger-type' ligands [9]. The co-ordination sphere of uranium is completed by a methanolato ligand which is formed from the solvent. It establishes a hydrogen bond to the $[NEt_3H]^+$ counter ion (N40-H40 0.91Å, O31-H40 1.74 Å, N40...O31 2.64(1)Å, N40-H40-O31 170.4°). This methanolato ligand is labile and can be replaced by dissolution of $[NEt_3H][UO_2(L^1)(OMe)]$ in warm DMSO which results in the formation of the neutral complex $[UO_2(L^1)(DMSO)]$. The product is formed quickly and the NMR spectrum of a solution of $[NEt_3H][UO_2(L^1)(OMe)]$ in DMSO immediately after dissolution shows practically exclusively the presence of $[UO_2(L^1)(DMSO)]$, NEt_3 and MeOH. $[UO_2(L^1)(DMSO)]$ crystallises upon cooling of a concentrated DMSO solution as red plates. Fig. 2 shows an ellipsoid representation of the structure of the complex. The bonding situation is similar to that in $[NEt_3H][UO_2(L^1)(OMe)]$. The ester substituents are almost coplanar with their chelate arms which maximises their electron-withdrawing potential, but unlike the situation in similar copper compounds [9c], the ligand is not planar and shows the same distortions as described above for $[NEt_3H][UO_2(L^1)(OMe)]$.

A completely different type of uranium complexes is obtained when the potentially tridentate azomethine

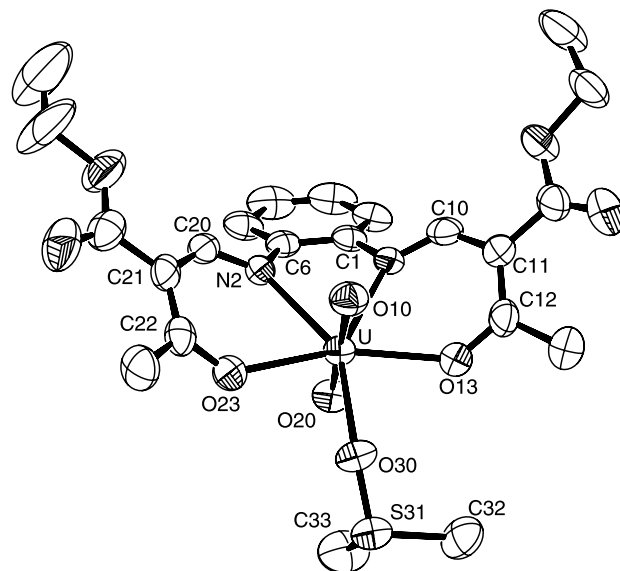H_2L^2 is used. The phenolato oxygen acts as bridge between two metal atoms and the trinuclear complex $[\{UO_2(L^2)\}_3(\mu_3\text{-}O)]^{2-}$ is formed which has been isolated as triethylammonium salt. It is a new representative of the small group of dioxouranium complexes with an additional central μ_3-bridging oxo ligand, which has been confirmed by an X-ray structure analysis. More details of the structure of this compound will be published elsewhere [8]. The capability of phenolato groups in 'jaeger-type' ligands to bridge metal centres has been demonstrated previously [9b] and the fact that this also can be achieved with uranium recommends this class of ligands for the synthesis of larger uranium-containing aggregates.
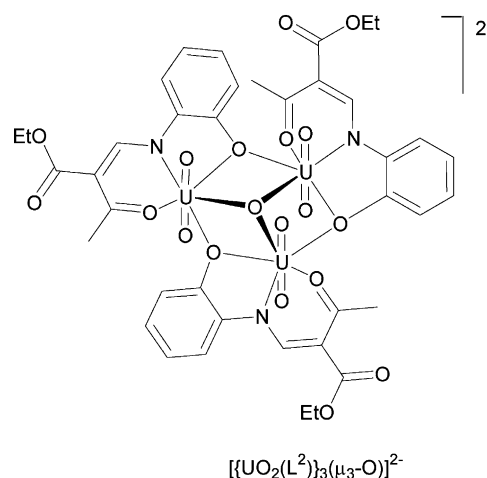
$[\{UO_2(L^2)\}_3(\mu_3\text{-}O)]^{2-}$

References

[1] E.G. Jäger, E. Häussler, M. Rudolph, A. Schneider, Z. Anorg. Allg. Chem. 525 (1985) 67.

[2] K. Müller, D. Seidel, E.G. Jäger, Z. Anorg. Allg. Chem. 561 (1988) 38, and references cited therein.

[3] E.G. Jäger, J. Knaudt, M. Rudolph, M. Rost, Chem. Ber. 129 (1996) 1041, and references cited therein.

[4] *Synthesis of* $[NEt_3H][UO_2(L^1)(OMe)]$: $UO_2(NO_3)_2 \cdot 6\,H_2O$ (502 mg, 1 mmol) in 5 ml MeOH was mixed with a solution of H_2L^1 (388 mg, 1 mmol) in 15 ml MeOH and NEt_3 (0.1 ml) was added. The colour of the solution turned red. After heating on reflux for 1 h, a red solid deposited from the solution. Single crystals which were appropriate for X-ray diffraction were obtained directly from the mother liquor upon standing overnight. Yield: 686 mg, 87%. $UC_{27}H_{41}N_3O_9$ (789.7); C 41.38 (calc. 41.07); H 5.21 (5.23); N 5.22 (5.32)%.
Synthesis of $[UO_2(L^1)(DMSO)]$: $[NEt_3H][UO_2(L^1)(OMe)]$ is dissolved in a small amount of warm DMSO. Red crystals deposit upon cooling. Yield: ca. 80%. $UC_{22}H_{28}N_2O_9S$ (734.6); C 35.93 (calc. 35.99); H 3.81 (3.75); N 3.81 (3.80). *Synthesis of* $[NEt_3H]_2[\{UO_2 (L^2)\}_3(\mu_3\text{-}O)] \cdot H_2O$: $UO_2(NO_3)_2 \cdot 6H_2O$ (502 mg, 1 mmol) in 5 ml MeOH was mixed with a solution of H_2L^1 (388 mg, 1 mmol) in 15 ml MeOH and NEt_3 (0.1 ml) was added. The colour of the solution turned red. After heating on reflux for 1h, a red solid deposited from the solution. Yield: 370 mg, 62%. $UC_{51}H_{71}N_5O_{20}$ (1788.2); C 34.22 (calc. 34.22); H 4.01 (4.11); N 3.84 (3.91)%.

[5] *Crystal data for* $[NEt_3H][UO_2(L^1)(OMe)]$: monoclinic, space group $P2_1/c$, $a = 11.524(7)$, $b = 15.959(2)$, $c = 17.061(2)$ Å, $\beta = 94.84(1)$, $V = 3126(2)$ Å^3, $Z = 4$. CAD4 (Enraf Nonius), Mo-Kα radiation ($\lambda = 0.71073$ Å), $T = 293$ K, 7777 reflections measured, 6763 independent, 362 parameter, $\mu = 1.678$ mm^{-1}, absorption correction: Psi scans: $T_{\min} = 0.44$, $T_{\max} = 0.89$. Structure solution and refinement: SHELXS97, SHELXL97 [7], $R1 = 0.0521$, $wR2 = 0.0881$, $GooF = 0.738$. Further details have been deposited with the Cambridge Crystallographic Data Centre under the deposition number CCDC-208434.
Crystal data for $[UO_2(L^1)(DMSO)]$: triclinic, space group $P\bar{1}$, $a = 8.908(1)$, $b = 11.337(2)$, $c = 13.783(2)$ Å, $\alpha = 110.39(1)$, $\beta = 91.14(1)$, $\gamma = 93.59(2)$, $V = 1300.9(3)$ Å^3, $Z = 2$. CAD4 (Enraf Nonius), Mo-Kα radiation ($\lambda = 0.71073$ Å), $T = 293$ K, 6764 reflections measured, 5653 independent, 316 parameter, $\mu = 6.370$ mm^{-1}, absorption correction: DIFABS: $T_{\min} = 0.322$, $T_{\max} = 0.753$. Structure solution and refinement: SHELXS97, SHELXL97 [7], $R1 = 0.0484$, $wR2 = 0.1122$, $GooF = 1.007$. Further details have been deposited with the Cambridge Crystallographic Data Centre under the deposition number CCDC-208435.

[6] L.J. Farrugia, J. Appl. Cryst. 30 (1997) 565.

[7] G.M. Sheldrick, SHELXS97 and SHELXL97 – programs for the solution and refinement of crystal structures, University of Göttingen, Germany, 1997.

[8] C.C. Gatto, E. Schulz Lang, A. Kupfer, A. Hagenbach, U. Abram, Z. Anorg. Allg. Chem., submitted.

[9] (a) D. Hess, H. Ellias, H. Paulus, Z. Anorg. Allg. Chem. 577 (1989) 135; (b) H. Ellias, D. Hess, H. Paulus, E.G. Jäger, F. Gräfe, Z. Anorg. Allg. Chem. 589 (1990) 101; (c) H. Keutel, D. Seidel, M. Klussmann, H. Görls, Inorg. Chem. 39 (2000) 1608; (d) U. Abram, S. Abram, R. Münze, E.G. Jäger, J. Stach, R. Kirmse, G. Admiraal, P.T. Beurskens, Inorg. Chim. Acta 182 (1991) 233.

Dioxouranium Complexes with Acetylpyridine Benzoylhydrazones and Related Ligands

C. C. Gatto, E. Schulz Lang

Santa Maria/Brazil, Department of Inorganic Chemistry of the University of Santa Maria

A. Kupfer, A. Hagenbach, D. Wille, U. Abram*

Berlin, Institut für Chemie der Freien Universität Berlin

Abstract. Acetylpyridine benzoylhydrazone and related ligands react with common dioxouranium(VI) compounds such as uranyl nitrate or [NBu$_4$]$_2$[UO$_2$Cl$_4$] to form air-stable complexes. Reactions with 2,6-diacetylpyridinebis(benzoylhydrazone) (H$_2$L^{1a}) or 2,6-diacetylpyridinebis(salicylhydrazone) (H$_2$L^{1b}) give yellow products of the composition [UO$_2$(L^1)]. The neutral compounds contain doubly deprotonated ligands and possess a distorted pentagonal-bipyramidal structure. The hydroxo groups of the salicylhydrazonato ligand do not contribute to the complexation of the metal. The equatorial coordination spheres of the complexes can be extended by the addition of a monodentate ligand such as pyridine or DMSO. The uranium atoms in the resulting deep-red complexes have hexagonal-bipyramidal coordination environments with the oxo ligands in axial positions.

The sterical strains inside the hexagonal plane can be reduced when two tridentate benzoylhydrazonato ligands are used instead of the pentadentate 2,6-diacetylpyridine derivatives. Acetylpyridine benzoylhydrazone (HL^2) and bis(2-pyridyl)ketone benzoylhydrazone (HL^3) deprotonate and form neutral, red [UO$_2$(L)$_2$] complexes. The equatorial coordination spheres of these complexes are puckered hexagons.

X-ray diffraction studies on [UO$_2$(L^{1a})(pyridine)], [UO$_2$(L^{1b})(DMSO)], [UO$_2$(L^2)$_2$] and [UO$_2$(L^3)$_2$] show relatively short U$-$O bonds to the benzoylic oxygen atoms between 2.328(6) and 2.389(8) Å. This suggests a preference of these donor sites of the ligands over their imino and amine functionalities (U$-$N bond lengths: 2.588(7)$-$2.701(6) Å).

Keywords: Uranium; Benzoylhydrazonato ligands, Actinides, Uranyl chelates; Structure analysis

Dioxouranium-Komplexe mit Acetylpyridinbenzoylhydrazon und verwandten Liganden

Inhaltsübersicht. Acetylpyridinbenzoylhydrazon und davon abgeleitete Liganden reagieren mit Uranylnitrat oder [NBu$_4$]$_2$[UO$_2$Cl$_4$] unter Bildung luftstabiler Dioxouranium(VI)-Komplexe. Bei Reaktionen mit 2,6-Diacetylpyridinbis(benzoylhydrazon) (H$_2$L^{1a}) und 2,6-Diacetylpyridinbis(salicylhydrazon) (H$_2$L^{1b}) entstehen gelbe Pulver der Zusammensetzung [UO$_2$(L^1)]. Die Koordination des Uranatoms in den Neutralkomplexen mit doppelt deprotonierten organischen Liganden ist verzerrt pentagonal-bipyramidal. Die Hydroxosubstituenten des Salicylhydrazonato-Liganden [L^{1b}]$^{2-}$ sind an der Komplexierung des Metallatoms nicht beteiligt. Reaktionen von [UO$_2$(L^1)]-Komplexen mit monodentaten Liganden wie Pyridin oder DMSO führen zur Aufweitung der äquatorialen Koordinationssphäre und zur Bildung von tiefroten, kristallinen Verbindungen mit einer verzerrten, hexagonal-bipyramidalen Koordination um die Uranatome.

Die sterische Belastung der äquatorialen Koordinationsebene kann verringert werden, wenn anstelle der fünfzähnigen H$_2$L^1-Liganden dreizähnige Benzoylhydrazonato-Liganden verwendet werden. 2-Acetylpyridinbenzoylhydrazon (HL^2) und Bis(2-pyridyl)keton-benzoylhydrazon (HL^3) bilden unter einfacher Deprotonierung neutrale Komplexe der Zusammensetzung [UO$_2$(L)$_2$]. Die hexagonalen Grundflächen der gebildeten Bipyramiden sind in diesen Produkten deutlich gewellt.

Kristallstrukturanalysen von [UO$_2$(L^{1a})(Pyridin)], [UO$_2$(L^{1b})(DMSO)], [UO$_2$(L^2)$_2$] und [UO$_2$(L^3)$_2$] zeigen relativ kurze Bindungen zwischen den Uranatomen und den Benzoylgruppierungen (2.328(6)$-$2.389(8) Å). Das legt eine bevorzugte Bindung an die Sauerstoffatome der Liganden nahe, während die Uran$-$Stickstoff-Bindungen deutlich länger sind (2.588(7)$-$2.701(6) Å).

Introduction

As a part of our systematic studies of the coordination chemistry of the early actinide elements, we recently published a report on the structural chemistry of thiosemicarbazonato complexes of uranium(VI) [1]. The formation of complexes with medium stability was observed with acetylpyridine thiosemicarbazone in which the pyridine nitrogen atom provides an additional donor site to the metal atoms. More stable complexes are expected with 'harder' donor atoms such as oxygen, as is provided by semicarbazones or hydrazones. A number of studies have been undertaken with both ligand systems and the formation of chelates with various compositions have been suggested on the basis of spec-

---

* Prof. Dr. Ulrich Abram
Freie Universität Berlin
Institut für Chemie
Fabeckstraße 34$-$36
D-14195 Berlin
Email: abram@chemie.fu-berlin.de

troscopic data [2]. Some of the compounds have been proposed for the spectrophotometric determination of metal ions including UO_2^{2+} [3], but less is known about the composition of the coordination environment of the metal. First structural reports performed with 2,6-diacetylpyridinebis(2′-pyridyl)hydrazones [4] and benzoylhydrazones [5] describe uranyl complexes having pentagonal bipyramidal or hexagonal-bipyramidal coordination spheres at the uranium atoms. The reasons for the respective composition of the equatorial coordination spheres and the influence of substituents are not yet clear. In the present paper, we describe the reactions of uranyl nitrate and $[NBu_4]_2[UO_2Cl_4]$ with 2,6-diacetylpyridinebis(benzoylhydrazone) (H_2L^{1a}), 2,6-diacetylpyridinebis(salicylhydrazone) (H_2L^{1b}), 2-acetylpyridine benzoylhydrazone (HL^2) and bis(2-pyridyl)ketone benzoylhydrazone (HL^3), Scheme 1, and the solid state structures of the products.

**H₂L¹ᵃ (R¹= R² = H)**   **H₂L¹ᵇ (R¹ = OH, R² = H)**   **HL²**   **HL³**
H₂L¹ᶜ (R¹=H, R²= OMe)
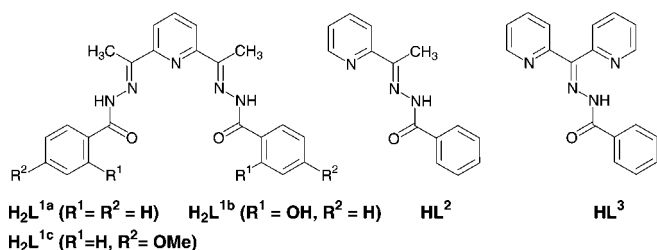
Scheme 1

Results and Discussion

$UO_2(NO_3)_2 \cdot 6H_2O$ as well as $[Bu_4N]_2[UO_2Cl_4]$ react with the benzoylhydrazone or salicylhydrazone ligands $H_2L^1-HL^3$ in boiling methanol under complete substitution of the equatorial coordination sphere of the metal atom. Under these conditions, complete deprotonation of the ligands is observed independent of the uranium precursor used, and neutral dioxouranium complexes are formed. No evidence has been found for the formation of complexes with non-deprotonated or semi-deprotonated (H_2L^1) hydrazone ligands as has been observed for related semicarbazones of chromium(III) [6] and other highly charged metal ions including the uranyl ion [7]. A complicated coordination pattern has also been described for products obtained from reactions of uranyl salts and 2,6-diacetylpyridine bis(p-methoxybenzoylhydrazone), where different structures have been assigned on the basis of spectroscopic

data in dependence on the solvents and the uranium starting materials used [5b]. The only compound in this report which has been characterized by X-ray crystallography, however, is a neutral dioxouranium(VI) complex with a doubly deprotonated organic ligand in which the uranium atom is seven-coordinate.

Similar complexes are obtained when the ligands H_2L^{1a} or H_2L^{1b} are heated with $UO_2(NO_3)_2 \cdot 6 H_2O$ or $[NBu_4]_2$-$[UO_2Cl_4]$ in boiling methanol. The reaction is faster when a supporting base such as triethylamine is added, but this is not mandatory. Yellow precipitates are formed upon cooling, which have been isolated and characterized by elemental analysis, IR and NMR measurements showing that the products formed from the different uranium precursors were identical. The U=O double bonds show characteristic IR bands between 900 and 905 cm^{-1}. This value is in accord with the neutral uranyl complexes in ref. [5b], whereas anionic derivatives absorb in the range between 920 and 950 cm^{-1}. The proton NMR spectra prove the absence of the NH protons of the organic ligands, whereas an OH signal for the complex with ligand $[L^{1b}]^{2-}$ was observed at 12.9 ppm. This is in the same position as in H_2L^{1b}, which suggests that the hydroxylic group of the salicylhydrazone does not contribute to the coordination of the metal atom. No evidence was found for the coordination of methanol or water. This allows the conclusion that complexes of the composition $[UO_2L^1]$ have been formed. These complexes possess the same coordination sphere at the metal atoms as the uranyl complex with 2,6-diacetylpyridine bis(methoxybenzoylhydrazone), which shows distorted pentagonal-bipyramidal coordination of the metal atom [5b]. No evidence could be found for anionic uranyl complexes with non-deprotonated or monodeprotonated ligands. The bond angles between neighbouring atoms inside the equatorial coordination sphere are approximately 63° (4 times) and 107° (between the oxygen atoms of the benzoyl groups) [5b] (see also Table 1 and Fig. 4), which suggests the possibility of the extension of the coordination number by the addition of an appropriate monodentate ligand. This has been proven by heating the $[UO_2(L^1)]$ complexes in coordinating solvents such as DMSO, pyridine or THF. The yellow solids slowly dissolve in these solvents and the colour changes to red. A reaction sequence resulting in the formation of neutral $[UO_2(L^1)(solvent)]$ complexes can be derived (see Scheme 2). The products can be isolated in crystalline form by the slow evaporation of the solvents (THF and pyridine) or addition of a small amount of water and slow cooling (DMSO). The U=O stretching vibrations are shifted to
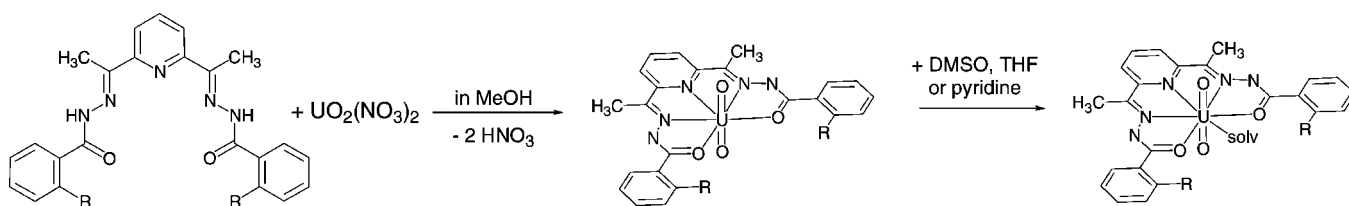
Scheme 2
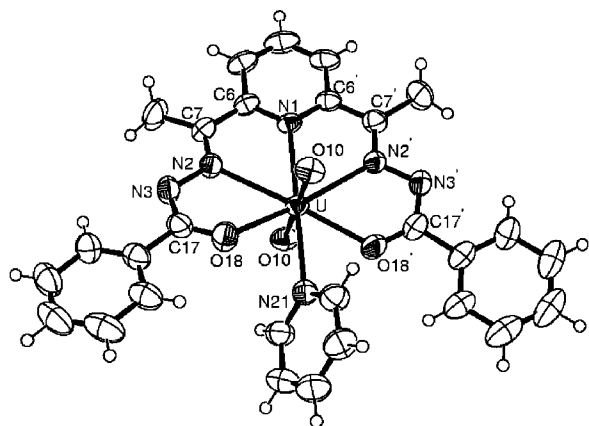
Figure 1 Ellipsoid presentation [13] of [UO$_2$(L^{1a})(pyridine)]. Thermal ellipsoids represent 50 per cent probability.

Table 1 Selected bond lengths /Å and angles/° in [UO$_2$(L^{1a})-(pyridine)], [UO$_2$(L^{1b})(DMSO)] and [UO$_2$(L^{1c})].

	[UO$_2$(L)^{1a}(pyridine)]	[UO$_2$(L)^{1b}(DMSO)]	[UO$_2$(L)^{1c}]a)
U−O10	1.774(2)	1.77(1)	1.77
U−O20	–	1.777(9)	1.77
U−O18	2.356(3)	2.389(8)	2.32/2.30b)
U−N2	2.630(3)	2.613(9)	2.47/2.49b)
U−N1	2.685(8)	2.65(1)	2.52
U−N21/O30	2.68(1)	2.527(9)	–
O18−C17	1.280(5)	1.28(1)	1.26/1.30b)
C17−N3	1.293(5)	1.32(1)	1.33/1.30b)
N3−N2	1.398(5)	1.38(1)	1.41/1.40b)
N2−C7	1.284(4)	1.31(1)	1.31/1.31b)
C7−C6	1.455(6)	1.45(1)	1.50/1.48b)
C7−C8	1.502(6)	1.49(1)	1.50/1.51b)
O18−U−N2	60.07(9)	60.3(3)	63.5/63.3b)
N2−U−N1	59.34(7)	59.8(2)	63.3/63.3b)
O18−U−N21/O30	61.39(7)	61.8(2)	–
O18−U−O18′	122.8(1)c)	119.2(4)d)	106.8
N1···N2	2.631(5)	2.62/2.63	
N2···O18	2.507(4)	2.52/2.52	

a) Values taken from ref. [5b] and adopted to the atomic labelling schemes given in Figures 1 and 2. b) Two values since there is no intramolecular symmetry in this complex. c) Symmetry operation: 1−x, −y, z. d) Symmetry operation: x, −0.5−y, z.

higher frequencies compared with the values in the [UO$_2$(L^1)] complexes and occur between 914 and 920 cm^{-1}. Similar changes in the position of the uranyl bands in dependence on the coordination number of the metal atom have been observed previously [5b].

Single crystals of [UO$_2$(L^{1a})(pyridine)] and [UO$_2$(L^{1b})(DMSO)] have been studied by X-ray crystallography, showing that the complexes possess eight-coordinate uranium atoms. An ellipsoid representation of the molecular structure of [UO$_2$(L^{1a})(pyridine)] is shown in Figure 1. Selected bond lengths and angles are summarised in Table 1. The coordination environment of the uranium atom can be described as an almost perfect hexagonal bipyramid with a planar equatorial coordination sphere (maximum deviation from a mean least-square plane

formed by the atoms U, N21, O18, N2, N1 N2′ and O18′: 0.201(3) Å for O18 and O18′, r.m.s. 0.1455). The X−U−Y angles (X and Y are neighbouring equatorial donor atoms) range from 59.34 to 61.39°. The torsion angle between the pyridine ring and the hexagonal plane is 61.4(1)°, which minimises steric hindrance between the pyridine ligand and the benzoylhydrazonato arms of the pentadentate ligand and the two oxo oxygen atoms. The extension of the coordination number of uranium causes lengthening of the U−N bonds to the chelating ligand as can be seen from a comparison with the corresponding data in the seven-coordinate complex [UO$_2$(L^{1c})] [5b]. Selected bond lengths and angles of this compound are included in Table 1; the atomic numbering has been adopted to fit the labelling scheme applied in the present paper. No significant change can be derived for the bonding situation inside the hydrazonato ligands, which are doubly deprotonated in all complexes described in this paper. Whereas the double bond between C7 and N2 is almost localised, a delocalisation of the electron density of the C17−O18 double bond can be concluded, which results in a significant shortening of the C17−N3 bond as a consequence of complex formation. This situation can best be described by the bonding scheme represented in **I**, irrespective of the coordination number of the uranium atom. It has also been found in [UO$_2$(L^{1b})(DMSO)], which has been prepared by heating of [UO$_2$(L^{1b})] in DMSO.
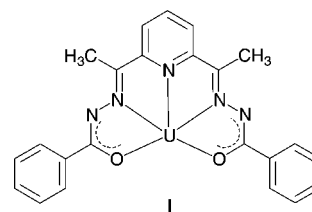
Scheme 3

[UO$_2$(L^{1b})(DMSO)] crystallizes as large red blocks, and the results of an X-ray structure analysis confirm the spectroscopic conclusion that the hydroxylic group of the salicylhydrazone is not involved in the coordination of the metal atom. The structure of the complex is illustrated in Figure 2. The OH substituents of the salicylic groups are disordered. The occupation of the two positions is about 0.8/0.2 with a preference of the position on C16 (Figure 2) which allows intramolecular hydrogen bonds to O18 and O30. The overall bonding pattern in [UO$_2$(L^{1b})(DMSO)] is similar to that in [UO$_2$(L^{1a})(pyridine)], with the uranium atom in an almost regular hexagonal-bipyramidal coordination environment. Only small deviations from planarity can be found for the hexagonal plane (maximum deviation: 0.170(4) Å for O30, r.m.s. 0.1459), and the bond angles are very close to 60°. The corresponding values and selected bond lengths are listed in Table 1. It is interesting to note that the increase in coordination number and the observed lengthening of the uranium-nitrogen bonds are not related to an increase of the bite angles of the binding sites, which
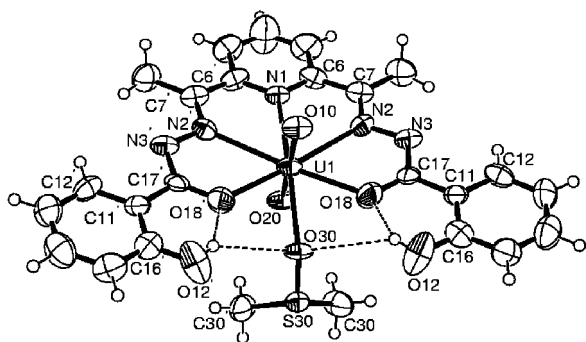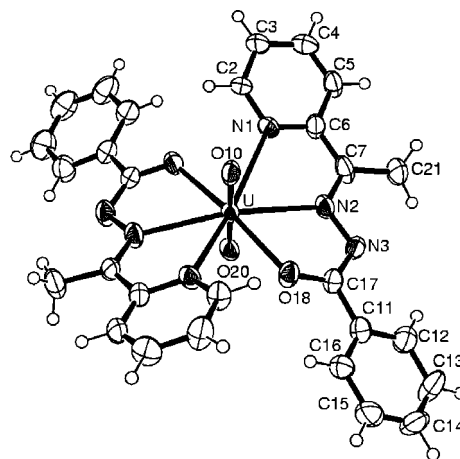
Figure 2 Ellipsoid presentation [13] of $[UO_2(L^{1b})(DMSO)]$. Thermal ellipsoids represent 50 per cent probability.

can be estimated by the intramolecular distances between the donor atoms N1 and N2 or N2 and O18. The corresponding values are also listed in Table 1.

More distortions from an ideal hexagonal bipyramid are found in the structures of the complexes $[UO_2(L^2)_2]$ and $[UO_2(L^3)_2]$, which also possess coordination number 8 at the uranium atoms. The compounds are formed during reactions of uranyl nitrate or $[NBu_4]_2[UO_2Cl_4]$ with an excess of the ligands in boiling methanol. They precipitate as orange-red solids directly from the reaction mixtures and recrystallisation from hot methanol or $CHCl_3$/methanol mixtures results in red crystals. The IR spectra show the expected $\nu(UO_2)$ bands at 912 cm^{-1} ($[UO_2(L^2)_2]$) and 911 cm^{-1} ($[UO_2(L^3)_2]$). The absences of NH bands indicates deprotonation of the hydrazones; the coordination of the benzoyl group is strongly suggested by the shift of the corresponding $\nu(C=O)$ bands to lower frequencies. A shift of the band at 990 cm^{-1} in the spectra of the proligands, which can be assigned to the breathing motion of the pyridine ring, to higher frequencies indicates the coordination of the pyridyl groups and, thus, a tridentate, monoanionic bonding scheme is expected for both of these hydrazones, irrespective of the possible binding mode of HL^3 as a bidentate, neutral bipyridine analogue, which has been observed recently for a rhenium(I) tricarbonyl complex [8].

The coordination environments of the uranium atoms in the molecular structures of $[UO_2(L^2)_2]$ (Fig. 3) and $[UO_2(L^3)_2]$ (Fig. 4) are similar and can best be described as a strongly distorted hexagonal bipyramid. Selected bond lengths and angles of both complexes are summarized in Table 2. For $[UO_2(L^2)_2]$, the atomic labelling scheme of $[UO_2(L^3)_2]$ has been applied, with the exception that the second $[L^2]^-$ ligand is symmetry-generated in $[UO_2(L^2)_2]$ since the atoms O10, U and O20 are situated on a 2-fold crystallographic axis. The U–N bond lengths in both complexes are in the same range as has been found in $[UO_2(L^1)-$ (solvent)] complexes with 8-coordinate uranium atoms and are accordingly longer than the values in $[UO_2(L^{1c})]$. This is another indication that the observed bond lengthening is due to steric overcrowding of the equatorial coordination spheres in the compounds with coordination number 8 at the metal atoms.

Figure 3 Ellipsoid presentation [13] of $[UO_2(L^2)_2]$. Thermal ellipsoids represent 50 per cent probability.
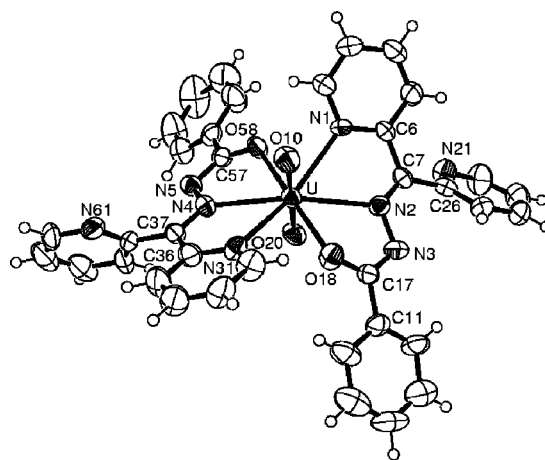
**Figure 4** Ellipsoid presentation [13] of $[UO_2(L^3)_2]$. Thermal ellipsoids represent 50 per cent probability.

The six equatorial atoms in $[UO_2(L^2)_2]$ and $[UO_2(L^3)_2]$ form puckered hexagons in which the five-membered chelate rings are almost planar and angles between 13° and 18° are established between them. This allows for the minimisation of steric interaction. Figure 5 shows a comparison of the coordination spheres of $[UO_2(L^{1c})]$, $[UO_2(L^{1a})$-(pyridine)] and $[UO_2(L^3)_2]$ containing uranium atoms with the coordination numbers seven and eight. Particularly the side views indicate that the sterical hindrance inside the equatorial coordination sphere is reduced by the coordination of two tridentate ligands rather than a 5+1 coordination as is established in $[UO_2(L^{1a})(pyridine)]$ or $[UO_2(L^{1b})(DMSO)]$. The views along the uranyl units, however, show almost regular hexagons for the equatorial coordination spheres of both structural types.

The present study shows that acetylpyridine benzoylhydrazones and related ligands are well suited for the formation of stable complexes with dioxouranium(VI) units. All hydrazone units of the ligands are deprotonated in the

Table 2 Selected bond lengths/Å and angles/° in $[UO_2(L^2)_2]$ and $[UO_2(L^3)_2]$.

	$[UO_2(L^2)_2]$	$[UO_2(L^3)_2]$
U−O10	1.725(9)	1.771(6)
U−O20	1.727(9)	1.756(6)
U−O18	2.371(6)	2.328(6)
U−N2	2.612(7)	2.610(7)
U−N1	2.701(6)	2.635(7)
U−N31	2.701(6)[a]	2.670(7)
U−N4	2.612(7)[a]	2.588(7)
U−O58	2.371(6)	2.355(6)
C7−N2	1.30(1)	1.28(1)
N2−N3	1.377(9)	1.376(9)
C17−O18	1.28(1)	1.29(1)
C37−N4	1.30(1)[a]	1.31(1)
N4−N5	1.377(9)[a]	1.385(9)
C51−O58	1.28(1)[a]	1.27(1)
O18−U−N2	60.0(2)	59.9(2)
N2−U−N1	59.5(2)	59.1(2)
N1−U−O18′/O58	65.3(2)[b]	64.8(2)
O58−U−N4	60.0(2)[a]	61.0(2)
N4−U−N31	59.5(2)[a]	59.4(2)
O18−U−N1′/N31	65.3(2)[a]	67.1(2)
O10−U−O20	180	177.3(3)

[a] Symmetry-related bond lengths or angles due to an intramolecular 2-fold axis. [b] Symmetry operation: 1−x, y, 0.5−z. [d] Symmetry operation: x, −0.5−y, z.
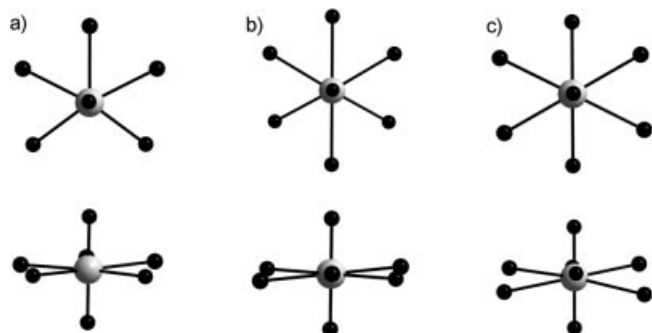
Figure 5 Representation [14] of the coordination spheres of a) $[UO_2(L^{1c})]$ [5b], b) $[UO_2(L^{1a})(pyridine)]$ and c) $[UO_2(L^2)_2]$ in top and side views with respect to the O−U−O axis showing the distortions of the equatorial coordination spheres of the complexes in dependence on the chelating ligands.

uranium complexes studied in this paper. This is in contrast to the behaviour in some lanthanide complexes, where only partial deprotonation of the NH groups was observed [9]. The ready extension of a pentagonal equatorial coordination sphere in the complexes of the type $[UO_2(L^1)]$ indicates a higher stability of the products with coordination number 8 at the uranium atoms, despite the resulting steric strains due to the relatively rigid pentadentate ligands, which obviously cannot fully be compensated for by distortions of the coordination sphere.

Experimental

HL^{1a}, HL^{1b}, HL^2 and HL^3 were prepared by refluxing equivalent amounts of 2,6-diacetylpyridine (ALDRICH), 2-acetylpyridine (ALDRICH) or di(2-pyridine)ketone (ACROS) with equivalent amounts of benzoylhydrazine (ACROS) or salicylhydrazine (ACROS) in ethanol and recrystallized from ethanol/water [8,10]. $[NBu_4]_2[UO_2Cl_4]$ was prepared following a standard procedure from uranyl nitrate, aqueous HCl and tetrabutylammonium chloride. Infrared spectra were recorded for KBr pellets on a Shimadzu FT IR spectrometer between 4000 and 400 cm^{-1}.

$[UO_2(L^{1a})]$. HL^{1a} (440 mg, 1.1 mmol) was partially dissolved in about 5 ml methanol and added to a solution of $UO_2(NO_3)_2 \cdot 6$ H_2O (502 mg, 1 mmol) in 3 ml methanol. After heating the mixture to reflux, a clear yellow solution was formed, from which a bright yellow powder began to precipitate after about 15 min. After an overall reflux time of 2 h, the mixture was cooled to room temperature and the yellow solid was filtered off.
The reaction rate can be increased by the addition of two drops of triethylamine. In this case, the precipitation of the solid is complete after 30 min. The solid is almost insoluble in alcohols. Yield: 633 mg (95%). Elemental analysis, Found: C, 41.2; H, 2.7; N, 10.5%; Calcd. for $C_{23}H_{19}N_5O_4U$: C, 41.4; H, 2.8; N, 10.5%. IR (ν_{max}/cm^{-1}): 1590 (C=N), 900 (O=U=O).
The same procedure can be applied when the reaction is performed with $[NBu_4]_2[UO_2Cl_4]$ instead of uranyl nitrate.

$[UO_2(L^{1b})]$. The complex was prepared following the procedure given above for $[UO_2(L^{1a})]$ starting from $UO_2(NO_3)_2 \cdot 6$ H_2O (502 mg, 1 mmol) and HL^{1b} (517 mg, 1.2 mmol). Yellow, sparingly soluble solid. Yield: 629 mg (90%). Elemental analysis, Found: C, 39.2; H, 2.7; N, 10.3%; Calcd. for $C_{23}H_{19}N_5O_6U$: C, 39.5; H, 2.7; N, 10.0%. IR (ν_{max}/cm^{-1}): 3209 (OH), 1591 (C=N), 902 (O=U=O).
The same procedure can be applied when the reaction is performed with $[NBu_4]_2[UO_2Cl_4]$ instead of uranyl nitrate.

$[UO_2(L^{1a})(DMSO)]$. $[UO_2(L^{1a})]$ (333 mg, 0.5 mmol) was dissolved in about 1 ml hot DMSO. Large red blocks deposited upon slow cooling of the solvent. More product could be obtained by diffusion of water into the DMSO solution. Yield: 224 mg (60%). Elemental analysis, Found: C, 41.2; H, 3.3; N, 9.7; S, 4.5%; Calcd. for $C_{25}H_{25}N_5O_5SU$: C, 41.2; H, 3.4; N, 9.6; S, 4.4%. IR (ν_{max}/cm^{-1}): 1585 (C=N), 914 (O=U=O).

$[UO_2(L^{1a})(pyridine)]$. The compound was prepared from $[UO_2(L^{1a})]$ and pyridine following the procedure given for $[UO_2(L^{1a})(DMSO)]$. Yield: 60%. Elemental analysis, Found: C, 45.0; H, 3.0; N, 11.0%; Calcd. for $C_{28}H_{24}N_6O_4U$: C, 45.0; H, 3.2; N, 11.3%. IR (ν_{max}/cm^{-1}): 1587 (C=N), 912 (O=U=O). Single crystals suitable for X-ray diffraction were obtained directly from the reaction mixture.

$[UO_2(L^{1a})(THF)]$. The compound was prepared from $[UO_2(L^{1a})]$ and THF following the procedure given for $[UO_2(L^{1a})(DMSO)]$. The large red crystals immediately decompose after removal from the solvent. This is most probably due to the loss of solvent incorporated in the crystal lattice. Elemental analysis was performed with the remaining red powder after drying in vacuum and confirmed the presence of coordinated THF. Yield: 80%. Elemental analysis, Found: C, 43.8; H, 3.6; N, 9.4%; Calcd. for $C_{27}H_{27}N_5O_5U$: C, 43.8; H, 3.7; N, 9.5%. IR (ν_{max}/cm^{-1}): 1594 (C=N), 917 (O=U=O).

$[UO_2(L^{1b})(DMSO)]$. The compound was prepared from $[UO_2(L^{1b})]$ and DMSO following the procedure given for

Table 3 X-ray structure data collection and refinement parameters

	[UO$_2$(L^{1a})(pyridine)]	[UO$_2$(L^{1b})(DMSO)]	[UO$_2$(L^2)$_2$]	[UO$_2$(L^3)$_2$]
Formula	C$_{28}$H$_{24}$N$_6$O$_4$U	C$_{25}$H$_{25}$N$_5$O$_7$SU	C$_{28}$H$_{24}$N$_6$O$_4$U	C$_{36}$H$_{26}$N$_8$O$_4$U
M /g mol^{-1}	746.56	777.60	746.56	872.68
Crystal system	Orthorhombic	Orthorhombic	Orthorhombic	Monoclinic
Space group	Fdd2	Pnma	Pbcn	P2$_1$/n
Unit cell a	11.191(2)	17.979(2)	14.641(2)	11.863(1)
b	19.620(3)	17.716(1)	7.834(1)	15.127(2)
c	24.248(3)	8.300(1)	23.163(3)	18.780(2)
β				100.72(2)
V /Å^3	53234(1)	2642(5)	2656.7(6)	3311.3(6)
Z	8	4	4	4
D$_c$ /g cm^{-3}	1.863	1.955	1.866	1.751
Measuring device and temperature /°C	SMART CCD / −100	CAD4 / 20	CAD4 / 20	CAD4 / 20
Linear absorption coefficient /mm^{-1}	6.144	6.276	6.156	4.955
Absorption correction	SADABS	Psi Scans	Psi Scans	Psi Scans
T$_{min}$ / T$_{max}$	0.4601 / 0.5088	0.7583 / 0.9750	0.6754 / 0.8621	0.2419 / 0.6371
Measured reflections	16098	3148	7990	8449
Independent reflections / R$_{int}$	4004 / 0.035	2970 / 0.072	3517 / 0.1076	7201 / 0.0628
Refined parameters	179	197	178	442
R1 (F) / wR2 (F^2) (I > 2σ(I))$^{a)}$	0.0208 / 0.0464	0.0626 / 0.0906	0.0495 / 0.1047	0.0526 / 0.0951
GooF	0.972	0.973	0.966	0.978
Deposit No.	CCDC 229649	CCDC 229650	CCDC 229651	CCDC 229652

$^{a)}$ R1 = $|F_o - F_c|/|F_o|$; wR2 = $[w(F_o{}^2 - F_c{}^2)^2/(wF_o{}^2)]^{-1/2}$.

[UO$_2$(L^{1a})(DMSO)]. Yield: 60%. Elemental analysis, Found: C, 38.5; H, 3.2; N, 8.8; S, 4.4%; Calcd. for C$_{25}$H$_{25}$N$_5$O$_7$SU: C, 38.6; H, 3.2; N, 9.0; S, 4.1%. IR (ν_{max}/cm^{-1}): 3053 (OH), 1591 (C=N), 914 (O=U=O).

Single crystals for the X-ray structure analysis were obtained by slow diffusion of water into a DMSO solution of the complex.

[UO$_2$(L^{1b})(pyridine)]. The compound was prepared from [UO$_2$(L^{1b})] and pyridine following the procedure given for [UO$_2$(L^{1a})(pyridine)]. Yield: 85%. Elemental analysis, Found: C, 43.2; H, 3.0; N, 12.1%; Calcd. for C$_{28}$H$_{24}$N$_6$O$_6$U: C, 43.2; H, 3.1; N, 12.3%. IR (ν_{max}/cm^{-1}): 3005 (OH), 1588 (C=N), 915 (O=U=O).

[UO$_2$(L^2)^2]. HL^2 (526 mg, 2.2 mmol) was dissolved in about 10 ml methanol and added to a solution of UO$_2$(NO$_3$)$_2$ · 6 H$_2$O (502 mg, 1 mmol) in 5 ml methanol. The mixture was heated at reflux for 1 h. During this period the solution turned red. A red, crystalline solid precipitated after reducing the volume to about 5 ml and cooling to room temperature. Addition of a few drops of triethylamine increased the rate of the reaction, but did not influence the overall yield of the product. The red solid was filtered off, washed with a small amount of cold methanol and dried in vacuum. Yield: 595 mg (80%). Elemental analysis, Found: C, 45.2; H, 3.3; N, 11.6%; Calcd. for C$_{28}$H$_{24}$N$_6$O$_4$U: C, 45.0; H, 3.2; N, 11.3%. IR (ν_{max}/cm^{-1}): 1575 (C=N), 912 (O=U=O).

The same procedure can be applied when the reaction is performed with [NBu$_4$]$_2$[UO$_2$Cl$_4$] instead of uranyl nitrate.

Single crystals suitable for X-ray diffraction were obtained from hot methanol.

[UO$_2$(L^3)$_2$]. The compound was prepared as reported for [UO$_2$(L^2)$_2$] starting from HL^3 (665 mg, 2.2 mmol) and UO$_2$(NO$_3$)$_2$ · 6 H$_2$O (502 mg, 1 mmol). Red blocks were deposited directly from the reaction mixture. Yield: 785 mg (90%). Elemental analysis, Found: C, 49.8; H, 3.3; N, 12.8%; Calcd. for C$_{36}$H$_{26}$N$_8$O$_4$U: C, 49.5; H, 3.0; N, 12.8%. IR (ν_{max}/cm^{-1}): 1574 (C=N), 911 (O=U=O).

Single crystals suitable for X-ray diffraction were obtained from a CHCl$_3$/methanol mixture.

X-Ray structure determinations

The X-ray diffraction data were collected on an automated single crystal diffractometer of the type CAD4 (Enraf-Nonius, Delft) or a BRUKER SMART CCD with Mo Kα radiation. The structures were solved by direct methods using SHELXS-97 [11]. Subsequent Fourier-difference map analyses yielded the positions of the non-hydrogen atoms. Refinement was performed using SHELXL-97 [12]. The positions of the hydrogen atoms were calculated for idealised positions and treated with the 'riding model' option of SHELXL-97. Crystal data and more details of the data collections and refinements are contained in Table 3. Additional information on the structure determinations have been deposited at the Cambridge Crystallographic Data Centre. See information for Authors, Issue No. 1.

References

[1] U. Abram, E. Schulz Lang, E. Bonfada, *Z. Anorg. Allg. Chem.* **2002,** *626*, 1873.

[2] a) B. V. Argawala, S. Hingorani, G. A. Gowda, *Inorg. Chim. Acta* **1990**, *176*, 149; b) J. B. Gandi, N. D. Kulkarni, *Transition Met. Chem.* **2001**, *26*, 96; c) J. B. Gandi, N. D. Kulkarni, *Transition Met. Chem.* **2000**, *25*, 209; d) R. A. Lal, S. Adhikari, A. Kumar, *Indian J. Chem. Section A*, **1997**, *36*, 1063; e) Xiao-Yuan Chen, Shu-Zhong Zhan, Qing-Jin Meng, *Transition Met. Chem.* **1996**, *21*, 345; f) R. A. Lal, A. N. Siva, S. Adhikari, A Pal, *Indian J. Chem. Section A*, **1995**, *34*, 1000; g) M. Husain, S. S. Bhattacharjee, K. B. Singh, R-A. Lal, *Polyhedron* **1991**, *10*, 779.

[3] a) R. K. Agarwal, N. Tyagi, I. Chakraborti, Egyptian *J. Anal. Chem.* **1998**, *7*, 127; b) P. L. Lopez de Alba, E. O. Ramirez, *J. Radioanalyt. Nucl. Chem.* **1986**, *104*, 255; c) C. Ramachand-

raiah, D. Vijayakumari, K. Lakshminarayana, *J. Radioanalyt. Nucl. Chem*. **1993**, *175*, 185; d) D. Vijayakumari, K. Lakshminarayana, *J. Radioanalyt. Nucl. Chem.* **1993**, *175*, 1; e) M. Abu-Eid, N. A. Zatar, M. A. Al-Nuri, M. Khamis, S. Khalaf, *Israel. Spectr. Letters* **1992**, *25*, 585; f) M. V. Main, J. S. James, *Anal. Chem*. **1989**, *61*, 1272; g) J. L. Gomez Ariza, M. L. Marques Gonzalez, M. T. Montana Gonzalez, *Analyst* **1984**, *109*, 885.

[4] a) G. Bandoli, D. A. Clemente, G. Marangoni, G. Paolucci, *J. Chem. Soc. Chem. Commun*. **1978**, 235; b) G. Paolucci, G. Marangoni, *Inorg. Chim. Acta* **1977**, *24*, L5.

[5] a) C. E. Kyriakidis, P. C. Christidis, P. J. Rentzeparis, I. A. Tossidis, *Z. Kristallogr.* **1992**, 200, 15; b) G. Paolucci, G. Marangoni, G. Bandoli, D. A. Clemente, *J. Chem. Soc. Dalton Trans.* **1980**, 1304.

[6] a) M. T. Benson, T. R. Cundari, L. C. Saunders, S. O. Sommerer, *Inorg. Chim. Acta* **1997**, *258*, 127; b) J. E. Thomas, R. C. Palenik, G. J. Palenik, *Inorg. Chim. Acta* **1979**, *37*, L459;

c) D. G. Paschalidis, I. A. Tossidis, M. Gdaniec, *Polyhedron* **2000**, *19*, 2629.

[7] A. Bino, R. Frim, M. van Genderen, *Inorg. Chim. Acta* **1987**, *127*, 95.

[8] J. Grewe, A. Hagenbach, B. Stromburg, R. Alberto, E. Vazquez-Lopez, U. Abram, *Z. Anorg. Allg. Chem.* **2003**, *629*, 303.

[9] F. B. Tamboura, M. Diop, M. Gaye, A. S. Sall, A. H. Barry, T. Jouini, *Inorg. Chem. Commun.* **2003**, *6*, 1004.

[10] U. Abram, C. C. Gatto, E. Bonfada, E. Schulz Lang, *Inorg. Chem. Commun*. **2002**, *5*, 461.

[11] G. M. Sheldrick, SHELXS-97, A program for the solution of crystal structures, University of Göttingen, 1997.

[12] G. M. Sheldrick, SHELXL-97, A program for the refinement of crystal structures, University of Göttingen, 1997

[13] L. J. Farrugia, *J. Appl. Crystallogr.* **1997**, *30*, 565.

[14] H. Brandenburg, DIAMOND- A program for the representation of crystal structures.

Mono-, Di- and Trinuclear Dioxo Complexes of Uranium Containing Hydrazonato and Azomethine Ligands

C. C. Gatto[a], E. Schulz Lang[a], A. Kupfer[b], A. Hagenbach[b], U. Abram[b],*

[a] Santa Maria/Brazil, Department of Inorganic Chemistry of the Federal University
[b] Berlin, Institut für Chemie der Freien Universität Berlin

Abstract. Mono-, di or trinuclear dioxouranium complexes with benzoylhydrazonato or azomethine ligands were prepared by reactions of common dioxouranium precursors such as $UO_2(NO_3)_2 \cdot 6$ H_2O or $[NBu_4]_2[UO_2Cl_4]$ with vanillin benzoylhydrazone (H_2L^4), salicylaldehyde benzoylhydrazone (H_2L^5), 2-hydroxyacetylbenzene salicylhydrazone (H_3L^6) or N-(2-ethoxycarbonyl-3-oxo-but-1-en(1)yl)-2-aminophenol (H_2L^7).
Spectroscopic and X-ray crystallographic studies on the complexes $[NBu_4]_2[UO_2Cl_4] \cdot 2$ H_2L^4, $[UO_2(HL^5)(H_2L^5)_2](NO_3)$, $[HNEt_3]_2$-$[\{UO_2(L^6)\}_2]$ and $[HNEt_3]_2[\{UO_2(L^7)_3O]$ confirm that the individual donor atom constellation, the size of the potential chelate rings and the acidity of the OH and NH functionalities of the proligands have a strong influence on the structure of the products.

Keywords: Uranium; Benzoylhydrazonato ligands; Actinides; Azomethines; Structure analysis

---

Ein-, zwei- und dreikernige Dioxouranium(VI)-Komplexe mit Hydrazonat- und Azomethin-Liganden

Inhaltsübersicht. Ein-, zwei oder dreikernige Dioxouranium(VI)-Komplexe entstehen bei der Umsetzung einfacher Uranylverbindungen wie $UO_2(NO_3)_2 \cdot 6$ H_2O oder $[NBu_4]_2[UO_2Cl_4]$ mit Vanillinbenzoylhydrazon (H_2L^4), Salicylaldehydbenzoylhydrazon (H_2L^5), 2-Hydroxyacetylbenzensalicylhydrazon (H_3L^6) oder N-(2-ethoxycarbonyl-3-oxo-but-1-en(1)yl)-2-aminophenol (H_2L^7).
Spektroskopische und kristallographische Untersuchungen an den Komplexen $[NBu_4]_2[UO_2Cl_4] \cdot 2$ H_2L^4, $[UO_2(HL^5)(H_2L^5)_2](NO_3)$, $[HEt_3N]_2[\{UO_2(L^6)\}_2]$ und $[HEt_3N]_2[\{UO_2(L^7)_3O]$ zeigen, dass die individuelle Donoratomkonstellation in den Liganden, die Größe der potentiellen Chelatringe und die Acidität der OH- und NH-Gruppierungen in den Proliganden einen starken Einfluss auf die Struktur der Metallkomplexe haben.


Introduction

As a part of our systematic studies on the coordination chemistry of the early actinide elements we recently published reports on the structural chemistry of dioxouranium(VI) complexes with acetylpyridine thiosemicarbazonato, semicarbazonato, benzoylhydrazonato and related ligands [1−3]. The formation of complexes with medium stability was observed with acetylpyridine thiosemicarbazone (HL^{1a}) in which the pyridine nitrogen atom provides an additional donor site to the metal atom. More stable complexes are formed with 'harder' donor atoms such as oxygen as is provided by semicarbazones [HL^{1b}] or benzoylhydrazones (HL^2). They react with common dioxouranium precursors such as uranyl nitrate or $[NBu_4]_2[UO_2Cl_4]$ to form $[UO_2(L)_2]$ complexes with eight-coordinate uranium atoms.
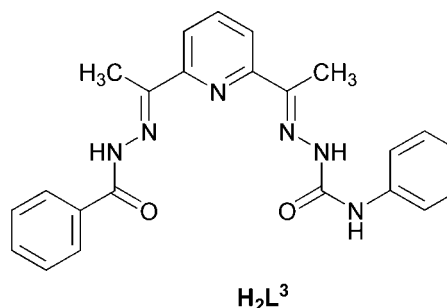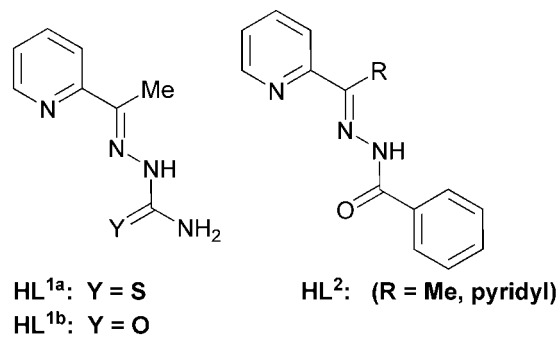
HL^{1a}: Y = S HL^2: (R = Me, pyridyl)
HL^{1b}: Y = O

H_2L^3

* Prof. Dr. Ulrich Abram
Freie Universität Berlin
Institut für Chemie
Fabeckstraße 34-36
D-14195 Berlin
Email: abram@chemie.fu-berlin.de
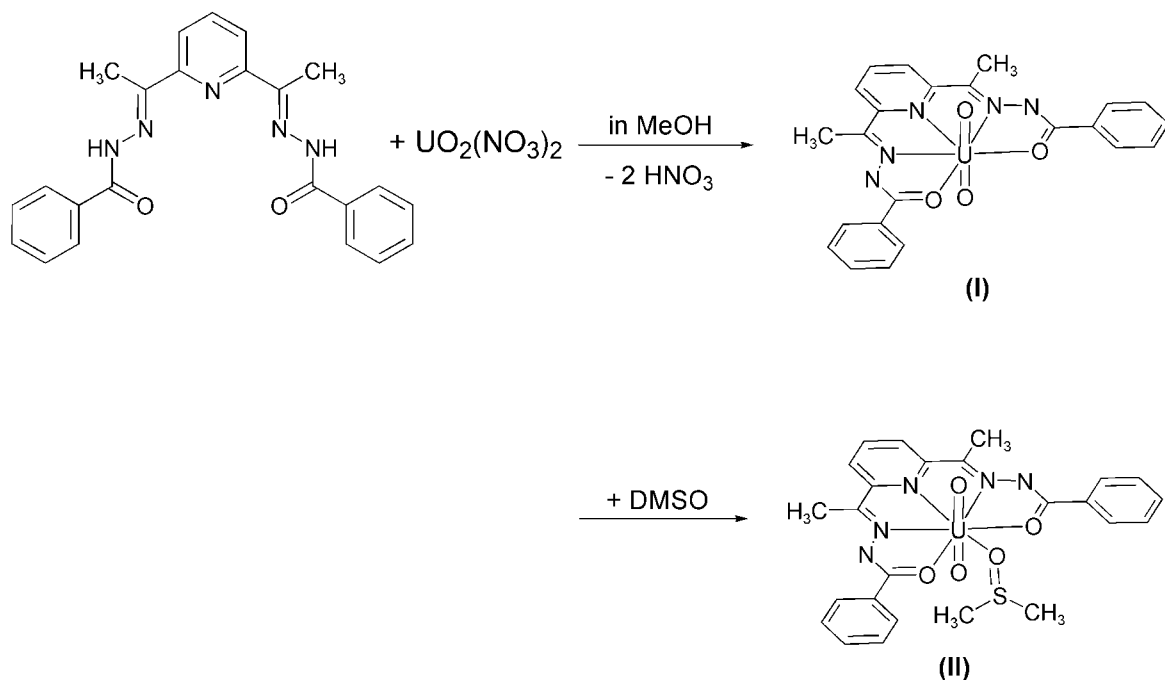
Scheme 1

The semicarbazones [4] and benzoylhydrazones [2] of type HL^{1b} and HL^2 act as tridentate, singly deprotonated ligands in these complexes. Ligands of the type H$_2$L^3 and their symmetric bis(benzoylhydrazone) or bis(semicarbazone) analogues coordinate to uranyl ions under double deprotonation and the formation of complexes containing uranium atoms of the coordination number seven. The equatorial coordination spheres of these pentagonal bipyramidal uranium complexes are readily extended by the addition of a monodentate ligand such as pyridine or dimethyl sulfoxide following the general route of Scheme 1. The resulting complexes contain eight-coordinate uranium atoms with distorted hexagonal bipyramidal coordination environments. An interesting structural feature of the binding of an additional ligand to complexes of the type (**I**) is the fact that the uranium (pyridine) nitrogen bond length increases. This, however, is not related to an increase of the bite angles of the binding sites which can be estimated by the intramolecular distances between neighbouring donor atoms.

The presence of the additional pyridine donor function in the thiosemicarbazones, semicarbazones and benzoylhydrazones of the types HL^1, HL^2 and H$_2$L^3 has found to be mandatory for the formation of stable dioxouranium(VI) complexes. The substitution of the pyridine sites of these ligands by other appropriate donor functions such as hydroxo or amine functionalities allows control to the overall charge of the formed complexes and gives access to polynuclear uranium complexes.

In the present paper, we describe reactions of common dioxouranium(VI) starting materials with benzoylhydrazones and azomethines containing additional hydroxo groups (H$_2$L^4 – H$_2$L^7). The positions of the hydroxo

groups and the nature of the accompanying donor function allow the synthesis of mono-, di- and trinuclear uranium complexes.

H$_2$L^4 H$_2$L^5

H$_3$L^6 H$_2$L^7
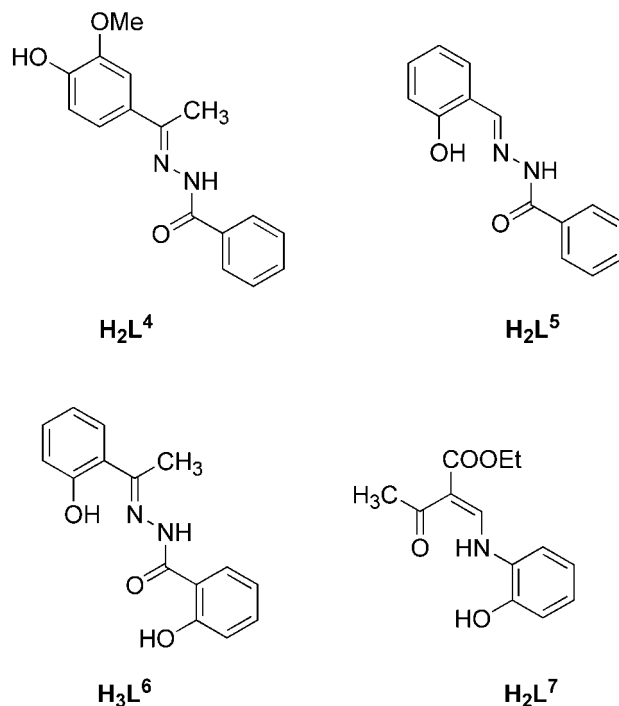
Results and Discussion

Vanillin benzoylhydrazone (H$_2$L^4) does not form uranium chelates during reactions with UO$_2$(NO$_3$)$_2$ · 6 H$_2$O or
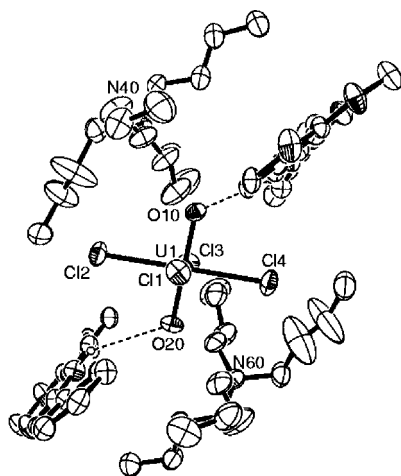
Fig. 1 Ellipsoid representation [16] of the [NBu₄]₂[UO₂Cl₄] · 2 H₂L⁴. Thermal ellipsoids represent 30 per cent probability.

Fig. 2 a) Ellipsoid representation [16] of the two crystallographically independent H₂L⁴ ligands b) Unit cell representation [19] showing the tube-like structure along the crystallographic *c* axis.

[NBu₄]₂[UO₂Cl₄]. From attempted reactions with uranyl nitrate in methanol, only the starting materials could be recovered. Addition of triethylamin resulted in the precipitation of a yellow polymeric, hydrolyzed material, which does not contain the benzoylhydrazone, as has been verified by IR spectroscopy. This behaviour of H₂L⁴ confirms the conclusion from previous reactions of benzoylhydrazones [2] and semicarbazones [3] derived from acetylpyridine and related carbonyl compounds, where the presence of the pyridine site was mandatory for the formation of stable dioxouranium complexes. The hydroxo group of proligand H₂L⁴ is in *trans* position to the benzoylhydrazone functionality and, thus, does not allow the formation of a second chelate ring. A similar result was observed for an attempted reaction with [NBu₄]₂[UO₂Cl₄]. The chloro ligands could not be replaced and the starting materials co-crystallized in the yellow crystals, which precipitated from the reaction mixture. The [UO₂Cl₄]²⁻ anion is located in the centre of two tetrabutylammonium cations and two molecules of vanillin benzoylhydrazone as is illustrated in Figure 1. Hydrogen bonds are established between the protonated hydrazone nitrogen atom of H₂L⁴ and an oxo ligand of the [UO₂Cl₄]²⁻ anions. This results in a twisting of the complex ion in this arrangement, which may be one of the reasons that the compound crystallizes in a non-centrosymmetric space group, despite the fact that each two tetrabutylammonium cations and H₂L⁴ molecules as well as a centrosymmetric complex anion are present.

The bond lengths and angles of the [UO₂Cl₄]²⁻ anion are in the same range as found for pure [NBu₄]₂[UO₂Cl₄] [5] and other tetrachlorodioxouranate(VI) salts [6]. The bonding situation inside H₂L⁴ (Fig. 2a) can best be described as a benzoylhydrazone with located C7−N8, C27−N28, C10−O12 and C30−O32 double bonds and N−N single bonds. An extended network of hydrogen bonds organizes the constituents of [NBu₄]₂[UO₂Cl₄] ·2 H₂L⁴ in a tube-like arrangement along the crystallographic *c* axis as is shown
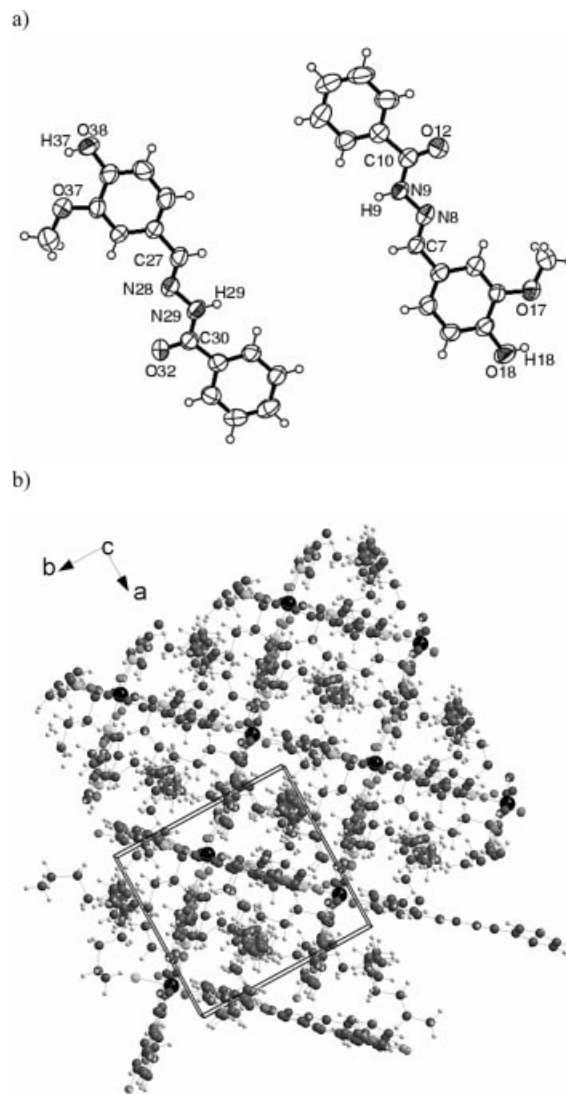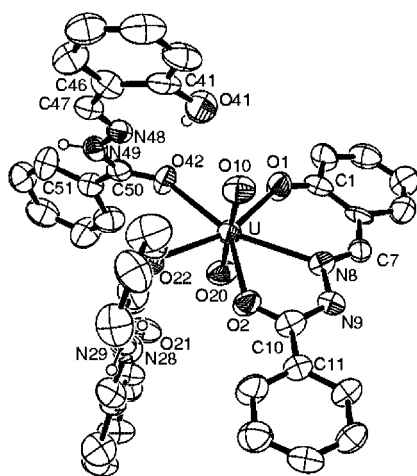
in Figure 2b. Selected bond lengths and angles as well as details of the hydrogen bonds are summarized in Table 1.

Whereas H₂L⁴ is obviously not able to form stable complexes with UO₂²⁺ ions, chelate formation was observed with salicylaldehyde benzoylhydrazone, H₂L⁵. UO₂(NO₃)₂ · 6 H₂O reacts with an excess of H₂L⁵ to form yellow crystals of [UO₂(HL⁵)(H₂L⁵)₂](NO₃). The product precipitates from the methanolic reaction mixture and is soluble in polar organic solvents such as dichloromethane or chloroform. The ¹H-NMR spectrum of the complex shows signals at 9.10 and 10.24 ppm, which suggest that the hydroxo and hydrazone functionalities are not deprotonated in the ligands. The IR spectrum, however, exhibits each two bands in the C=O and C=N region and the elemental analysis of the compound indicates the presence of three organic ligands per UO₂²⁺ unit. The IR frequency of the O=U=O unit is

Table 1 Selected bond lengths /Å and angles /° in $[NBu_4]_2[UO_2Cl_4]$ · $2H_2L^4$

U1−O10	1.757(6)	U1−Cl2	2.685(2)
U1−O20	1.777(6)	U1−Cl3	2.567(2)
U1−Cl1	2.656(3)	U1−Cl4	2.663(2)
C7−N8	1.25(1)	C27−N28	1.28(1)
N8−N9	1.39(1)	N28−N29	1.39(1)
N9−C10	1.33(1)	N29−C30	1.34(1)
C10−C12	1.22(1)	C30−C32	1.22(1)
C7−N8−N9	117.0(7)	C27−N28−N29	115.1(7)
N8−N9−C10	119.5(7)	N28−N29−C30	119.3(8)
N9−C10−O12	122.8(8)	N29−C30−O32	121.6(8)

Hydrogen bonds				
	D-H	H···A	D···A	D-H···A
O(18)-H(18)...O(12)#1	0.82	2.24	2.751(9)	121.1
O(18)-H(18)...O(17)	0.82	2.29	2.73(1)	113.7
O(18)-H(18)...N(8)#1	0.82	2.47	3.24(1)	157.2
N(9)-H(9)...O(10)	0.86	2.55	3.33(1)	151.2
O(38)-H(37)...O(37)	0.82	2.24	2.68(1)	114.5
O(38)-H(37)...O(32)#2	0.82	2.29	2.76(1)	117.5
O(38)-H(37)...N(28)#2	0.82	2.70	3.48(1)	161.4
N(29)-H(29)...O(20)	0.86	2.64	3.37(1)	143.4

Symmetry operations: #1 2−x, 0.5+y, −1−z; #2 1−x, −0.5+y, −z

Fig. 3 Ellipsoid representation [16] of the complex cation of $[\{UO_2(L^6)\}_2](NO_3)$. Thermal ellipsoids represent 50 per cent probability.

Table 2 Selected bond lengths /Å and angles /° in $[UO_2(HL^5)(H_2L^5)_2](NO_3)$

U−O10	1.785(9)	O1−C1	1.30(2)
U−O20	1.73(1)	C7−N8	1.46(2)
U−O1	2.18(1)	N8−N9	1.41(1)
U−N8	2.60(1)	N9−C10	1.34(2)
U−O2	2.435(9)	C10−O2	1.26(2)
U−O22	2.45(7)	O22−C30	1.32(2)
U−O42	2.365(8)	O42−C50	1.27(1)
O1−U−N8	68.8(3)	C7−N8−U	131.9(9)
N8−U−O2	61.9(3)	C7−N8−N9	112.8(9)
O2−U−O22	70.2(3)	U−N8−N9	115.3(7)
O22−U−O42	72.0(3)	N8−N9−C10	117.3(9)
O42−U−O1	87.1(3)	N9−C10−O2	118.6(9)
U−O1−C1	145.9(9)	C10−O2−U	126.8(9)
O1−C1−C6	124.3(9)	U−O22−C30	136.4(9)
C1−C6−C7	123.0(9)	U−O42−C50	146.3(9)
C6−C7−N8	124.4(9)		

are due to the restricting bite angle of the 5-membered chelate ring. This results in bond angles between neighbouring donor atoms of about 70° (3 times), 61° (5-membered chelate ring) and 87°. The chelating and one of the monodentate coordinated ligands are almost planar (main deviations from least square planes: 0.29(2) Å, r.m.s. 0.1669, and 0.09(2) Å, r.m.s. 0.0537), whereas the benzoyl phenyl ring of the third one is twisted by 22.7(6)° against the least square plane of the remaining ligand. The uranium−hydroxo bond (U−O1) is markedly shorter than the bonds to the benzoyl functionalities, which range between 2.365(8) and 2.45(1) Å. Nevertheless, the benzoyl functionality of H_2L^5 seems to be the preferred bonding side for uranium(VI) as is suggested by the monodentate coordination of the ligands at this position.

The reaction of $[NBu_4]_2[UO_2Cl_4]$ with an excess of H_2L^5 in methanol leads to the formation of the same complex cation, which precipitates from the reaction mixture as chloride salt. Reactions of equimolar amounts of H_2L^5 and the uranium precursors did not give pure crystalline products. Spectroscopic studies on the obtained yellow-orange powders suggest the formation of oxo or hydroxo bridged dioxouranium compounds when performed in methanol, whereas a complex with coordinated DMSO was obtained when the reaction was done in dimethylsulfoxide. A compound of the composition $[UO_2(HL^5)(DMSO)_2](NO_3)$ was also obtained from a prolonged heating of $[UO_2(HL^5)(H_2L^5)_2](NO_3)$ in DMSO (Scheme 2).

The addition of a hydroxo group in *ortho* position of the benzoylic phenyl ring changes the complex formation capabilities of the ligand and allows to connect two uranyl units. This has been demonstrated by reactions of H_3L^6 with uranyl nitrate and tetrachlorodioxouranate(VI). Both reactions result in the formation of the anionic dimeric complex $[\{UO_2(L^6\text{-}O,N,O',O'')\}_2]^{2-}$, which crystallizes as triethylammonium or tetrabutylammonium salt. The triply deprotonated organic ligands act as bridges between two uranyl units in a fashion that two 6-membered and one 5-membered chelate rings are established. The oxygen atoms of the

found at 908 cm^{-1} and is in accord with the expected value for a cationic uranyl complex [7]. A band at 1390 cm^{-1} suggests the presence of nitrate anions. The latter band is not present in the spectrum of the corresponding product that has been prepared from $[NBu_4]_2[UO_2Cl_4]$ and H_2L^5.

The crystal structure of $[UO_2(HL^5)(H_2L^5)_2](NO_3)$ confirms the spectroscopic results and shows that the uranyl core is coordinated by one tridentate, singly deprotonated salicylaldehyde benzoylhydrazonato and two neutral H_2L^5 ligands. The latter ones bind via their benzoyl oxygen atoms. An ellipsoid representation of the complex cation is shown in Figure 3, Table 2 contains selected bond lengths and angles. The coordination sphere of the uranium atom can best be described as a distorted pentagonal bipyramid with the oxo ligands in apical positions. Main distortions
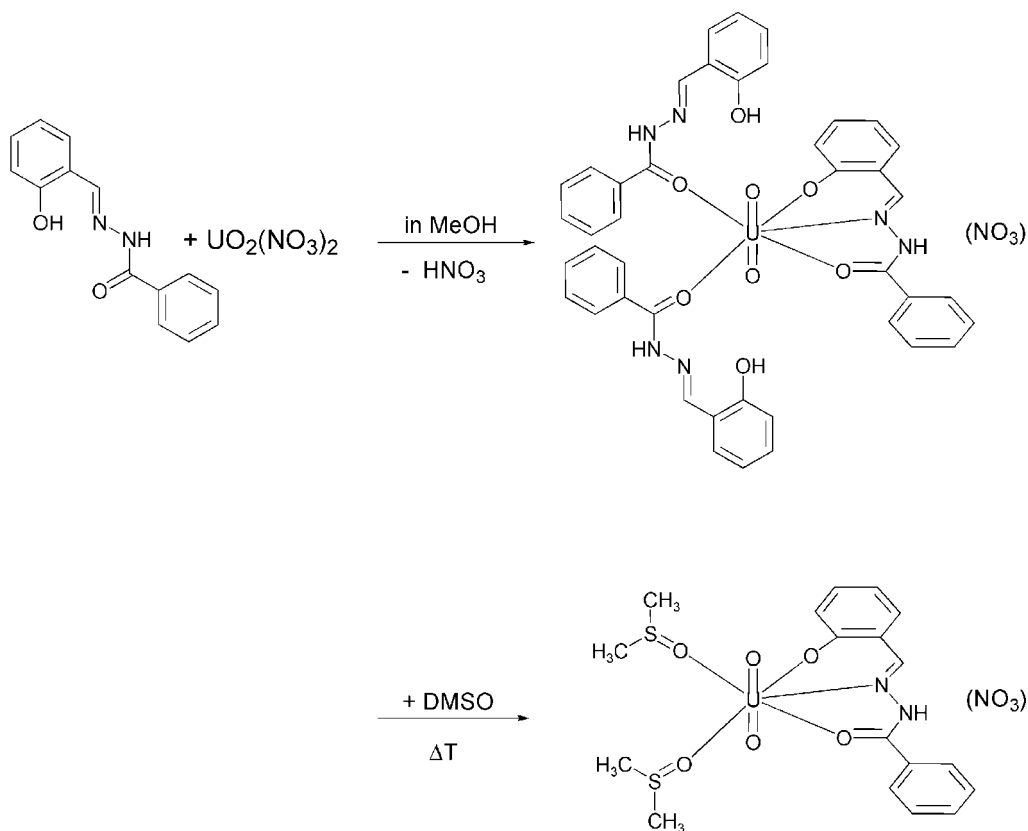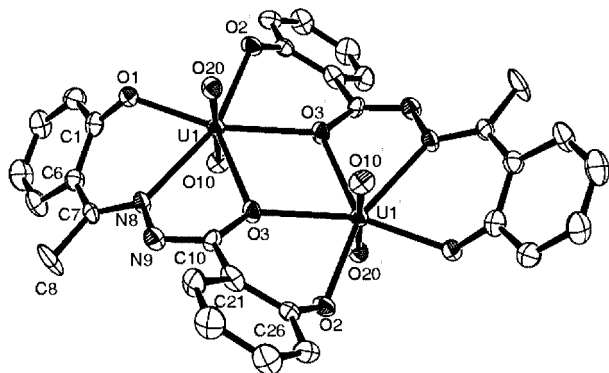
Scheme 2

Fig. 4 Ellipsoid representation [16] of the complex anion of $[HNEt_3]_2[\{UO_2(L^6)\}_2]$. Thermal ellipsoids represent 30 per cent probability.

**Table 3** Selected bond lengths /Å and angles /° in $[HNEt_3]_2[\{UO_2(L^6)\}_2]$

U1−O10	1.798(5)	C1−C6	1.44(1)
U1−O20	1.776(5)	C6−C7	1.460(9)
U1−O1	2.219(4)	C7−N8	1.312(8)
U1−N8	2.512(5)	N8−N9	1.415(7)
U1−O3	2.433(4)	N9−C10	1.298(8)
U1−O3#1	2.436(4)	C10−O3	1.322(7)
U1−O2#1	2.283(4)	C26−O2	1.330(8)
O1−C1	1.320(8)		
U1−O3−U1#1	112.6(2)	C6−C7−N8	119.3(6)
O1−U1−N8	70.5(2)	C7−N8−U1	130.0(4)
N8−U1−O3	62.5(2)	C7−N8−N9	113.9(5)
O3−U1−O3#1	67.4(2)	U1−N8−N9	115.9(4)
O3#1−U1−O2#1	71.7(2)	N8−N9−C10	111.6(5)
O2#1−U1−O1	88.9(2)	N9−C10−O3	123.9(5)
U1−O1−C1	124.7(4)	C10−O3−U1#1	129.0(4)
O1−C1−C6	121.8(6)	C10−O3−U1	116.4(4)
C1−C6−C7	122.2(6)	C26−O2−U1#1	123.2(4)

Symmetry operations: #1 1−x, 1−y, −z

benzoyl groups are μ_2-bonded and form a planar central $\{U_2O_2\}$ ring. This bonding mode results in a U−U distance of 4.051(1) Å which is similar to the values observed in hydroxo bridged dimers. An ellipsoid representation of the complex anion is shown in Figure 4, Table 3 contains selected bond lengths and angles. The U−O bond lengths range between 2.22 (hydroxylic) and 2.43 Å (benzoyl). Thus, the

formation of an oxygen bridge between two uranium atoms does not result in a significant lengthening of the corresponding U−O bonds (c.f. U−(benzoyl)O bond lengths between 2.37 and 2.45 Å in $[UO_2(HL^5)(H_2L^5)_2](NO_3)$). The coordination of a benzoyl group as bridging functionality

is without precedent in the uranium chemistry, whereas a number of compounds are reported with μ_2-bonded secondary or tertiary alkoxo groups [8].


III
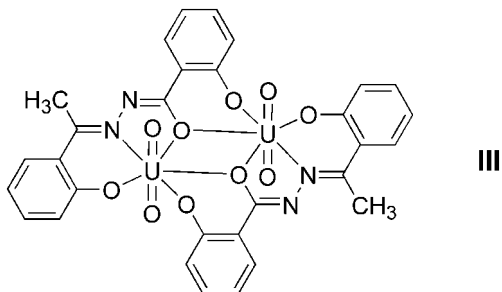
All the chelate rings are non-planar in $[\{UO_2(L^6\text{-}O,N,O',O'')\}_2]^{2-}$ and almost regular C=N double bonds with bond lengths of 1.312(8) and 1.298(8) Å are observed for C7-N8 and N9–C10. This results in a bonding mode of the benzoylhydrazone as is indicated in **III**. The phenyl rings are bent out of the coordination planes of the metal atoms which minimizes sterical strains and allows the unusual tetradentate bonding mode of the ligands.

The uranium atoms are 7-coordinate with the oxo ligands as apexes of a strongly distorted hexagonal bipyramids. Distortions in the equatorial coordination sphere are due to the restrictions induced by the tetradentate organic ligands and the presence of 5- and 6-membered chelate rings. This results in a puckered pentagonal base plane with deviations up to 0.174 Å (for O3′) from a least square plane formed by the uranium atom and the corresponding donor atoms.

The angles between neighbouring donor atoms are between 62.5(2) and 70.5(2)° (chelate rings and $\{U_2O_2\}$ ring) and 88.9(2)° (O–U–O2′). The relatively large value for the latter angle suggests the possibility to extend the coordination number of the uranium atom by the addition of a sixth ligand in this plane as has been observed for a number of diacetylpyridine benzoylhydrazonato [2] and semicarbazonato [3] complexes of uranium(VI). All attempts to coordinate an additional solvent molecule to $[\{UO_2(L^6\text{-}O,N,O',O'')\}_2]^{2-}$ by recrystallization from DMSO or pyridine, however, failed.

The azomethine ligand H_2L^7 has the same O,N,O donor atom constellation like H_2L^5 and H_3L^6. The peripheral electron-withdrawing ester functionalities, however, often provide distinct coordination capabilities to this type of ligands, for which frequently the term 'Jäger-type' ligands is used. This has been demonstrated for a large number of metals [9, 10]. The resulting complexes have been considered for their catalytic behaviour and to mimic metal sides in enzymes [11]. First uranium complexes have been published recently with the tetradentate ligand H_2L^8, which doubly deprotonates and occupies the equatorial coordination sphere of the $\{UO_2\}^{2+}$ core together with one additional monodentate ligand as is shown in Scheme 3 [12].

A trinuclear dioxouranium(VI) complex was obtained from reactions of uranyl nitrate with the 'Jäger-type' ligand H_2L^7. Contrasting the behaviour of H_2L^5 and H_3L^6, this compound is able to connect three uranium atoms by the formation of each one U–O–U bridge by the phenolato functionalities of three ligands. The trinuclear complex $[\{UO_2(L^7)\}_3O]^{2-}$ (**VI**) contains doubly deprotonated azo-
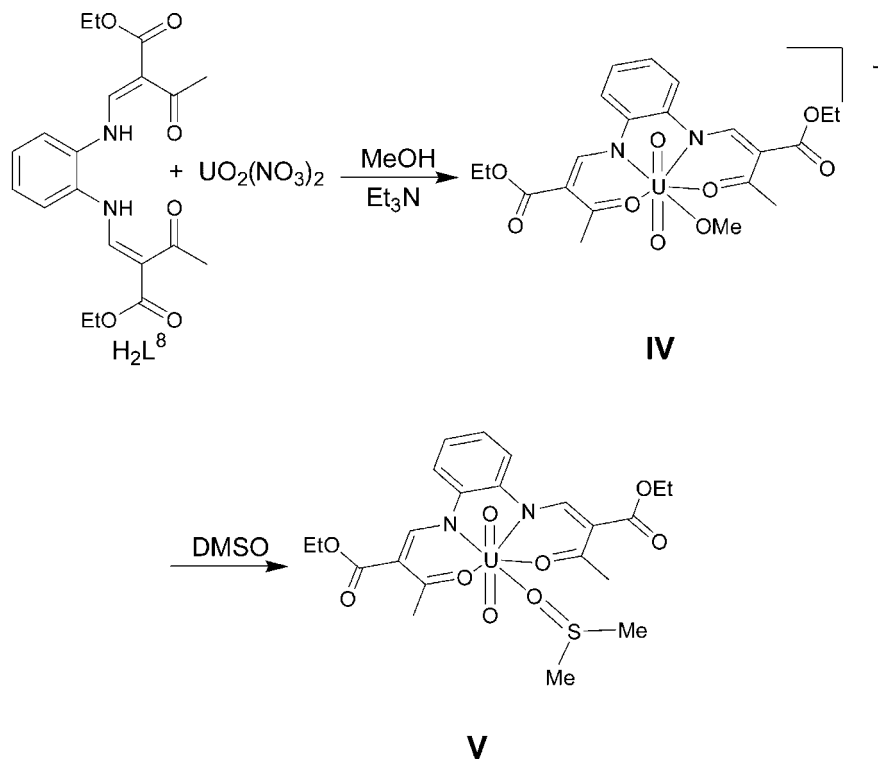

Scheme 3
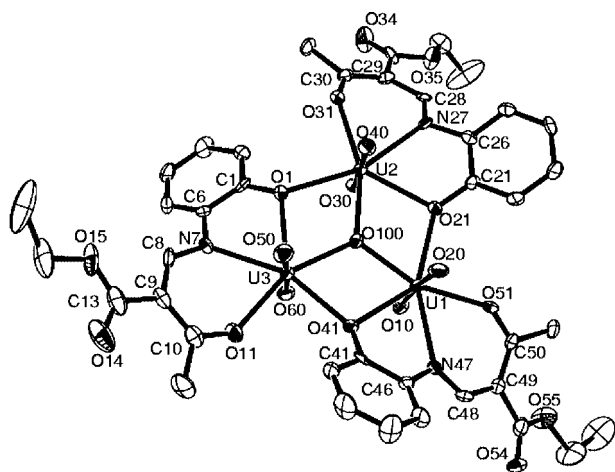
Fig. 5 Ellipsoid representation [16] of the complex anion of $[HNEt_3]_2[\{UO_2(L^7)\}_3O]$. Thermal ellipsoids represent 30 per cent probability.

Table 4 Selected bond lengths /Å and angles /° in $[HNEt_3]_2[\{UO_2(L^7)\}_3O](H_2O)$

U1−O10	1.775(5)	U2−O30	1.799(5)	U3−O50	1.782(5)
U1−O20	1.779(5)	U2−O40	1.773(5)	U3−O60	1.787(5)
U1−O41	2.445(5)	U2−O21	2.473(5)	U3−O1	2.476(5)
U1−N47	2.493(6)	U2−N27	2.484(6)	U3−N7	2.489(6)
U1−O51	2.306(5)	U2−O31	2.331(5)	U3−O11	2.319(5)
U1−O21	2.398(5)	U2−O1	2.445(5)	U3−O41	2.428(4)
U1−O100	2.190(4)	U2−O100	2.220(5)	U3−O100	2.224(5)
N47−C48	1.292(9)	N27−C28	1.283(8)	N7−C8	1.295(9)
C48−C49	1.412(9)	C28−C29	1.436(9)	C8−C9	1.423(9)
C49−C50	1.398(9)	C29−C30	1.389(9)	C9−C10	1.40(1)
C50−O51	1.283(8)	C30−O31	1.283(8)	C10−O11	1.282(9)
C41−O41	1.337(8)	C21−O21	1.335(8)	C1−O1	1.366(8)
U1−O100−U2	120.5(2)		O100−U1−O21		66.9(2)
U1−O100−U3	118.6(2)		O21−U2−N27		65.0(2)
U2−O100−O3	120.1(2)		O31−U2−O1		90.9(2)
U1−O21−U2	103.6(2)		O1−U2−O100		68.7(2)
U1−O41−U3	102.3(2)		O100−U2−O21		66.9(2)
U2−O1−U3	103.0(2)		O1−U3−N7		65.7(2)
O21−U1−O51	89.2(2)		N7−U3−O11		69.5(2)
O51−U1−N47	68.6(2)		O11−U3−O41		88.5(2)
N47−U1−O41	65.8(2)		O41−U3−O100		68.2(2)
O41−U1−O100	68.4(2)		O100−U3−O1		68.1(2)
N27−U2−O31	68.6(2)				

methine ligands and has been isolated as triethylammonium salt. It belongs to the small group of dioxouranium complexes with an additional central μ_3-bridging oxo ligand [13], what has been confirmed by an X-ray crystal structure. An ellipsoid representation of the complex anion is illustrated in Figure 5. Selected bond lengths and angles are summarized in Table 4. The most striking feature of the compound is the μ_3-oxo ligand which is located in the centre of the three uranium atoms with U−O100 bond lengths between 2.190(4) and 2.224(5) Å. This results in an almost equilateral triangle of uranium atoms with U−U distances of 3.7961(1), 3.828(1) and 3.851(1) Å. These distances are long enough to preclude any direct uranium-uranium interactions. The coordination environments of the individual

uranium atoms can best be described as pentagonal bipyramids. Distortions from the ideal symmetry are due to the 5- and 6-membered chelate rings and the two 4-membered $\{U_2O_2\}$ rings in the central part of the molecule. This results in X−U−Y angles between neighbouring donor atoms between 56 and 89°. The pentagonal plane is puckered with a maximum deviation from the planarity of about 0.16 Å for the bridging hydroxo oxygen atoms.
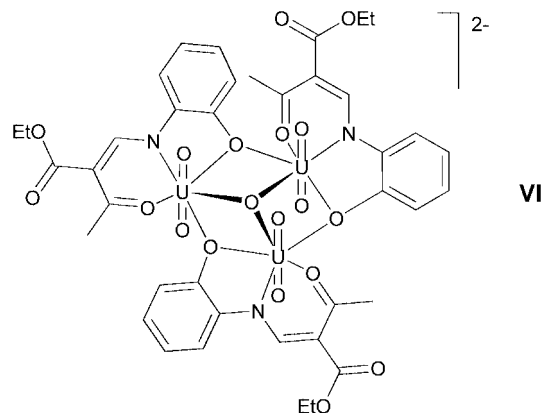
The coordination of the organic ligands is non-planar as a consequence of the restrictions by the formation of a pentagonal basal plane of the bipyramid. In octahedral or square-pyramidal complexes such as $[Ni(L^7)(L')]$ (L′ = PPh$_3$, 2,6-dimethylpyridine, NH$_3$, thiourea) [14, 15] or $[TcN(L^7)(PPh_3)]$ [16], an almost planar coordination mode is observed. This suggests considerable sterical strains for the uranium complex under study. Nevertheless, a shift of the π-system of H_2L^7 is observed upon coordination to the metal atom. This is obvious from the bond lengths in the backbone of the ligand. An almost located double bond with bond lengths of approximately 1.29 Å is observed between N7 and C8 (and the corresponding atoms in the other ligands), whereas the double bond in H_2L^7 is delocated between N7−C8 and C8−C9. Figure 6 shows an ellipsoid representation of the molecular structure of the proligand. Selected bond lengths are given in the corresponding Figure Caption. Spectroscopic studies and the crystal structure of the compound indicate protonation of the nitrogen atom N4 and the formation of a hydrogen bond between N7 and O11. The resulting 6-membered ring stabilizes this conformation of the proligand. Deprotonation which occurs during the formation of metal complexes results in a bond length shift inside the backbone of the ligand, which increases the electron density at the corresponding oxygen and nitrogen atoms and their ability to act as donors to metal ions.

Conclusions

The present paper shows that ligands with azomethine functions are well suited for the coordination of uranyl ions. Additional donor functionalities such as hydroxylic or car-
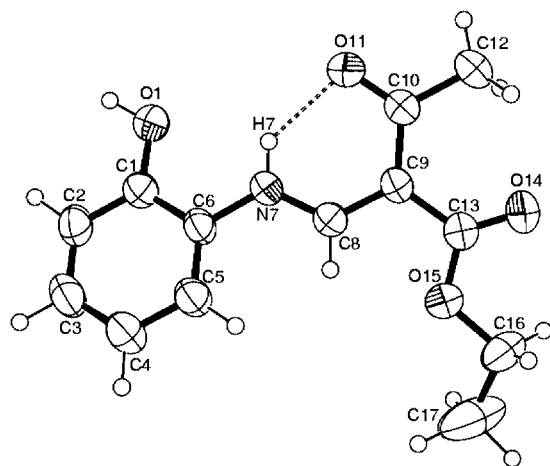
Fig. 6 Ellipsoid representation [16] of H_2L^7. Thermal ellipsoids represent 50 per cent probability.

Selected bond lengths /Å: C1−O1 1.356(3), C6−N7 1.424(2). N7−C8 1.321(4), C8−C9 1.388(4), C9−C10 1.442(4), C10−O11 1.249(3). Hydrogen bond: N7−H7 0.87(4) Å, H7...O11 1.96(4) Å, N7...O11 2.647(3) Å, N7−H7−O11 135(3)°.

bonyl groups increase the stability of the products. Mono-, di- or trinuclear dioxouranium compounds are formed depending on the donor atom constellation and the size of the potential chelate rings. Deprotonation of the ligands and condensation to multinuclear arrangements lead to anionic complexes. The new compounds serve as structural models for uranium complexes with biodegradation products and studies to check the potential of the ligands for the liquid-liquid extraction of uranium from radioactive waste solutions.

Experimental

$UO_2(NO_3)_2 \cdot 6 H_2O$ was purchased from Merck. $[NBu_4]_2[UO_2Cl_4]$ was prepared following a standard procedure from uranyl nitrate, aqueous HCl and tetrabutylammonium chloride. H_2L^4, H_2L^5 and H_3L^6 were prepared by heating equimolar amounts of the corresponding carbonyl components vanillin, salicyl aldehyde or 2-hydroxyacetylbenzene with benzoylhydrazine or salicylhydrazine in ethanol. The products were characterized by elemental analysis and standard spectroscopic methods. H_2L^7 was a gift of Professor E.G. Jäger (Jena).

Infrared spectra were recorded for KBr pellets on a FT IR Shimadzu spectrometer in the range between 4000 and 400 cm^{-1}. A Jeol FX400 NMR spectrometer was used to record the ^{1}H-NMR spectra.

[UO₂(HL⁵-O,O′)₂(H₂L⁵-O)₂](NO₃). $UO_2(NO_3)_2 \cdot 6 H_2O$ (502 mg, 1 mmol) was dissolved in 5 ml of methanol and H_2L^5 (1.2 g, 5 mmol) was added in 10 ml of methanol. The mixture was heated on reflux for 2 h. Yellow plates of $[UO_2(HL^5-O,O')_2(H_2L^5-O)_2](NO_3)$ were formed upon cooling directly from the reaction mixture. More material was obtained by slow evaporation of the solvent. Yield: 893 mg (85 %). Elemental analysis, Found: C, 48.4; H, 3.0; N, 9.2 %; Calcd. for $C_{42}H_{34}N_7O_{11}U$: C, 48.0; H, 3.2; N, 9.3 %. IR (ν_{max}/cm^{-1}): 3475, 3050, 2932 (OH, NH), 1623, 1605 (C=O), 1522, 1491 (C=N), 1390 (NO₃⁻), 908 (O=U=O).

[UO₂(HL⁵-O,O′)₂(H₂L⁵-O)₂]Cl. The complex was prepared as described for the nitrate salt, starting from $[NBu_4]_2[UO_2Cl_4]$ (896 mg, 1 mmol) and H_2L^5 (1.2 g, 5 mmol). A pale yellow powder of $[UO_2(HL^5-O,O')_2(H_2L^5-O)_2]Cl \cdot 3MeOH$ precipitated upon concentration of the reaction mixture. Yield: 477 mg (40 %). Elemental analysis, Found: C, 49.4; H, 3.1; N, 6.7 %; Calcd. for $C_{44}H_{34}N_6O_{11}U$: C, 49.8; H, 3.2; N, 6.8 %. IR (ν_{max}/cm^{-1}): 3466, 3007, 2872 (OH, NH), 1623, 1610 (C=O), 1530, 1500 (C=N), 909 (O=U=O).

[UO₂(HL⁵-O,O′)₂(DMSO)₂](NO₃). $UO_2(NO_3)_2 \cdot 6 H_2O$ (502 mg, 1 mmol) was dissolved in 3 ml of DMSO and H_2L^5 (240 mg, 1 mmol) was added. The mixture was heated to about 100 °C for 1 h. Yellow microcrystals of $[UO_2(HL^5-O,O')_2(DMSO)_2](NO_3)$ slowly deposited upon diffusion of water into the reaction mixture. Yield: 74 mg (10 %). Elemental analysis, Found: C, 30.7; H, 2.8; N, 5.6; S, 8.7 %; Calcd. for $C_{19}H_{23}N_3O_9S_2U$: C, 30.8; H, 3.1; N, 5.7; S, 8.7 %. IR (ν_{max}/cm^{-1}): 1610 (C=O), 1492 (C=N), 1370 (NO₃⁻), 909 (O=U=O).

[HNEt₃]₂[{UO₂(L⁶)}₂]. $UO_2(NO_3)_2 \cdot 6 H_2O$ (502 mg, 1 mmol) was dissolved in 5 ml of methanol and H_3L^6 (1.35 g, 5 mmol) was added in 5 ml of methanol. Three drops of NEt₃ were added and the mixture was heated on reflux for 2 h. The volume of the resulting red-brown solution was reduced to about 3 ml. An orange-red solid deposited upon cooling. Recrystallization from DMSO gave red crystalline blocks. Yield: 447 mg (70 %). Elemental analysis, Found: C, 39.4; H, 4.2; N, 6.5 %; Calcd. for $C_{42}H_{54}N_6O_{10}U_2$: 39.4; H, 4.2; N, 6.6 %. IR (ν_{max}/cm^{-1}): 1587 (C=N), 893 (O=U=O).

[NBu₄]₂[{UO₂(L⁶)}₂]. $[NBu_4]_2[UO_2Cl_4]$ (896 mg, 1 mmol) was dissolved in 3 ml of methanol and H_3L^6 (1.35 g, 5 mmol) was added in 3 ml of methanol. Three drops of NEt₃ were added and the mixture was heated on reflux for 2 h. Concentration of the solution and cooling gave dark crystals of $[NBu_4]_2[\{UO_2(L^6)\}_2]$. Yield: 430 mg (55 %). Elemental analysis, Found: C, 48.2; H, 6.2; N, 5.2 %; Calcd. for $C_{62}H_{94}N_6O_{10}U_2$: 47.8; H, 6.0; N, 5.4 %. IR (ν_{max}/cm^{-1}): 1590 (C=N), 897 (O=U=O).

[HNEt₃]₂[{UO₂(L⁷)}₃O](H₂O). $UO_2(NO_3)_2 \cdot 6 H_2O$ (502 mg, 1 mmol) was dissolved in 5 ml of methanol and H_2L^7 (1.245 g, 5 mmol) was added in 5 ml of methanol. Three drops of NEt₃ were added and the mixture was heated on reflux for 2 h. The volume of the resulting red solution was reduced to about 3 ml. Red crystals deposited upon cooling. Yield: 358 mg (60 %). Elemental analysis, Found: C, 34.2; H, 4.0; N, 3.8 %; Calcd. for $C_{51}H_{73}N_5O_{20}U_3$: C 34.2; H, 4.1; N, 3.9 %. IR (ν_{max}/cm^{-1}): 1695 (C=O), 1655 (C=O-U), 1583 (C=N), 897 (O=U=O). Recrystallization from hot DMSO gave large red blocks of $[HNEt_3]_2[\{UO_2(L^7)\}_3O]$ suitable for X-ray crystallography. Elemental analysis, Found: C, 33.9; H, 4.0; N, 4.2 %; Calcd. for $C_{51}H_{71}N_5O_{19}U_3$: C 34.5; H, 4.0; N, 3.9 %.

X-Ray structure determinations

The intensities for the X-ray determinations were collected on an automated single crystal diffractometer of the type CAD4 (Enraf-Nonius, Delft) or a Bruker Smart CCD with Mo Kα (λ = 0.71073 Å) or Cu Kα (λ = 1.54184 Å) radiation. The structures were solved by direct methods using SHELXS-97 [17]. Subsequent Fourier-difference map analyses yielded the positions of the non-hydrogen atoms. Refinement was performed using SHELXL-97 [18]. The positions of the hydrogen atoms in the uranium complexes were calculated for idealized positions and treated with the 'riding model' option of SHELXL-97. For H_2L^7, the H atoms were de-

Table 5 X-ray structure data collection and refinement parameters

	$[NBu_4]_2[UO_2Cl_4]\cdot 2H_2L^4$	$[UO_2(HL^5)(H_2L^5)_2](NO_3)$	$[HNEt_3]_2[\{UO_2(L^6)\}_2]$	$[HNEt_3]_2[\{UO_2(L^7)_3O\}\cdot H_2O$	H_2L^7
Crystal dimensions (mm³)	$0.2\cdot0.2\cdot0.2$	$0.5\cdot0.3\cdot0.05$	$0.2\cdot0.2\cdot0.2$	$0.3\cdot0.1\cdot0.1$	$0.35\cdot0.25\cdot0.1$
Formula	$C_{62}H_{100}Cl_4N_6O_8U$	$C_{42}H_{34}N_7O_{11}U$	$C_{42}H_{54}N_6O_{10}U_2$	$C_{51}H_{73}N_5O_{20}U_3$	$C_{13}H_{15}NO_4$
M/(g mol⁻¹)	1437.31	1050.79	1278.97	1790.23	249.26
Crystal system	monoclinic	monoclinic	orthorhombic	monoclinic	orthorhombic
Space group	$P2_1$	$P2_1/c$	Pbca	$P2_1/n$	$Pna2_1$
Unit cell	a = 11.128(1)	a = 13.432(2) Å	a = 19.413(4) Å	a = 19.754(4) Å	a = 7.517(1)
	b = 11.504(1)	b = 25.502(3) Å	b = 8.752(2) Å	b = 14.312(3) Å	b = 16.224(3) Å
	c = 27.218(5)	c = 13.528(2) Å	c = 26.986(5) Å	c = 22.241(4) Å	c = 10.807(1)
	β = 99.12(1)	β = 117.15(1)		b = 107.12(1)°	
V/Å³	3440.3(8)	4123(1)	4585(2)	6009(2)	1318.0(3)
Z	2	4	4	4	4
D_c/(g cm⁻³)	1.387	1.693	1.853	1.979	1.256
Measuring temperature/°C	20	20	−100	−100	20
Linear absorption coefficient/mm⁻¹	2.568	4.006	7.115	8.139	0.779
Absorption correction	DELABS [17]	DELABS [17]	SADABS [18]	DELABS [17]	None
T_{min}	0.437	0.2393	0.3303	0.235	−
T_{max}	0.813	0.8248	0.8352	0.672	−
Measured reflections	15762	9849	53696	53009	4991
Independent reflections / R_{int}	14814 / 0.049	8627 / 0.081	7039 / 0.111	12304 / 0.079	2211 / 0.028
Refined parameters	730	550	271	712	224
R1 (F) / wR2 (F²) (I > 2σ(I))	0.0505 / 0.1264	0.0568 / 0.1340	0.0376 / 0.0820	0.0345 / 0.0628	0.0458 / 0.1302
Device	CAD4	CAD4	BRUKER Smart	BRUKER Smart	CAD4
Radiation	Mo Kα	Mo Kα	Mo Kα	Mo Kα	Cu Kα
GooF	1.035	0.824	0.817	0.956	1.035
Flack parameter	0.008(7)	−	−	−	0.2(3)
Deposit	CCDC-235132	CCDC-235133	CCDC-235134	CCDC-235135	CCDC-235136

rived from the final Fourier map and refined. Crystal data and more details of the data collections and refinements are contained in Table 5. Additional information on the structure determinations have been deposited at the Cambridge Crystallographic Data Centre. See information for Authors, Issue No. 1.

References

[1] U. Abram, E. Schulz Lang, E. Bonfada, *Z. Anorg. Allg. Chem.* **2002,** *626*, 1873.

[2] C.C. Gatto, E. Schulz Lang, A. Kupfer, A. Hagenbach, D. Wille, U. Abram, *Z. Anorg. Allg. Chem.* **2004**, *628*, 735.

[3] C.C. Gatto, E. Schulz Lang, A. Jagst, U. Abram, *Inorg. Chim. Acta*, in press.

[4] A. Bino, R. Frim, M. van Genderen, *Inorg. Chim. Acta* **1987**, *127*, 95.

[5] L. di Sipio, E. Tondello, G. Pelizzi, G. Ingletto, A. Montenero, *Cryst. Struct. Commun.* **1974**, *3*, 527.

[6] Cambridge Crystallographic Structural database, vers. 5.25, Cambridge, **2004**.

[7] G. Paolucci, G. Marangoni, G. Bandoli, D.A. Clemente, *J. Chem. Soc. Dalton Trans.* **1980**, 1304.

[8] a) R.L. Lintvedt, H.J. Heeg, N. Ahmad, M.D. Glick, *Inorg. Chem.* **1982**, *21*, 2350 ; b) P. Thuery, M. Nierlich, B. Souley, Z. Asfari, J. Vicens, *J. Chem. Soc. Dalton Trans.* **1999**, 2589 ; c) F.A. Cotton, D.O. Marler, W. Schwotzer, *Inorg. Chim. Acta* **1984**, *85*, L31 ; F.A. Cotton, D.O. Marler, W. Schwotzer, *Inorg.*

Chem. **1984**, *23*, 4211 ; d) C.J. Burns, A.P. Sattelberger, *Inorg. Chem.* **1988**, *27*, 3692 ; e) M. Brunell, C. Pereggo, G. Lugli, A. Mazzei, *J. Chem. Soc. Dalton Trans.* **1979**, 861 ; f) U. Casellato, P. Guerriero, S. Tamburini, P.A. Vigato, R. Graziani, *J. Chem. Soc. Dalton Trans.* **1990**, 1533 ; g) T. Arliguie, D. Baudry, M. Ephritikhine, M. Nierlich, M. Lance, J. Vigner, *J. Chem. Soc. Dalton Trans.* **1992**, 1019 ; h) W.G. Van der Sluys, J.C. Huffman, D.S. Ehler, N.N. Sauer, *Inorg. Chem.* **1992**, *31*, 1316 ; i) M.P. Wilkerson, J. Burns, H.J. Dewey, J.M. Martin, D.E. Morris, R.T. Paine, B.L. Scott, *Inorg. Chem.* **2000**, *39*, 5277 ; j) M.P. Wilkerson, J. Burns, D.E. Morris, R.T. Paine, B.L. Scott, *Inorg. Chem.* **2002**, *41*, 3110.

[9] E.G. Jäger, E. Häussler, M. Rudolph, A. Schneider, *Z. Anorg. Allg. Chem.* **1985**, *525*, 67.

[10] K. Müller, D. Seidel, E.G. Seidel, *Z. Anorg. Allg. Chem.* **1988**, *561*, 38 and refs. cited therein.

[11] E.G. Jäger, J. Knaudt, M. Rudolph, M. Rost, *Chem. Ber.* **1996**, *129*, 1041 and refs. cited therein.

[12] C.C. Gatto, E. Schulz Lang, U. Abram, *Inorg. Chem. Commun.* **2003**, *6*, 1001.

[13] a) R.L. Lintvedt, M.J. Heeg, N. Ahmad, M.D. Glick, *Inorg. Chem.* **1982**, *21*, 2350; b) P. Charpin, M. Lance, M. Nierlich, D. Vigner, J. Livet, C. Musikas, *Acta Crystallogr.* **1986**, *C42*, 1691; c) G. van der Bossche, M.R. Spirlet, J. Rebizant, J. Goffart, *Acta Crystallogr.* **1987**, *C43*, 837; d) O.A. Gerasko, D.G. Samsonenko, A.A. Sharonova, A.V. Virovets, J. Lipkowski, V.P. Fedin, *Izv. Akad. Nauk SSSR, Ser. Khim.* **2002**, 325; U. Turpeinen, R. Hamalainen, I. Mutikainen, O. Orama, *Acta Crystallogr.* **1996**, *C52*, 1169.

[14] D. Hess, H. Elias, H. Paulus, *Z. Anorg. Allg. Chem.* **1989**, *577*, 135.

[15] H. Elias, D. Hess, H. Paulus, E.-G. Jäger, F. Gräfe, *Z. Anorg. Allg. Chem.* **1990**, *589*, 101.

[16] U. Abram, S. Abram, R. Münze, E.-G. Jäger, J. Stach, R. Kirmse, G. Admiraal, P.T. Beurskens, *Inorg. Chim. Acta* **1991**, *182*, 233.

[17] G.M. Sheldrick, SHELXS97, a program for the solution of crystal structures, University of Göttingen, **1997**.

[18] G.M. Sheldrick, SHELXL97, a program for the refinement of crystal structures, University of Göttingen, **1997**.

[16] L.J. Farrugia, *J. Appl. Crystallogr.* **1997**, *30*, 565.

[17] A.L. Spek, *Acta Crystallogr.* **1990**, *A46*, C34.

[18] SADABS − a program for empirical absorption correction, BRUKER, **2002**.

[19] H. Brandenburg, DIAMOND- A program for the representation of crystal structures.

Dioxouranium(VI) complexes with 2,6-acetylpyridinebenzoylhydrazones and -semicarbazones

C.C. Gatto [a], E. Schulz Lang [a], A. Jagst [b], U. Abram [b],*

[a] *Departamento de Quimica, Universidade Federal de Santa Maria, 97.111 Santa Maria-RS, Brazil*
[b] *Freie Universität Berlin, Institute of Chemistry, Fabeckstr. 34-36, D-14195 Berlin, Germany*

Abstract

Benzoylhydrazones and semicarbazones derived from 2,6-diacetylpyridine react with common dioxouranium(VI) compounds such as uranyl nitrate or $[NBu_4]_2[UO_2Cl_4]$ to form air-stable complexes. 2,6-Diacetylpyridinebis(benzoylhydrazone) (H_2L^1), 2,6-diacetylpyridinebis(N4-phenylsemicarbazone) (H_2L^2) and the asymmetric proligand 2,6-diacetylpyridine(benzoylhydrazone)-(N4-phenylsemicarbazone) (H_2L^3) give yellow products of the composition $[UO_2(L)]$. The neutral compounds contain doubly deprotonated ligands and possess uranium atoms with distorted pentagonal-bipyramidal coordination spheres. The equatorial coordination spheres of the metal atoms can be extended by the addition of a monodentate ligand such as pyridine or DMSO. The uranium atoms in the resulting complexes have hexagonal-bipyramidal coordination environments with the oxo ligands in axial positions.

X-ray diffraction studies on $[UO_2(L^1)(DMSO)]$, $[UO_2(L^2)]$, $[UO_2(L^2)(DMSO)]$ and $[UO_2(L^3)]$ show relatively short U–O bonds to the benzoylic oxygen atoms between 2.273(6) and 2.368(5) Å. This suggests a preference of these donor sites of the ligands over their imino and amine functionalities (U–N bond lengths: 2.502(7)–2.671(7) Å). The addition of a sixth ligand to the equatorial coordination sphere results in a lengthening of the metal–pyridine bonds.
© 2004 Elsevier B.V. All rights reserved.

Keywords: Uranium; Benzoylhydrazones; Semicarbazones; Actinides; Structure analysis

1. Introduction

As a part of our systematic studies of the coordination chemistry of the early actinide elements, we recently published a report on the structural chemistry of thiosemicarbazonato complexes of uranium(VI) [1]. The formation of complexes with moderate stability was observed with acetylpyridine thiosemicarbazone. The presence of the pyridine nitrogen atom was mandatory for the formation of chelate complexes. This additional donor site is obviously essential

to establish a bond between the relatively 'hard' metal ion UO_2^{2+} and 'soft' donor sites such as the thione sulfur atoms in thiosemicarbazones. More stable complexes are expected with 'harder' donor atoms such as oxygen, as are provided by semicarbazones or hydrazones. A number of studies have been undertaken with both ligand systems and the formation of chelates with various compositions has been suggested on the basis of spectroscopic data [2]. Some of the compounds have been proposed for the spectrophotometric determination of metal ions including UO_2^{2+} [3], but less is known about the composition of the coordination environment of the metal. First structural reports of complexes with 2,6-diacetylpyridine-bis(2′-pyridyl)hydrazones [4], benzoylhydrazones [5]

* Corresponding author. Tel.: +49 30 83854002; fax: +49 30 838542676.
E-mail address: abram@chemie.fu-berlin.de (U. Abram).

and semicarbazones [6] describe uranyl complexes having pentagonal bipyramidal or hexagonal bipyramidal coordination spheres. The reasons for the respective composition of the equatorial coordination spheres and the influence of substituents are not yet clear. In the present paper, we describe the reactions of uranyl nitrate and $[NBu_4]_2[UO_2Cl_4]$ with 2,6-diacetyl-pyridinebis(benzoylhydrazone) (H_2L^{1a}), 2,6-diacetyl-pyridinebis(N4-phenylsemicarbazone) (H_2L^2), and 2,6-diacetylpyridine(benzoylhydrazone)(N4-phenylsemicarbazone) (HL^3), and the solid state structures of the products. H_2L^3 represents a prototype of new of asymmetric ligands, which combine three donor functionalities (aromatic amine, benzoylhydrazone and semicarbazone) in one molecule.

H_2L^{1a}: R^1 = H H_2L^{1b}: R^1 = OMe H_2L^2 H_2L^3
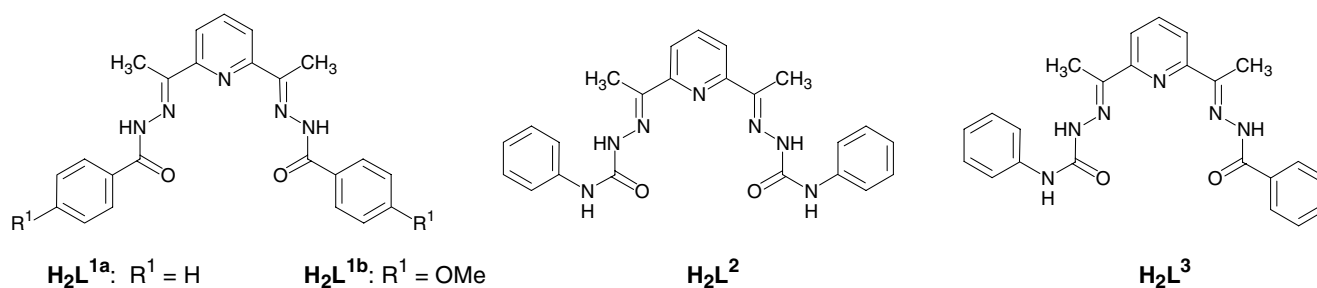
2. Experimental

HL^1 and HL^2 were prepared by refluxing equimolar amounts of 2,6-diacetylpyridine (Aldrich) and ben-zoylhydrazine (ACROS) or 4-phenylsemicarbazide (AC-ROS) in ethanol and recrystallizing from ethanol/water [6,7]. $[NBu_4]_2[UO_2Cl_4]$ was prepared from uranyl nitrate, aqueous HCl and tetrabutylammonium chloride following a standard procedure. Infrared spectra have been recorded for KBr pellets on a Shimadzu FT IR spectrometer in the range between 4000 and 400 cm^{-1}.

2.1. 2,6-Diacetylpyridinemono(4N-phenylsemicarbazone), HL^{3a}

2,6-Diacetylpyridine (1.63 g, 10.0 mmol) was dissolved in 50 ml of a hot 1:1 mixture of ethanol and water. A solution of 4-phenylsemicarbazide (1.51 g, 10.0 mmol) in 75 ml of water was slowly added to the reaction mixture. After heating at reflux for 1 h, the col-ourless precipitate was filtered off and washed with ethanol. Yield: 2.75 g (93%). *Anal.* Calc. for $C_{16}H_{16}N_4O_2$: C, 64.9; H, 5.4; N, 18.9. Found: C, 64.6; H, 5.5; N, 19.1%. IR (v_{max}/cm^{-1}): 3375, 3194 (NH), 1697,1680 (C=O). ^{1}H NMR (400 MHz, dmso-d_6): δ (ppm): CH$_3$ 2.20 (s, 3H), 2.67 (s, 3H); phenyl 7.03–8.65 (m, 8H); NH 9.01, 10.03 (s, 2H). FAB$^+$-MS: m/z = 297 ([M − H]$^+$); 204 (58%, [M − NH − Ph]$^+$).

2.2. H_2L^3

A suspension of HL^{3a} (340 mg, 1.2 mmol) and ben-zoylhydrazine (160 mg, 1.2 mmol) in 30 ml of iso-propanol was heated at reflux for 36 h. The hot reaction mixture was filtered and the bright-yellow precipitate was washed with 5 ml of ethanol. Yield: 0.33 g (66%). *Anal.* Calc. for $C_{23}H_{22}N_6O_2$: C, 66.7; H, 5.4; N, 20.3. Found: C, 66.5; H, 5.6; N, 19.9%. IR (v_{max}/cm^{-1}): 3389, 3201 (NH), 1689, 1653 (C=O). ^{1}H NMR (400 MHz, dmso-d_6): δ (ppm): CH$_3$ 2.42 (s, 3H,); 2.53 (s, 3H); phenyl 7.04–8.43 (m, 13H); NH 8.99 (s, 1H), 9.96 (s, 1H), 10.89 (s, 1H). FAB$^+$-MS: m/z = 415 (3%, [M − H]$^+$); 105 (12%, [Ph—C=O]$^+$).

2.3. $[UO_2(L^{1a})]$

HL^{1a} (440 mg, 1.1 mmol) was partially dissolved in 5 ml of methanol and added to a solution of UO_2-$(NO_3)_2 \cdot 6\, H_2O$ (502 mg, 1 mmol) in 3 ml of methanol. A clear yellow solution was formed while heating the mixture at reflux, and a bright yellow powder began to precipitate after about 15 min. After an overall refluxing time of 2 h, the mixture was cooled to room temperature and the yellow solid was filtered off.

The reaction rate can be increased by the addition of two drops of triethylamine. Then, the precipitation of the solid is complete after 30 min. The solid is almost insoluble in alcohols. Yield: 633 mg (95%). *Anal.* Calc. for $C_{23}H_{19}N_5O_4U$: C, 41.4; H, 2.8; N, 10.5. Found: C, 41.2; H, 2.7; N, 10.5%. IR (v_{max}/cm^{-1}): 1590 (C=N), 900 (O=U=O).

The same procedure can be applied when the reaction is performed with $[NBu_4]_2[UO_2Cl_4]$ instead of uranyl nitrate.

2.4. $[UO_2(L^{1a})(DMSO)]$

$[UO_2(L^{1a})]$ (333 mg, 0.5 mmol) was dissolved in about 1 ml of hot DMSO. Large red blocks deposited upon slow cooling of the solvent. More product could be obtained by diffusion of water into the DMSO solution. Yield: 224 mg (60%). *Anal.* Calc. for $C_{25}H_{25}N_5O_5$-SU: C, 41.2; H, 3.4; N, 9.6; S, 4.4. Found: C, 41.2; H,

3.3; N, 9.7; S, 4.5%. IR (v_{max}/cm^{-1}): 1585 (C=N), 914 (O=U=O).

Crystals suitable for X-ray diffraction were obtained directly from the reaction mixture.

2.5. [UO$_2$(L^2)]

The compound was prepared from UO$_2$(NO$_3$)$_2$ · 6H$_2$O or [NBu$_4$]$_2$[UO$_2$Cl$_4$] and H$_2$L^2 following the procedure given for [UO$_2$(L^{1a})]. Yellow powder. Yield: 60%. *Anal.* Calc. for C$_{23}$H$_{21}$N$_7$O$_4$U: C, 39.6; H, 3.0; N, 14.1. Found: C, 40.0; H, 3.1; N, 14.0%. IR (v_{max}/cm^{-1}): 1570 (C=N), 905 (O=U=O).

2.6. Attempts to prepare [UO$_2$(L^2)(DMSO)]

[UO$_2$(L^2)] (348 mg, 0.5 mmol) was dissolved in about 3 ml of hot DMSO. Orange-red crystals deposited upon diffusion of water into the DMSO solution. The crystals that deposit from such solutions have a composition of [UO$_2$(L^2)] · [UO$_2$(L^2)(DMSO)] · DMSO · H$_2$O and were suitable for X-ray diffraction. Yield: 176 mg (45%). *Anal.* Calc. for C$_{25}$H$_{25}$N$_5$O$_5$SU: C, 41.2; H, 3.4; N, 9.6; S, 4.4. Found: C, 41.2; H, 3.3; N, 9.7; S, 4.5%. IR (v_{max}/cm^{-1}): 1572 (C=N), 908 (O=U=O).

2.7. [UO$_2$(L^3)]

The compound was prepared from UO$_2$(NO$_3$)$_2$ · 6H$_2$O or [NBu$_4$]$_2$[UO$_2$Cl$_4$] and H$_2$L^3 following the procedure given for [UO$_2$(L^{1a})]. Yellow crystals suitable for X-ray diffraction deposited directly from the reaction mixture. Yield: 40%. *Anal.* Calc. for C$_{23}$H$_{20}$N$_6$O$_4$U: C, 40.5; H, 2.9; N, 12.3. Found: C, 40.1; H, 3.4; N, 11.7%. IR (v_{max}/cm^{-1}): 1591, 1554 (C=N), 908 (O=U=O).

2.8. X-ray structure determinations

The X-ray diffraction data were collected on an automated single crystal diffractometer of the type CAD4 (Enraf-Nonius, Delft) with Mo Kα radiation. The structures were solved by direct methods using SHELXS-97 [8]. Subsequent Fourier-difference map analyses yielded the positions of the non-hydrogen atoms. Refinement was performed using SHELXL-97 [9]. The positions of the hydrogen atoms were calculated for idealized positions and treated with the 'riding model' option of SHELXL-97. Crystal data and more details of the data collections and refinements are contained in Table 1. Additional information on the structure determinations have been deposited at the Cambridge Crystallographic Data Centre. See information for Authors, Issue No. 1.

3. Results and discussion

UO$_2$(NO$_3$)$_2$ · 6H$_2$O as well as [NBu$_4$]$_2$[UO$_2$Cl$_4$] react with the benzoylhydrazone or semicarbazone ligands H$_2$L^1–HL^3 in boiling methanol under complete substitution of the equatorial coordination sphere of the metal. Under these conditions, complete deprotonation of both ligand types is observed independent of the uranium precursor used, and neutral dioxouranium complexes are formed. No evidence has been found for the formation of complexes with non-deprotonated or semi-deprotonated organic ligands, as has been observed for related semicarbazones of lanthanides and chromium(III) [10], and other highly charged metal ions [6]. A complicated coordination pattern has also been described for products obtained from reactions of uranyl salts and 2,6-diacetylpyridine bis(*p*-methoxybenzoyl-hydrazone), where different structures have been assigned on the basis of spectroscopic data depending on the solvents and the uranium starting materials used [5b]. The only compound in this report which has been characterized by X-ray crystallography, however, is a neutral dioxouranium(VI) complex with a doubly deprotonated organic ligand in which the uranium atom is seven-coordinate.

Similar complexes are obtained when the ligands H$_2$L^{1a}, H$_2$L^2 or H$_2$L^3 are heated with UO$_2$(NO$_3$)$_2$ · 6H$_2$O or [NBu$_4$]$_2$[UO$_2$Cl$_4$] in boiling methanol. The reaction is faster when a supporting base such as triethylamine is added, but this is not mandatory. Yellow precipitates are formed upon cooling, which have been isolated and characterized by elemental analysis, IR and (partially) NMR measurements showing that the products formed from the different uranium precursors were identical. The compounds are poorly soluble in common solvents and, thus, do not allow a detailed NMR analysis, and in coordinating solvents such as DMSO or pyridine a conversion of the complexes is observed.

The U=O double bonds show characteristic IR bands between 900 and 908 cm^{-1}. This value is in accord with the neutral uranyl complexes in [5b], whereas anionic derivatives absorb in the range between 920 and 950 cm^{-1}. The proton NMR spectra prove the absence of NH protons of the organic ligands. No evidence was found for the coordination of methanol or water. This allows the conclusion that complexes of the composition [UO$_2$(L)] have been formed, despite the fact that the crystal structure of [UO$_2$(L^4)(H$_2$O)] (H$_2$L^4 = bis(2,6-diacetylpyridinebis(semicarbazone))) has been reported in a previous paper [6]. No evidence could be found for anionic uranyl complexes with non-deprotonated or monodeprotonated ligands. This strongly suggests that the hydrazonato and semicarbazonato complexes of the present study possess the same coordination sphere as the uranyl complex with 2,6-diacetylpyridine bis(methoxybenzoylhydrazone), H$_2$L^{1b}, which

Table 1
X-ray structure data collection and refinement parameters

	$[UO_2(L^{1a})(DMSO)]$	$[UO_2(L^2)] \cdot [UO_2(L^2)(DMSO)] \cdot DMSO \cdot H_2O$	$[UO_2(L^3)]$
Formula	$C_{25}H_{25}N_5O_5SU$	$C_{50}H_{54}N_{14}O_{11}S_2U_2$	$C_{23}H_{20}N_6O_4U$
M (g mol^{-1})	745.60	1567.25	682.48
Crystal system	orthorhombic	triclinic	monoclinic
Space group	*Pnma*	*P*$\bar{1}$	*P*2$_1$/*n*
Unit cell dimensions			
a	18.130(3)	8.284(1)	8.141(2)
b	17.514(1)	15.283(2)	10.985(2)
c	8.221(3)	23.700(3)	29.120(2)
α	90	75.52(1)	90
β	90	88.92(1)	93.71(9)
γ	90	78.30(1)	90
V (Å^3)	2610.5(6)	2843.1(7)	2598.7(8)
Z	4	2	4
D_c (g cm^{-3})	1.897	1.831	1.744
Linear absorption coefficient (mm^{-1})	6.343	5.832	6.284
Absorption correction	Ψ scans	Ψ scans	DELABS [13]
T_{min}/T_{max}	0.1339/0.4831	0.7094/0.9783	0.230/0.391
Measured reflections	6963	14998	3849
Independent reflections/R_{int}	2928/0.055	12389/0.033	3048/0.049
Refined parameters	178	716	307
$R_1(F)/wR_2(F^2)$ $(I > 2\sigma(I))$[a]	0.0459/0.0976	0.0459/0.0922	0.0677/0.1535
Goodness-of-fit	1.162	0.997	1.034
CCDC Deposit Nos.	230958	230959	230960

[a] $R_1 = |F_o - F_c|/|F_o|$; $wR_2 = [W(F_o^2 - F_c^2)^2/(wF_o^2)]^{-1/2}$.

shows a distorted pentagonal-bipyramidal coordination sphere of the metal atom [b]. The bond angles between neighbouring atoms inside the equatorial coordination sphere are approximately 63° (4 times) and 107° (between the oxygen atoms of the benzoyl groups) [5b] (see also Table 2), which suggests the possibility of the extension of the coordination number of the uranium atom by the addition of an appropriate monodentate ligand. This has been tested by heating the $[UO_2(L)]$ complexes in a strongly coordinating solvent such as DMSO. The yellow solids slowly dissolve in these solvents and the colour changes. Whereas a dark red solution was obtained with $[UO_2(L^{1a})]$, an orange-red colour was obtained with $[UO_2(L^2)]$. This behaviour suggests different reaction patterns for the hydrazonato and semicarbazonato complexes.

A reaction sequence according to Scheme 1 can be derived for HL^{1a}. It results in the formation of a neutral $[UO_2(L^{1a})(DMSO)]$ complex, which can be isolated in crystalline form by the addition of a small amount of water to the DMSO solution and slow cooling. The U=O stretching vibration is slightly shifted to higher frequencies. Similar changes in the position of the uranyl bands in dependence on the coordination number of the metal atom have been observed previously [5b].

Single crystals of $[UO_2(L^{1a})(DMSO)]$ have been studied by X-ray crystallography, showing that the complex possesses an eight-coordinate uranium atom. An ellipsoid representation of the molecular structure is shown in Fig. 1. Selected bond lengths and angles are summarized in Table 2. The coordination environment of the uranium atom can be described as a slightly distorted hexagonal bipyramid. Whereas the five donor atoms of the hydrazonato ligand and the uranium atom are almost perfectly coplanar (mean deviations from the mean least-square plane: 0.0816 Å, r.m.s. 0.0670), O30 deviated from this plane by 0.619(9) Å. The phenyl groups of the ligands are coplanar with the equatorial coordination sphere within 5°. The *X*–U–*Y* angles (*X* and *Y* are neighbouring equatorial donor atoms) range between 59.7(2)° and 61.6(1)°. The extension of the coordination number of the uranium atom causes lengthening of the uranium–nitrogen bonds to the chelating ligand as can be seen from a comparison with the corresponding data in the seven-coordinate complex $[UO_2(L^{1b})]$ [5b]. Selected bond lengths and angles of this compound are included in Table 1; the atomic numbering has been adopted to fit the labelling scheme applied in the present paper. No significant change can be derived for the bonding situation inside the hydrazonato ligand, which is doubly deprotonated in both compounds. Whereas the double bond between C7 and N2 is almost localized, a delocalization of the electron density of the C17–O18 double bond can be concluded. This results in a significant shortening of the C17–N3 bond as a consequence of complex formation and can best be described by the bonding scheme represented in **I**, irrespective of the coordination number of the uranium atoms and the ligand type, and has also been found in the semicarbazonato complexes $[UO_2(L^2)]$ and $[UO_2(L^2)(DMSO)]$.

Table 2
Selected bond lengths (Å) and angles (°) in [UO$_2$(L^{1a})(DMSO)], [UO$_2$(L^{1b})]^a, [UO$_2$(L^2)(DMSO)] and [UO$_2$(L^2)]

	[UO$_2$ (L^{1a})(DMSO)]	[UO$_2$(L^{1b})]^a	[UO$_2$(L^2)(DMSO)]	[UO$_2$(L^2)]
U–O10/O11	1.771(7)	1.77	1.752(5)	1.748(6)
U–O20/O12	1.764(6)	1.77	1.763(5)	1.762(6)
U–O18/O58	2.359(5)	2.32	2.360(5)	2.341(5)
U–O28/O68	^{b}	2.30	2.368(5)	2.273(6)
U–N2/N42	2.617(5)	2.47	2.559(6)	2.505(7)
U–N4/N44	^{b}	2.49	2.583(6)	2.503(7)
U–N1/N41	2.671(7)	2.52	2.610(6)	2.502(7)
U–O30	2.542(6)		2.673(6)	
O18/O58–C17/C57	1.265(8)	1.26	1.278(8)	1.27(1)
O28/O68–C27/C67	^{b}	1.30	1.259(9)	1.29(1)
C17/C57–N3/N43	1.306(9)	1.33	1.313(9)	1.33(1)
C27/C67–N5/N45	^{b}	1.30	1.34(1)	1.32(1)
N3/N43–N2/N42	1.380(8)	1.41	1.373(8)	1.381(9)
N4/N44–N5/N45	^{b}	1.40	1.385(8)	1.38(1)
N2/N42–C7/C47	1.303(8)	1.31	1.290(9)	1.29(1)
N4/N44–C9/C49		1.31	1.278(9)	1.28(1)
C7/C47–C6/C46	1.44(1)	1.50	1.45(1)	1.46(1)
C9/C49–C2/C42	^{b}	1.48	1.47(1)	1.48(1)
O18/O58–U–N2/N42	59.7(2)	63.5	61.5(2)	63.6(2)
O28/O68–U–N4/N44	59.7(2)^b	63.3	61.3(2)	63.6(2)
N2/N42–U–N1/N41	59.9(1)	63.3	61.6(2)	63.8(2)
N4/N44–U–N1/N41	59.9(1)^b	63.3	61.1(2)	63.5(2)
O18/–U–O30	61.6(1)		61.7(2)	
O18–U–O18′/O28				
O58–U–O68	120.6(2)	106.8	113.7(2)	105.5(2)
N1···N2/N41···N42	2.64	2.62	2.65	2.64
N1···N4/N41···N44	2.64^b	2.63	2.64	2.64
N2···O18/N21···O58	2.49	2.52	2.52	2.56
N4···O28/N44···O68	2.49^b	2.52	2.53	2.52

^{a} Values taken from [5b] and adopted to the atomic labelling schemes given in Figs. 1 and 2.
^{b} Symmetry related.

Scheme 1.

I R = Ph, NHPh
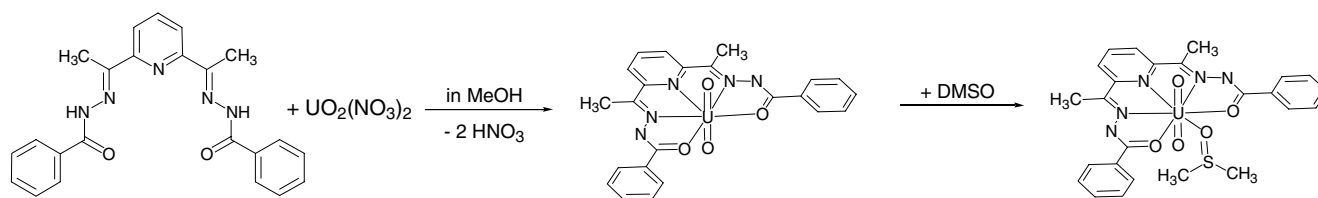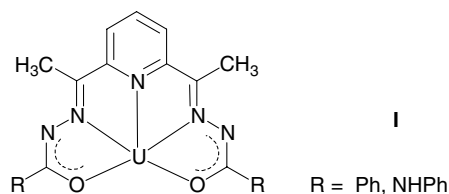
[UO$_2$(L^2)] and [UO$_2$(L^2)(DMSO)] co-crystallize as large orange-red plates when [UO$_2$(L^2)] is recrystallized from hot DMSO. The presence of two complexes with different coordination environments around uranium in the same crystals is somewhat surprising in light of the fact that the extension of the coordination number proceeds readily at [UO$_2$(L^1)] and that additional solvent molecules (H$_2$O and DMSO) are present. The structures of the complex molecules are illustrated in Fig. 2. The sulfur atom of the DMSO ligand in [UO$_2$(L^2)(DMSO)] is disordered over two positions. The overall bonding pattern in [UO$_2$(L^2)(DMSO)] is similar to that in [UO$_2$(L^{1a})(DMSO)] and [UO$_2$(L^4)-(H$_2$O)], with the uranium atom in an almost regular hexagonal-bipyramidal coordination environment. The pentadentate semicarbazonato ligands are almost
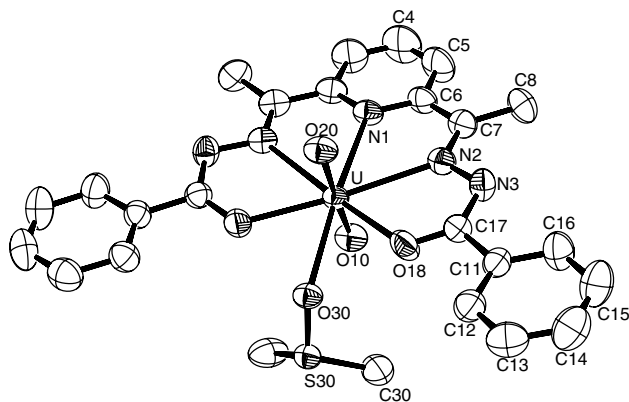
Fig. 1. Ellipsoid presentation [14] of [UO$_2$(L^{1a})(DMSO)]. Thermal ellipsoids represent 50% probability.

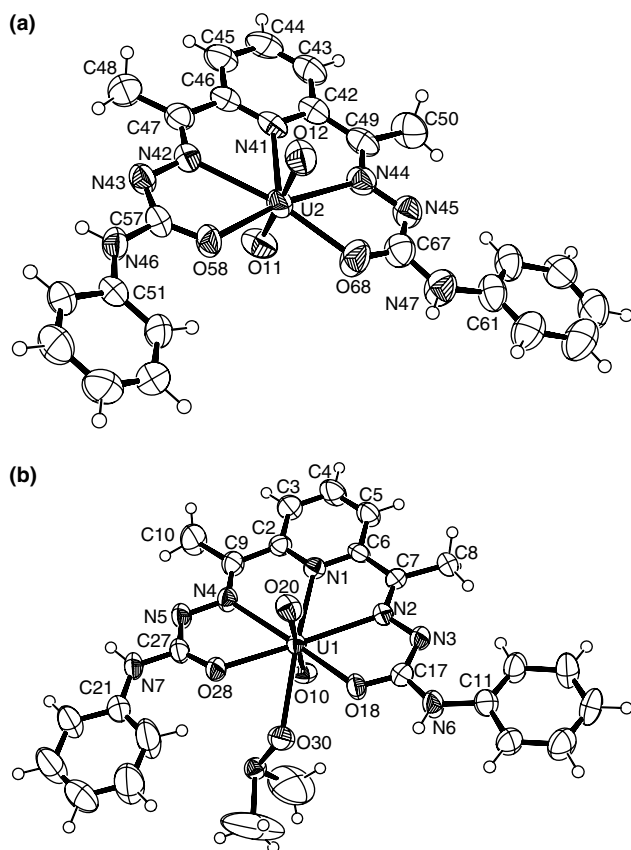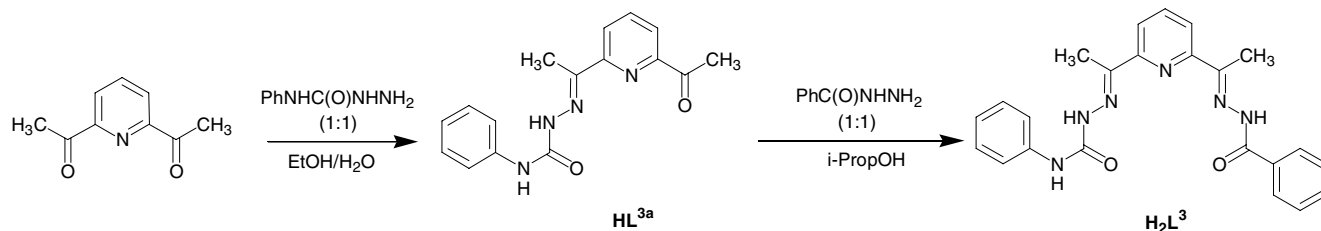Fig. 2. Ellipsoid presentations [14] of (a) [UO$_2$(L^2)] and (b) [UO$_2$(L^2)(DMSO)]. Thermal ellipsoids represent 50% probability.

perfectly planar in both complexes. There are maximum deviations from the mean least-squares planes which include all atoms of the L$_2^{2-}$ ligands, with the exception of the phenylrings of the semicarbazone units, of 0.18 Å (r.m.s.: 0.0747) in [UO$_2$(L^2)] and 0.081 Å (r.m.s.: 0.0351) in [UO$_2$(L^2)(DMSO)]. The phenyl rings are slightly twisted against these planes with angles between 2.1° and 11.8°. The oxygen atom of the DMSO ligand in [UO$_2$(L^2)(DMSO)] has a distance of 1.26 Å to the plane formed by the donor atoms of the pentadentate ligand. It is interesting to note that the increase of the coordination number and the observed lengthening of the uranium–nitrogen bonds are not related to an increase of the bite angles of the binding sites, which can be estimated by the intramolecular distances between the donor atoms of the five-membered chelate rings. The corresponding values are also listed in Table 2. A lengthening of the U–N1 bond by 0.18 Å is the result of the coordination of a DMSO ligand to [UO$_2$(L^2)], despite the fact that the resulting long U–O30 bond length of 2.673(6) Å reflects an only weak interaction (cf. uranium–DMSO bond lengths of 2.542(6) Å in [UO$_2$-(L^{1a})(DMSO)] or a mean value of 2.38 Å in [UO$_2$(DM-SO)$_5$][ClO$_4$]$_2$ [11]).

The U–N bond lengths are longer in the eight-coordinate [UO$_2$(L)(solvent)] complexes irrespective of the semicarbazonato or benzoylhydrazonato side arms. This is another indication that the observed bond lengthening is due to steric overcrowding of the equatorial coordination spheres in the compounds with coordination number eight.

The proligand H$_2$L^3 contains one benzoylhydrazone and one semicarbazone side arm and allows the coordination of metal atoms in an asymmetric manner. The synthesis of H$_2$L^3 succeeded by a stepwise condensation of 2,6-diacetylpyridine with N4-phenylsemicarbazide and benzoylhydrazine according to Scheme 2. This sequence is mandatory, since the reaction of 2,6-diacetyl-pyridine with semicarbazide always yields significant amounts of the bis-condensation product irrespective of the amounts of reactants applied. The general route of Scheme 2 can also be applied for the synthesis of other asymmetric ligands carrying Schiff base or thio-semicarbazone side arms. It gives approach to 'tailor-made' ligand systems in terms of 'hard' and 'soft'

Scheme 2.

donor atoms and/or their protonation/deprotonation behaviour.

Uranyl nitrate and $[NBu_4]_2[UO_2Cl_4]$ react with H_2L^3 in methanol to yield a yellow complex of the composition $[UO_2(L^3)]$. Expectedly, both side arms of the ligand are deprotonated and a neutral dioxouranium compound is formed. The U=O frequency is found at 908 cm^{-1}. The molecular structure of this compound, which is the first example of a mixed benzoyl-hydrazone/semicarbazone complex, is shown in Fig. 3. Selected bond lengths and angles are summarized in Table 3. The bonding situation inside the chelate rings is similar to those in the symmetric benzoylhydrazone and semicarbazone complexes. As has been observed previously, the U–N bond lengths are shorter in the seven-coordinate complexes compared with their analogues with coordination number eight, and almost localized C–N double bonds between the hydrazine nitrogen atoms and their neighbours can be stated. The O18–U–O28 angle of 109.9(6)° is larger than the corresponding value in $[UO_2(L^2)]$ and should allow the extension of the coordination sphere without intro-

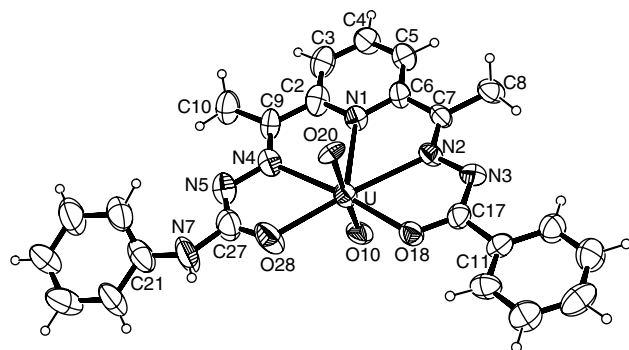duction of disproportional steric strain. This has been proven by heating $[UO_2(L^3)]$ in DMSO, which results in the formation of a deep red solution and the formation of the DMSO adduct is suggested with respect to the similar behaviour of $[UO_2(L^1)]$ and partially $[UO_2(L^2)]$. The red crystals, however, decompose rapidly when they are removed from the solvent to give an yellow-orange powder, the analysis of which did not give satisfactory evidence for an intact DMSO adduct. A mixed composition of the material containing $[UO_2(L^3)]$ and $[UO_2(L^3)(DMSO)]$ is strongly suggested, but we were not yet able to grow single crystals suitable for an X-ray structure analysis.

Fig. 4 shows a comparison of the coordination spheres of $[UO_2(L^{1a})(DMSO)]$, $[UO_2(L^2)]$ $[UO_2(L^2)(DMSO)]$ and $[UO_2(L^3)]$ containing uranium with the coordination numbers seven and eight. Particularly, the side views indicate the steric hindrance inside the equatorial coordination spheres of the metal atoms. The views along the uranyl units, however, show almost regular hexagons for the equatorial coordination spheres of $[UO_2(L^{1a})(DMSO)]$ and $[UO_2(L^2)(DMSO)]$, and the space between the oxygen donor atoms of the complexes with coordination number seven.

The present study shows that acetylpyridine benzoyl-hydrazones and semicarbazones are well suited to form stable complexes with dioxouranium(VI) units. All hydrazone and semicarbazone units of the ligands are deprotonated in the uranium complexes studied in this paper. This is in contrast to the behaviour in some lanthanide complexes where no or only partial deprotonation of the NH groups was observed [12]. The successful synthesis of the asymmetric ligand H_2L^3 and its uranium complex may provide a valuable tool for developing ligand systems, which can perfectly fit the coordination requirements of lanthanide and actinide ions.

Fig. 3. Ellipsoid presentation [14] of $[UO_2(L^3)]$. Thermal ellipsoids represent 50% probability.

Table 3
Selected bond lengths (Å) and angles (°) in $[UO_2(L^3)]$

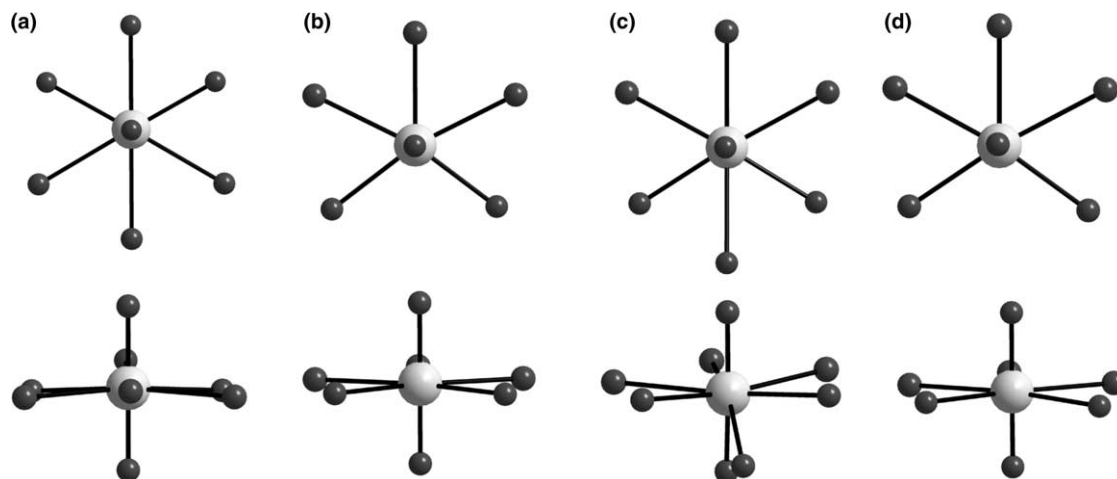|			
U–O10	1.726(1)	C17–N3	1.31(2)
U–O20	1.70(2)	N2-N3	1.39(2)
U–O18	2.30(1)	N2–C7	1.28(2)
U–O28	2.33(1)	C7–C6	1.44(3)
U–N1	2.54(2)	C27–O28	1.36(2)
U–N2	2.53(2)	C27–N5	1.25(3)
U–N4	2.55(2)	N4–N5	1.43(2)
C17–O18	1.32(2)	C27–N7	1.36(3)
N1–U–N2	61.2(5)	N2–U–O18	62.7(5)
N1–U–N4	62.4(6)	N4–U–O28	63.7(6)
O18–U–28	109.9(6)		
N1···N2	2.58	N2···O18	2.52
N1···N4	2.64	N4···O28	2.59

Fig. 4. Representation [15] of the coordination spheres of (a) $[UO_2(L^{1a})(DMSO)]$, (b) $[UO_2(L^2)]$, (c) $[UO_2(L^2)(DMSO)]$ and (d) $[UO_2(L^3)]$ in top and side views with respect to the O–U–O axis illustrating the distortions of the equatorial coordination spheres of the complexes in dependence on the chelating ligands and the coordination number of the metal atoms.

Acknowledgements

Appendix A. Supplementary material

Supplementary data associated with this article can be found, in the online version at doi:10.1016/j.ica.2004.07.011.

References

[1] U. Abram, E. Schulz Lang, E. Bonfada, Z. Anorg. Allg. Chem. 626 (2002) 1873.

[2] (a) B.V. Argawala, S. Hingorani, G.A. Gowda, Inorg. Chim. Acta 176 (1990) 149;
(b) J.B. Gandi, N.D. Kulkarni, Transition Met. Chem. 26 (2001) 96;
(c) J.B. Gandi, N.D. Kulkarni, Transition Met. Chem. 25 (2000) 209;
(d) R.A. Lal, S. Adhikari, A. Kumar, Indian J. Chem. Sect. A 36 (1997) 1063;
(e) Xiao-Yuan Chen, Shu-Zhong Zhan, Qing-Jin Meng, Transition Met. Chem. 21 (1996) 345;
(f) R.A. Lal, A.N. Siva, S. Adhikari, A. Pal, Indian J. Chem. Sect. A 34 (1995) 1000;
(g) M. Husain, S.S. Bhattacharjee, K.B. Singh, R.-A. Lal, Polyhedron 10 (1991) 779.

[3] (a) R.K. Agarwal, N. Tyagi, I. Chakraborti, Egyptian J. Anal. Chem. 7 (1998) 127;
(b) P.L. Lopez de Alba, E.O. Ramirez, J. Radioanalyt. Nucl. Chem. 104 (1986) 255;
(c) C. Ramachandraiah, D. Vijayakumari, K. Lakshminarayana, J. Radioanalyt. Nucl. Chem. 175 (1993) 185;

(d) D. Vijayakumari, K. Lakshminarayana, J. Radioanalyt. Nucl. Chem. 175 (1993) 1;
(e) M. Abu-Eid, N.A. Zatar, M.A. Al-Nuri, M. Khamis, S. Khalaf, Israel Spectr. Lett. 25 (1992) 585;
(f) M.V. Main, J.S. James, Anal. Chem. 61 (1989) 1272;
(g) J.L. Gomez Ariza, M.L. Marques Gonzalez, M.T. Montana Gonzalez, Analyst 109 (1984) 885.

[4] (a) G. Bandoli, D.A. Clemente, G. Marangoni, G. Paolucci, J. Chem. Soc., Chem. Commun. (1978) 235;
(b) G. Paolucci, G. Marangoni, Inorg. Chim. Acta 24 (1977) L5.

[5] (a) C.E. Kyriakidis, P.C. Christidis, P.J. Rentzeparis, I.A. Tossidis, Z. Kristallogr. 200 (1992) 15;
(b) G. Paolucci, G. Marangoni, G. Bandoli, D.A. Clemente, J. Chem. Soc., Dalton Trans. (1980) 1304.

[6] A. Bino, R. Frim, M. van Genderen, Inorg. Chim. Acta 127 (1987) 95.

[7] (a) J. Grewe, A. Hagenbach, B. Stromburg, R. Alberto, E. Vazquez-Lopez, U. Abram, Z. Anorg. Allg. Chem. 629 (2003) 303;
(b) U. Abram, C.C. Gatto, E. Bonfada, E. Schulz Lang, Inorg. Chem. Commun. 5 (2002) 461.

[8] G.M. Sheldrick, SHELXS-97, A program for the solution of crystal structures, University of Göttingen, 1997.

[9] G.M. Sheldrick, SHELXL-97, A Program for the Refinement of Crystal Structures, University of Göttingen, 1997.

[10] (a) M.T. Benson, T.R. Cundari, L.C. Saunders, S.O. Sommerer, Inorg. Chim. Acta 258 (1997) 127;
(b) J.E. Thomas, R.C. Palenik, G.J. Palenik, Inorg. Chim. Acta 37 (1979) L459;
(c) D.G. Paschalidis, I.A. Tossidis, M. Gdaniec, Polyhedron 19 (2000) 2629.

[11] J.M. Harrowfield, D.L. Kepert, J.M. Patrick, A.H. White, S.F. Lincoln, J. Chem. Soc., Dalton Trans. (1983) 393.

[12] F.B. Tamboura, M. Diop, M. Gaye, A.S. Sall, A.H. Barry, T. Jouini, Inorg. Chem. Commun. 6 (2003) 1004.

[13] A. Spek, PLATON – A Universal Crystallographic Tool, University of Utrecht, 2003.

[14] L.J. Farrugia, J. Appl. Crystallogr. 30 (1997) 565.

[15] H. Brandenburg, DIAMOND – A Program for the Representation of Crystal Structures.

Syntheses and Structures of 2-Acetylpyridine-(2-amino-benzoylhydrazone) and its Dioxouranium(VI) Complex

Claudia C. Gatto,[a] Ernesto S. Lang,[*,a] Robert A. Burrow [a] and Ulrich Abram[b]

[a] *Universidade Federal de Santa Maria, Departamento de Química, 97105-900 Santa Maria-RS, Brazil*

[b] *Freie Universität Berlin, Institute of Chemistry, Fabeckstr. 34-36, D-14195 Berlin, Germany*

A síntese e a caracterização da 2-acetilpiridina-(2-aminobenzoilhidrazona) (HL[1]) e do seu primeiro complexo com dióxido de urânio são descritas neste trabalho. A análise estrutural da hidrazona, HL[1], por difração de raios X do monocristal, mostra que sua estrutura molecular é quase planar no estado sólido, apresentando ligações de hidrogênio intermoleculares. O complexo $[UO_2(L^1)(dmf)_2](NO_3)$ é formado a partir de uma suspensão em refluxo de HL[1] com nitrato de uranila em metanol, na presença de pequena quantidade de trietilamina. A recristalização em dmf resulta na obtenção de cristais adequados para a difração de raios X. A análise por difração de raios X do complexo mostra uma geometria de coordenação bipiramidal de base pentagonal para o urânio(VI), formada pelos oxigênios da uranila nas posições apicais, uma molécula da hidrazona monodesprotonada e dois átomos de oxigênio das moléculas de dimetilformamida nas posições equatoriais.

We describe the synthesis and characterization of 2-acetylpyridine-(2-amino-benzoylhydrazone) (HL[1]) and its first dioxouranium complex. The single crystal X-ray structural analysis of the hydrazone, HL[1], reveals an almost planar structure with intermolecular hydrogen bonds. The complex $[UO_2(L^1)(dmf)_2](NO_3)$ is formed by refluxing a suspension of HL[1] with uranyl nitrate in methanol in the presence of a small quantity of triethylamine. Recrystallisation from dmf results in single crystals suitable for X-ray crystallography. The single crystal X-ray study of the complex shows a distorted pentagonal-bipyramidal coordination geometry around the uranium(VI) center, determined by two axial oxo ligands, two nitrogen and one oxygen atoms from a chelating monodeprotonated hydrazone and the oxygen donor atoms of two dimethylformamide molecules.

Keywords: uranium; hydrazones, actinides, structure analysis

Introduction

Schiff base complexes of uranium have aroused interest on account of their stability, high coordination numbers and usefulness in selective chemical separations. Uranyl complexes of ligands with O and N donors have been extensively reviewed and quite a few complexes of hydrazone Schiff bases have been reported.[1,2] As part of our systematic studies on the coordination chemistry of the early actinide elements, we recently published a report on the structural chemistry of thiosemicarbazonato complexes of uranium(VI).[3]

The formation of complexes with moderate stability is observed with acetylpyridine thiosemicarbazone. The presence of the pyridine nitrogen atom is essential for the formation of chelate complexes. This additional donor site is obviously essential to establish a bond between the relatively 'hard' UO_2^{2+} ions and 'soft' donor sites such as the thione sulphur atoms in thiosemicarbazones. More stable complexes are expected with 'harder' donor atoms such as oxygen, as provided by semicarbazones or hydrazones. A number of studies have been undertaken with both ligand systems and the formation of chelates with various compositions has been suggested on the basis of spectroscopic data.[4] Some derivatives of semicarbazones or hydrazones can be used for the spectrophotometric determination of metal ions including UO_2^{2+}.[5] In view of the structural interest involved in the coordination chemistry of uranium with Schiff base ligands, the synthesis and characterization of the Lewis base 2-acetylpyridine-(2-

*e-mail: eslang@quimica.ufsm.br

aminobenzoylhydrazone) and the first dioxouranium complex with this hydrazone are reported in this paper.

Experimental

Caution! *Uranium is a toxic metal and both ^{235}U and ^{238}U are radioactive isotopes. Good laboratory practices should be employed when working with any uranic material.*

$UO_2(NO_3)_2 \cdot 6H_2O$ was purchased from Merck. $(NBu_4)_2[UO_2Cl_4]$ was prepared following a standard procedure from uranyl nitrate, aqueous HCl and tetrabutyl-ammonium chloride. Infrared spectra were recorded for KBr pellets on a Shimadzu FTIR spectrophotometer between 4000 and 400 cm^{-1}. A Jeol FX400 NMR spectrometer was used to record the ^{1}H NMR spectra.

HL^1

2-Acetylpiridine (0.34 mL, 3 mmol) was added to a solution of 2-aminobenzoylhydrazide (453 mg, 3 mmol) dissolved in 20 mL of aqueous ethanol (1:1 v/v). The mixture was heated at reflux for 4 h and a yellow solution was formed. Single crystals suitable for X-ray diffraction analysis were obtained directly from the mother liquor upon standing overnight at room temperature. Yield: 708 mg, 93%. Elemental Analysis (Found/Calc. for $C_{14}H_{14}N_4O$): C, 66.05/66.13; H, 5.68/5.55; N, 22.37/22.03%. IR ν_{max}/cm^{-1}: 1705.0 (C=O), 1593.1, 1473.5 (C=N). ^{1}H NMR (400 MHz, DMSO-d_6), δ (ppm): CH$_3$ 2.45(s, 3H); phenyl 6.27-8.64 (m, 8H); NH 10.67 (s, 1H).

[UO$_2$(L^1)(dmf)$_2$](NO$_3$)

HL^1 (50 mg, 2 mmol) was partially dissolved in 10 mL of methanol and added to a solution of $UO_2(NO_3)_2 \cdot 6H_2O$ (100 mg, 2 mmol) in 5 mL of methanol. A few drops of NEt$_3$ were added and the mixture was heated at reflux for 2h. An orange powder was formed and filtered off. Single crystals suitable for X-ray diffraction analysis were obtained by slow cooling of a hot dmf solution. Yield: 94.7 mg, 65%. Elemental Analysis, (Found/Calc. for $C_{20}H_{27}N_7O_8U$): C, 32.62/32.84; H, 3.48/3.72; N, 13.83/13.40%. IR ν_{max}/cm^{-1}: 1654.8 (C=O), 1539.1 (C=N), 894.9 (O=U=O). The same procedure can be used when the reaction is performed with $(NBu_4)_2[UO_2Cl_4]$ instead of uranyl nitrate.

X-ray structure determinations

The X-ray diffraction data were collected on a Bruker Kappa APEX II single crystal diffractometer with Mo K$_\alpha$ radiation (0.71073 Å). SADABS was used to scale the data and perform the multi-scan absorption correction. The structures were solved by direct methods using SHELXS-97.[6] Subsequent Fourier-difference map analyses yielded the positions of the non-hydrogen atoms. Refinement was performed using SHELXL-97.[7] Hydrogen atoms were placed in idealized positions and treated with the 'riding model' option of SHELXL97. Crystal data and more details of data collections and refinements are presented in Table 1. Selected bond lengths and bond angles are given in Table 2.

Table 1. X-ray structure data collection and refinement parameters

	HL^1	[UO$_2$(L^1)(dmf)$_2$](NO$_3$)
Formula	$C_{14}H_{14}N_4O$	$C_{20}H_{27}N_7O_8U$
M / (g mol^{-1})	254.29	731.52
Crystal system	Orthorhombic	Monoclinic
Space group	*Pbca*	*C2/c*
Unit cell		
a/(Å)	11.475(2)	26.237(1)
b/(Å)	14.766(3)	7.945(4)
c/(Å)	15.177(3)	25.455(1)
β/(°)	90	107.507(3)
V/(Å^3)	2571.6(8)	5061.0(4)
Z	8	8
Linear absorption coefficient/(mm^{-1})	0.087	6.472
Measured reflections	12645	31092
Independent reflections / R_{int}	3562 / 0.0492	7429 / 0.0411
Refined parameters	169	325
t_{min} / t_{max}	0.7904 / 1.00	0.5955 / 1.00
F(000)	1072	2816
Goodness-of-fit (F^2)	0.994	0.854
R_1 (F) / wR_2 (F^2) ($I > 2\sigma$ (I))^a	0.0484 / 0.1073	0.0295 / 0.0776

^{a} $R_1 = |F_o - F_c| / |F_o|$; $wR_2 = [w(F_o^2 - F_c^2)^2/(wF_o^2)]^{-1/2}$.
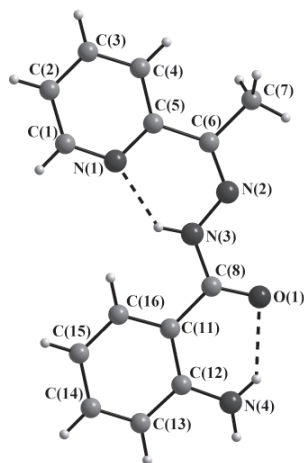
Table 2. Selected bond lengths (Å) and bond angles (°) for HL^1 and [UO$_2$(L^1)(dmf)$_2$](NO$_3$)

HL^1	[UO$_2$(L^1)(dmf)$_2$](NO$_3$)
C(6)-N(2) = 1.295(2)	U(1)–O(20) = 1.761(4)
N(2)-N(3) = 1.366(2)	U(1)–O(1) = 2.298(4)
N(3)-C(8) = 1.360(2)	U(1)–N(1) = 2.581(4)
N(4)-C(12) = 1.354(2)	U(1)–N(2) = 2.513(4)
N(1)-C(1) = 1.330(2)	C(6)–N(2) = 1.297(6)
O(1)-C(8) = 1.228(2)	U(1)–O(2) = 2.365(4)
N(3)-H(3)⋯N(1) = 2.617(2)	U(1)–O(3) = 2.329(4)
N(4)-H(4B)⋯O(1) = 2.667(2)	N(4)-H(4B)⋯N(3) = 2.705(7)
N(4)-H(4A)⋯N(2)^i = 3.126(2)	N(4)-H(4A)⋯O(5)^{ii} = 3.145(8)
O(1)–C(8)–N(3) = 120.95(1)	O(10)–U(1)–O(20) = 176.23(2)
C(6)–N(2)–N(3) = 118.57(1)	O(1)–U(1)–N(2) = 62.84(1)
O(1)–C(8)–C(11) = 123.93(1)	N(2)–U(1)–N(1) = 62.83(1)
N(3)–C(8)–C(11) = 115.12(1)	O(1)–U(1)–O(2) = 157.01(1)
C(8)–N(2)–N(3) = 118.57(1)	O(1)–U(1)–O(3) = 78.63(1)
	O(20)–U(1)–N(2) = 90.63(2)
	O(10)–U(1)–O(3) = 90.63(2)

Symmetry operations: ^{i} x–½, –y+½ –z+1; ^{ii} –x+1, y+1, –z+½
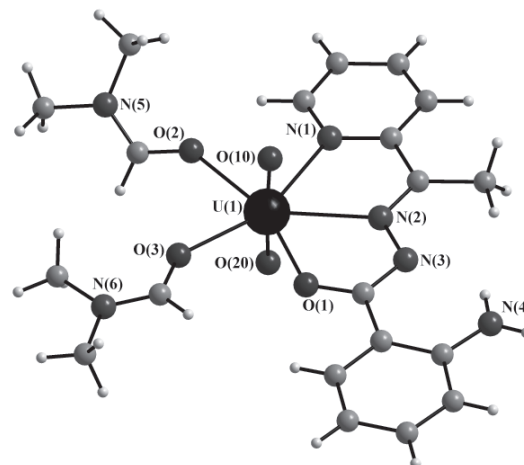
Results and Discussion

The synthesis of 2-acetylpyridine-(2-amino-benzoylhydrazone), HL^1, was performed by a condensation reaction in almost quantitative yield. The single crystal X-ray analysis of the product shows that the molecule is almost planar, with the pyridine ring N(1)-C(5) (r.m.s. = 0.0071 Å) and the phenyl ring C(11)-C(16) (r.m.s. = 0.0062 Å) lying 2.70(1)° and 12.93(9)° away, respectively, from the mean plane of the HN$_2$CO central unit. The double bonds N(2)=C(6) and C(8)=O(1) are localized, with bond lengths of 1.295(2) and 1.228(2) Å, respectively. The distance N(2)–N(3) of 1.366(2) Å is intermediate between those of an N–N single bond (1.425(27) Å)[8] and an N=N double bond (1.222(6) Å).[8] Figure 1 shows an representation of the molecular structure of HL^1.

Selected bond lengths and bond angles are given in Table 2.

The results of spectroscopic and X-ray diffraction studies of HL^1 indicate the protonation of the N(3) atom and the formation of intramolecular hydrogen bonds N(3)–H(3)⋯N(1) and N(4)–H(4B)⋯O(1) (Table 3). Additionally, the intermolecular hydrogen bond N(4)–H(4A)⋯N(2)^i is observed in the crystal structure (symmetry operation: ^{i} x+½, –y+½ –z+1). The molecules are packed in layers parallel to the *ac* plane and are held together essentially by van der Waals interactions.

UO$_2$(NO$_3$)$_2$·6H$_2$O or (NBu$_4$)$_2$[UO$_2$Cl$_4$] react with 2-acetylpyridine-(2-aminobenzoyl-hydrazone) to form an orange precipitate. The composition of the product is solvent dependent due to solvent complexation at the free coordination sites *trans* to the hydrazone. The crystal structure determination confirms that two molecules of dimethylformamide bind to the uranium center, producing [UO$_2$(L^1)(dmf)$_2$](NO$_3$) when the reaction is performed in dmf and the product is crystallized from that solvent. The hydrazone binds in its mono-deprotonated form. An representation of the molecular structure is illustrated in Figure 2 and selected bond lengths and angles are given in Table 2. The coordination sphere of the metal center can be described as a distorted pentagonal bipyramid with the oxo ligands in the axial positions and with a planar equatorial coordination environment (maximum deviation from the mean least-square plane formed by the atoms U(1), N(1), N(2), O(1), O(2) and O(3): r.m.s. 0.0466 Å). The X-ray structural analysis confirms the spectroscopic conclusion that the NH$_2$ group of the hydrazone is not involved in coordination to the metal center. The infrared spectrum of the complex shows a band at 2800 cm^{-1}, which suggests hydrogen bonds in the solid state and could be assigned to the NH$_2$ group. The presence of the UO$_2$$^{2+}$ unit is confirmed by a strong band at 894.9 cm^{-1}, and the

Figure 1. Graphical representation of the molecular structure of the 2-acetylpyridine-(2-aminobenzoylhydrazone).[10]

Figure 2. Graphical representation of the molecular structure of [UO$_2$(L^1)(dmf)$_2$]$^+$.[10]

Table 3. Hydrogen bonding distances (Å) and angles (°) in HL^1 and [UO$_2$(L^1)(dmf)$_2$](NO$_3$)

D–A···H	d(D–H)	d(H···A)	d(D···A)	<(DHA)
HL^1				
N(3)–H(3)···N(1)	0.86	1.94	2.617(2)	134.6(9)
N(4)–H(4B)···O(1)	0.86	2.02	2.677(2)	131.3(5)
N(4)–H(4A)···N(2)^i	0.86	2.34	3.126(2)	152.3(7)
[UO$_2$(L^1)(dmf)$_2$](NO$_3$)				
N(4)–H(4B)···N(3)	0.86	2.07	2.705(7)	130.4
N4–H(4A)···O(5)^{ii}	0.86	2.50	3.145(8)	132.0

Symmetry operations: ^{i} x–½, –y+½ –z+1; ^{ii} –x+1, y+1, –z+½

typical pattern for 2-acetylpyridine-(2-aminobenzoylhydrazone), with C=O and C=N vibrations, appears between 1654.8 and 1539.1 cm^{-1}.

The hydrazone ligand is almost planar, as a consequence of the constraints imposed by the formation of the pentagonal basal plane. This suggests considerable steric strain for the uranium complex under study. Principal distortions are due to the small bite angles of the hydrazone, which result in bond angles between 62.83(1) and 78.63(1)° for neighboring atoms in the equatorial plane. Deprotonation of the N(2) atom, which occurs during the formation of the metal complex, results in a shift of the double bonds within the backbone of the ligand, increasing the electron density at the corresponding oxygen and nitrogen atoms and their ability to act as donors to metal ions. A shift of the π-system of HL^1 from C(6) to C(8) and a delocalization of the electron density of the C(8)–O(1) double bond over the N(3)–C(8)–O(1) amide system is observed.

The hydrazone unit is deprotonated in the uranium complexes studied in this paper. This is in contrast to the behavior in some lanthanide complexes where no or only partial deprotonation of the NH groups was observed.[9] There are intramolecular hydrogen bonds between N(4)–H(4B)···N(3) and intermolecular hydrogen bonds between N(4)–H(4A)···O(5)^{ii}, Table 3 (symmetry operation ^{ii} –x+1, y+1, –z+½).

The present study shows that acetylpyridine benzoylhydrazones are well suitable to form stable complexes with dioxouranium(VI) units. The successful synthesis of the 2-acetylpyridine-(2-aminobenzoylhydrazone) and its uranium complex may constitute a starting point to the development of new ligand systems which can perfectly fit the coordination requirements of lanthanide and actinide ions.

Acknowledgments

Supplementary Information

Crystallographic data (excluding structure factors) for the structures in this paper have been deposited with the Cambridge Crystallographic Data Centre, CSD numbers CCDC 606778 and CCDC 609303. Copies of the data can be obtained, free of charge, via www.ccdc.cam.ac.uk/conts/retrieving.html, or from the Cambridge Crystallographic Data Centre, CCDC, 12 Union Road, Cambridge CB2 1EZ, UK; fax: +44 1223 336033; e-mail: deposit@ccdc.cam.ac.uk.

References

1. RadeckaParyzek, W.; Jankowska, E.; Luks, E.; *Polyhedron* **1988**, *7*, 439; Aggarwal, R.C.; Prasad, B.; *J. Inorg. Nucl. Chem.* **1971**, *33*, 3984.

2. Bandoli, G.; Clemente, D.A.; Marangoni, G.; Paolucci, G.; *J. Chem. Soc., Chem. Commun.* **1978**, 235; Paolucci, G.; Marangoni, G.; *Inorg. Chim. Acta* **1977**, *24*, L5; Kyriakidis, C.E.; Christidis, P.C.; Rentzeparis, P.J.; Tossidis, I.A.; *Z. Kristallogr.* **1992**, *200*, 15; Paolucci, G.; Marangoni, G.; Bandoli, G.; Clemente, D.A.; *J. Chem. Soc., Dalton Trans.* **1980**, 1304; Gulbaev, Y.I.; Azizov, T.A.; Khudoyarov, A.B.; Sharipov, K.T.; *Uzb. Khim. Sh.(Russ.)(Uzbek Chem. J.)* **1997**, 28; Gatto, C.C.; Lang, E.S.; Kupfer, A.; Hagenbach, A.; Wille, D.; Abram, U.; *Z. Anorg. Allg. Chem.* **2004**, *630*, 735; Gatto, C.C.; Lang, E.S.; Kupfer, A.; Hagenbach, A.; Abram, U.; *Z. Anorg. Allg. Chem.* **2004**, *630*, 1286; Gatto, C. C.; Lang, E.S.; Jagst, A.; Abram, U.; *Inorg. Chim. Acta* **2004**, *357*, 4405.

3. Abram, U.; Lang, E.S.; Bonfada, E.; *Z. Anorg. Allg. Chem.* **2002**, *626*, 1873.

4. Argawala, B.V.; Hingorani, S.; Gowda, G. A.; *Inorg. Chim. Acta* **1990**, *176*, 149; Gandi, J.B.; Kulkarni, N.D.; *Transition Met. Chem.* **2001**, *26*, 96; Gandi, J.B.; Kulkarni, N.D.; *Transition Met. Chem.* **2000**, *25*, 209; Lal, R.A.; Adhikari, S.; Kumar, A.; *Indian J. Chem., Section A* **1997**, *36*, 1063.

5. Agarwal, R.K.; Tyagi, N.; Chakraborti, I.; *Egyptian J. Anal. Chem.* **1998**, *7*, 127; Lopez de Alba, P.L.; Ramirez, E.O.; *J. Radioanalyt. Nucl. Chem.* **1986**, *104*, 255; Ramachandraiah, C.;

Vijayakumari, D. ; Lakshminarayana, K.; *J. Radioanalyt. Nucl. Chem*. **1993**, *175*, 185; Vijayakumari, D. ; Lakshminarayana, K.; *J. Radioanalyt. Nucl. Chem.* **1993**, *175*, 1.

6. Sheldrick, G. M.; *SHELXS97- A Program for the Solution of Crystal Structures*, University of Göttingen: Germany, 1997.

7. Sheldrick, G. M.; *SHELXL97 - A Program for the Refinement of Crystal Structures*, University of Göttingen: Germany, 1997.

8. Allen, F. H; Kennard, O.; Watson, D. G.; Brammer, L.; Orpen, A. G.; *J. Chem. Soc., Perkin Trans. II* **1987**, S1.

9. Jagst, A.; Sanchez, A.; Lopez, E.M.V.; Abram, U.; *Inorg. Chem.* **2005**, *44*, 5738.

10. Brandenburg, H., *DIAMOND - A Program for the Representation of Crystal Structures*, Bohn: Germany, 2006.